RADC-TDR-64-322

STUDIES OF THE EFFECT OF CIRCUIT TAPERING ON TWT PERFORMANCE

TECHNICAL DOCUMENTARY REPORT NO. RADC-TDR-64-322

135 p

September 1964

Techniques Branch
Rome Air Development Center
Research and Technology Division
Air Force Systems Command
Griffiss Air Force Base, New York

Project No. 5573, Task No. 557303

(Prepared under Contract AF30(602)-2575 by C.C. Lo, Microwave Laboratory, W.W. Hansen Laboratories of Physics, Stanford University, Stanford, California)

DISCLAIMER NOTICE

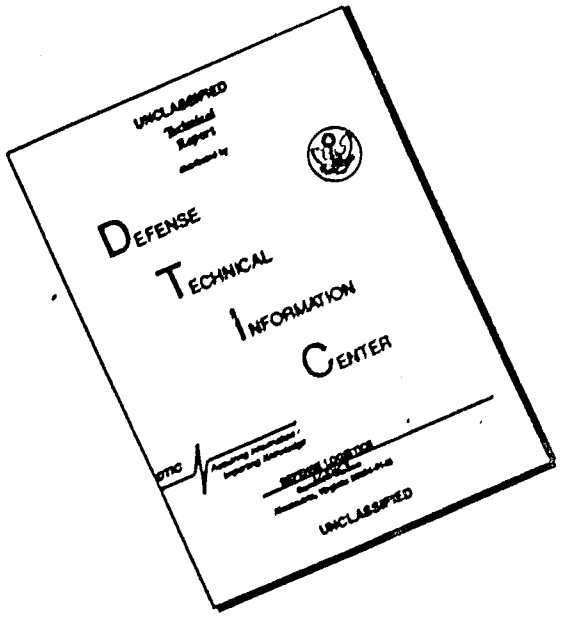

THIS DOCUMENT IS BEST QUALITY AVAILABLE. THE COPY FURNISHED TO DTIC CONTAINED A SIGNIFICANT NUMBER OF PAGES WHICH DO NOT REPRODUCE LEGIBLY.

FOREWORD

The author would like to express his appreciation to Professor M. Chodorow and Dr. R. A. Craig for their guidance and constant interest, and to Dr. D. K. Winslow for many helpful discussions. Thanks are also due to Messrs. W. H. Holmes, W. Sward, W. Heintzen and S. Sangyimpahn for their contributions in constructing the experimental tube and their help in making measurements.

The author would also like to thank Mr Al Braun, the ladies of the Reports Office, and the staff of the Drafting Room of the W. W. Hansen Laboratories, as well as Mrs. Barbara Sturges and Messrs. Al Bahr and T. Reeder for their contribution in making this thesis into final readable form.

ABSTRACT

The main object of this research was to show that by proper tapering of the circuit characteristics of a pulsed, high-power traveling-wave amplifier, long-persisting pulse-edge oscillations could be successfully eliminated. Several types of circuit tapering have been considered, and a particular one was chosen for this empirical study. The type of circuit taper, which appears to have several advantages over others for suppression of pulse-edge oscillations, has both the π-mode frequency increased and the phase velocity for the passband frequencies decreased gradually toward the output end of the tube.

The effect of circuit tapering on forward-wave amplification has also been studied. A method was introduced for calculating the performance and an increase in gain was predicted for the aforementioned taper by this method when the tube was operated beyond the small-signal level. This effect was also measured experimentally on a high-power tube constructed for this purpose.

The effect of circuit tapering on tube efficiency has been studied qualitatively. By using the conventional velocity-phase diagram, the possibility of improving the efficiency is indicated. However, a different kind of circuit tapering other than that used for this study is required.

Two versions of a demountable experimental tube with the aforementioned circuit tapering have been designed, built, and tested. The first version of the tapered tube suffered a vacuum leak, but during its short life period, it proved to have no pulse-edge oscillations in the tapered output section of the tube, although the forward-wave gain was smaller than expected. Since the absence of pulse-edge oscillations might possibly have been due to insufficient gain, the tube was repaired and a middle section was added to increase the gain. The performance of the second version of the tube was good and no pulse-edge oscillations could be found which originated in the tapered output section. Under typical operating conditions at a beam

voltage equal to 120 kV, the maximum power output was 3 MW at a mid-band frequency of 3.0 kMc with a 3 db bandwidth of 12.2% and an efficiency of 26 percent. The forward-wave gain had a maximum increase of 2.3 db over the small-signal gain at 3.06 kMc as the input power was increased beyond the small signal operation level. This effect agreed well with the theoretical prediction; however, as expected, no efficiency improvement was evident. For higher voltages, the power output increased without the appearance of pulse-edge oscillations in the tapered output section, and the gain increase characteristic was still maintained. The bandwidth and the efficiency remained at the same value as that obtained at 120 kV beam voltage.

PUBLICATION REVIEW

This report has been reviewed and is approved. For further technical information on this project, contact 2/Lt William E. Wilson, EMATE.

Approved: William E. Wilson
WILLIAM E. WILSON, 2/Lt, USAF
Project Engineer
Electron Devices Section

Approved:
ARTHUR J. FROHLICH
Chief, Techniques Branch
Surveillance & Control Division

TABLE OF CONTENTS

LIST OF FIGURES

CHAPTER I

INTRODUCTION

In the design of pulsed, high-power traveling-wave amplifiers, the pulse-edge oscillations occurring on the rising and falling edges of the voltage pulse have been one of the most persistent problems. These oscillations, in general, appear with fixed frequencies at the comparatively high impedance points at, or near, the cutoff frequencies of the passband. This is because synchronism between the electromagnetic wave and the electron beam in this region requires a beam voltage considerably lower than the normal operating values. Therefore, under most operating conditions, the circuit wave in this region is not synchronous with the beam during the flat top of the voltage pulse unless the voltage is decreased purposely to the critical value for oscillation. In the transient region, the leading and trailing edges of the pulse, the beam voltage sweeps from zero to full operating voltage in a finite time interval so the critical conditions for start oscillation can be satisfied if the sweep is sufficiently slow to allow buildup to occur. If the rectified rf output pulse is viewed on a scope, the oscillations will appear in the form of irregular pips on the two sides of the amplified rf pulse. The tendency toward these oscillations limits the usable length of the tube, and the allowable gain and the efficiency of the output section of the amplifier will be reduced.

The nature of the pulse-edge oscillations has been discussed in the literature.[1,2,3,4] The buildup of such oscillations could be attributed to, at least, the following kinds of beam-wave interactions. These are: (1) Forward-wave interaction combined with the high reflections at the couplers at, or near, the upper cutoff frequency of the circuit. This kind of oscillation is possible because, at the critical value of beam voltage, the forward-wave gain is high, peaking near the upper cutoff frequency, and the reflections there are generally approaching unity such

that the loop gain could exceed unity. (2) Backward-wave oscillations. Since at the pulse edges the beam voltage sweeps through the backward space-harmonic region, if the tube is sufficiently long, such oscillations are possible. For traveling-wave tubes built for forward-wave amplification, the output section is usually long enough to allow the buildup of backward-wave oscillations. (3) Oscillations due to the simultaneous interaction with a backward-wave and a forward-wave. Near the circuit cutoff frequency, it is possible to have such waves at nearly the same phase velocity with comparable high magnitudes of interaction impedance.

Several ways of suppressing pulse-edge oscillations have been proposed, and some of them have been tried. An obvious example is that of using the gridded gun, so that the beam current can be turned on and off after the anode voltage has reached its operating value. However, in high power applications, the existing designs of gridded guns either intercept some beam current which can cause a serious heat dissipation problem at the grid when the beam power is high; or they have too small a ratio of beam anode voltage to the grid voltage such that a large value of grid voltage is required, and as a consequence a complicated modulating system is inevitable.

In this report, we shall consider another approach to the solution of this problem; the method consists of tapering the circuit velocity so that it is gradually decreasing and simultaneously varying the dispersion characteristic of each section of the tapered circuit in some prescribed fashion. If the tapering is proper, it will result in a condition such that in the region where oscillation is most likely to occur, all the mechanisms contributing to the oscillation are disrupted, without seriously deteriorating the amplification. In other words, a tapered tube can be made longer, thus having higher gain but still maintaining good stability.

In fact, if the circuit tapering is also proper for the normal amplification region which, in general, lies in the middle of the passband, the electronic efficiency as well as the forward-wave gain of the tube can also be enhanced. This is because a properly tapered slow-wave structure provides a better synchronism condition for high level operation of the tube

than that of an untapered slow-wave structure. The success of the circuit tapering technique would result in an output section long enough for sufficient gain, provide high electronic efficiency, and the input section, or sections, could be short enough to preclude pulse-edge oscillations in these regions so that traveling-wave tubes could be made unconditionally stable.

There are several theoretical approaches one can use in studying the effect of circuit tapering. One of these is by extending the nonlinear analysis used in the study of the large-signal behavior of uniform circuit tubes to take account of the circuit variation due to tapering. However, the existing large-signal theories consider, in general, one-dimensional, nonrelativistic, uniform circuit cases only. In some cases, large discrepancies between the calculated and experimental values of uniform circuit tube efficiency have been observed.[5] If more hypothetical assumptions were added in order to solve the effects of circuit tapering, then the validity of the approach would become questionable. Furthermore, a great amount of numerical computation must be performed before any general conclusion on circuit tapering can be reached. If successful modification were made on the nonlinear theory, such an analysis would be excellent for studying the effect of a particular tapered circuit but would still be impractical for the design of a tapered traveling-wave tube. The approach adopted here is a simpler but approximate one. It is essentially that of considering the tapered circuit as a variation of uniform slow-wave circuits; by extending the theories and results of the uniform circuit traveling-wave tube the effect of circuit tapering can be estimated approximately. Such an approach may not be a rigorous theoretical treatment of the problem; however, it provides a simple and useful tool in the design of tapered, pulsed, high-power traveling-wave tubes, as well as a clear interpretation of the actual behavior of circuit tapering on the tube performance.

Several different types of circuit tapering are briefly considered in Chapter II, and the one which appears to have the best chance of suppressing pulse-edge oscillations was chosen for use in an experimental

high-power, pulsed traveling-wave amplifier. This taper results in a variation of both the phase velocity in the passband and the upper cutoff frequency of the passband in a particular fashion. The amount of circuit tapering is determined by the required change in the propagation constant necessary to ensure that the circuit wave is sufficiently out of synchronism with the beam when the beam voltage sweeps through the possible pulse-edge oscillation region.

From an equivalent study of voltage taper on uniform circuit tubes by Hess[6] at the University of California, it is also known that such a tapered circuit is, at least, an adequate one for forward-wave interaction. His data show that, if starting from a voltage less than the synchronous voltage, one increases the dc beam voltage linearly along the length of a uniform circuit tube, the output power and efficiency are maximized at a point where the beam voltage is about 1.4 times the synchronous voltage. Equivalently, therefore, by slowing down the circuit phase velocity linearly, it is possible to obtain an enhanced forward-wave amplification.

The effect of circuit tapering on the amplification when the average velocity of electrons in the beam is decreased due to the increase of input power will also be discussed in Chapter II, and the actual six-cavity linear taper in the experimental tube will be used as an example to illustrate an approximate method which can give a gain increase approximating the value actually obtained from the experimental tube. This will be shown in Chapter IV together with other test results.

A qualitative discussion of the effect on efficiency based on Cutler's results[5] will also be given in the last section of Chapter II. The mechanism of efficiency improvement due to circuit tapering is also presented.

In order to check the theoretical predictions, an experimental tube was made to evaluate the circuit tapering effects empirically. The type of circuit tapering chosen in Chapter II was applied to the clover-leaf circuit, in which the cavity height and the size of the apertures in the coupling plates are gradually changed from cavity to cavity to provide the required changes in frequency and in phase constant, and thus, in the

circuit phase velocity. The detail of the design, as well as the cold circuit measurements and small-signal parameter computations on the actual experimental tapered tube are given in Chapter III.

The experimental tapered tube consisted of the six-cavity linear taper which formed the last six cavities at the output end of the tube, and of other untapered cavities which formed the rest of the circuit of the tube. The tube was designed with demountable connections at the severs which divide the circuit into output section and input section or sections, such that it can be easily rebuilt for testing other tapered circuits in the future.

Results of the experimental tube performance are given in Chapter IV. It can be seen that the pulse-edge oscillations can actually be stopped in the output section of the tube by use of the linearly tapered circuit. The tapered circuit also shows a distinct effect on the forward-wave gain; it exhibits a sudden increase when the input drive is sufficient to cause the onset of saturation in the beam. This effect agrees well with the theoretical prediction shown in Chapter II. However, as compared with an earlier uniform circuit tube built with the same uniform clover-leaf structure, the efficiency and bandwidth of the tapered tube seem to remain unchanged. This is because the experimental tube was purposely designed to have moderate circuit tapering in the forward-wave amplification region, but which was sufficient to suppress pulse-edge oscillations. Greater tapering should result in increased efficiency.

CHAPTER II

SOME THEORETICAL ASPECTS OF CIRCUIT TAPERING IN TRAVELING-WAVE TUBES

A. INTRODUCTION

It has long been known that by properly tapering the slow-wave structure of a traveling-wave amplifier that the forward-wave amplification and the efficiency of the tube might be improved. However, a great part of this chapter will be devoted to a discussion of possible improvements in the control of pulse-edge oscillations. This problem of oscillation has long been a persistent one in the design of pulsed, high-power traveling-wave tubes.

As mentioned in Chapter I, pulse-edge oscillations generally appear as irregular pips on the leading and the trailing edge of the pulse at frequencies near or at the upper cutoff frequency. For a typical slow-wave circuit used in a pulsed, high-power traveling-wave amplifier such as a clover-leaf or a centipede structure,[7] the ω-β diagram for the amplification passband has a form as shown in Fig. 2.1. In the transient regions of the beam voltage pulse edges, oscillations usually exist at the heavy line region of the ω-β diagram in Fig. 2.1 with frequencies near or equal to f_π, and with phase constant, β, slightly less or slightly more than π/L. This means that pulse-edge oscillations may exist in a region extending from the forward-wave to the backward-wave space-harmonic regions.

To illustrate how circuit tapering can be used to preclude the build-up of the pulse-edge oscillations as well as to improve the forward-wave amplification, a hypothetical and simplified example will be considered as follows. Let the block in Fig. 2.2 represent a tapered slow-wave circuit which is designed in such a way that at its output end the phase velocity of both forward-wave and backward-wave regions

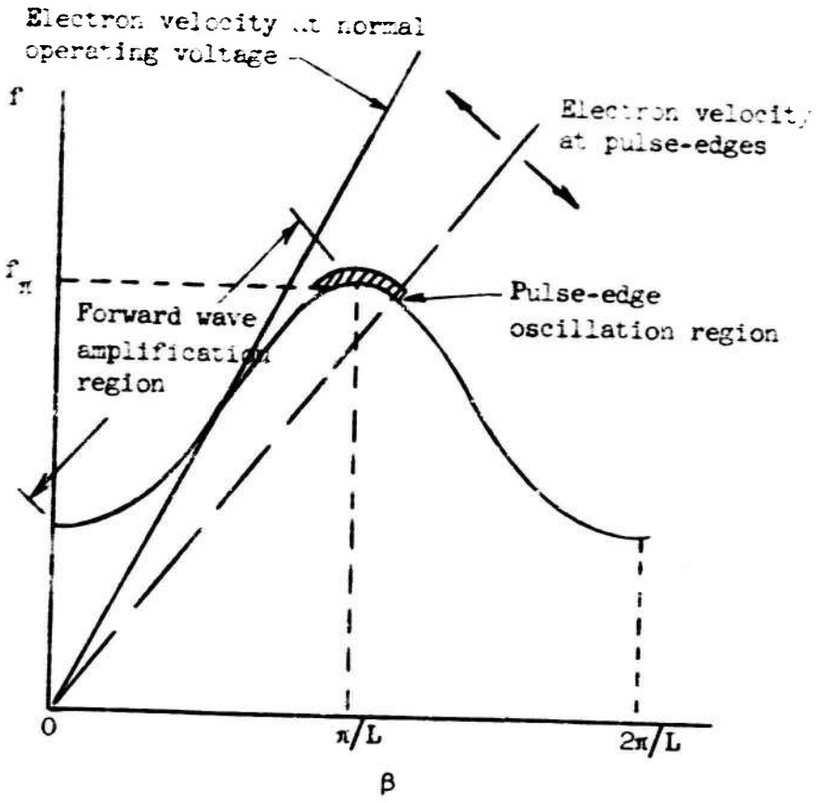

FIG. 2.1--ω - β diagram for a typical slow-wave structure used in a high-power, traveling-wave amplifier. Here, only the fundamental passband and one space harmonic are shown.

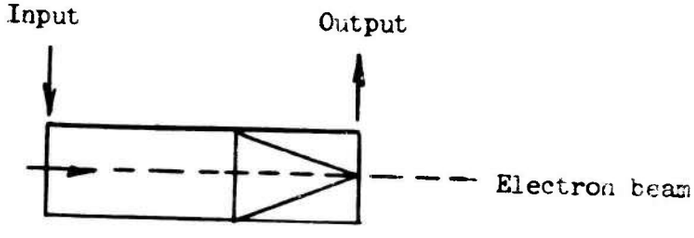

FIG. 2.2--Backward-wave interaction circuit block diagram.

is decreased when one proceeds from left to right. Assume an electron beam is passing through the circuit and is also going from left to right. For the purpose of simplicity, only pulse-edge oscillations due to backward-wave interaction are considered to be important in this particular example. When the input power level is increased beyond the level for small signal operation, the electron velocity of the beam becomes multivalued, and most electrons in the beam reach velocities at the output end of the tube lower than the original values at the input end of the tube. Since the phase velocity of the forward-wave is also decreased in the same direction, the forward-wave amplification will be improved if proper tapering is maintained. If, however, the phase velocity in the backward-wave region is made to decrease more rapidly than that in the forward-wave region, the electrons in the beam can be made to fall out of synchronism with the backward wave when conditions are optimum for forward-wave amplification. Therefore, with a single taper which provides different rates of velocity tapering in the forward-wave and the backward-wave regions, the amplification and the stability of the tube can both be improved simultaneously.

The method adopted in this chapter in studying the effect of circuit tapering is essentially an extension of the uniform circuit traveling-wave tube theories. These theories are not applicable directly to the tapered tube case because the circuit is now no longer periodic. Nevertheless, if the effect of each cavity in the taper is considered discretely, then the summation of these discrete results will give an approximation to the effect of the entire taper. For a taper sufficiently gradual, such an approximation should be a close one. This method is by no means a rigorous theoretical treatment of the problem of circuit tapering; however, it provides a simple and reliable method for design of a tapered-circuit, pulsed, high-power traveling-wave amplifier, and also indicates its expected performance.

In actual tubes, oscillations due to other circuit-beam interactions are also important. In Section B which follows, various types of oscillations as well as the effect on these oscillations of different kinds of possible circuit tapering will be considered individually.

The effect of circuit tapering on forward-wave amplification, and on tube efficiency, will be discussed in Sections C and D, respectively.

B. EFFECT OF CIRCUIT TAPERING ON THE PULSE-EDGE OSCILLATIONS

In the earlier studies of uniform circuit traveling-wave tubes, it was found that the pulse-edge oscillations generally appear with fixed frequency at, or near, the upper cutoff frequency of the passband which corresponds to beam voltages lower than the normal operating values, as mentioned in the preceding section. Hence, the rf output due to pulse-edge oscillations will not appear in the region corresponding to the flat top of the beam voltage pulse when it is at the rated voltage, but will appear in the transient regions of the rise and fall of the voltage pulse. Therefore, these two irregular pips occur where the beam voltage is proper for the electron beam velocity to be synchronous with the rf circuit wave velocity as the voltage sweeps from zero to the normal operating value.

The dynamics of such oscillations are rather complicated. However, it has been found that they may at least be caused by the following three kinds of beam-wave interactions. They are: 1) forward-wave interaction combined with the high reflections at the couplers at, or near, the upper cutoff frequency of the passband; 2) backward-wave interaction; and 3), simultaneous interaction of both the forward-wave and backward-wave spatial harmonics. More details of these interactions as well as the effect of circuit tapering on each of them will be given in later parts of this chapter.

First of all, let us consider the means of tapering the slow-wave circuit of a traveling-wave tube and the classification of these tapers. One may wish to classify them according to their effects on the circuit characteristics. Thus, according to the change in phase velocity, interaction impedance, etc., that they introduce, they are known as velocity-taper, impedance-taper, etc. They can be subgrouped further according to the manner in which the circuit parameters change from cavity to cavity along the taper: thus we might have the linear velocity-taper, exponential impedance-taper, etc. On the other hand, in the study

of their effects on suppressing the pulse-edge oscillations, the change of the final dispersion characteristics with respect to the original one is of importance. Hence, one may classify them accordingly. Several possible types of tapers are shown in Figs. 2.3 to 2.6. They are classified by their final changes with respect to the original characteristics and will be referred to as different tapering schemes hereafter.

As in the study of uniform circuit traveling-wave tubes, the use of ω-β diagrams of the slow-wave structures facilitates the understanding of the beam-wave interaction. Furthermore, some of the effects of circuit tapering can readily be visualized from such diagrams. Figure 2.3 shows the ω-β diagram of a simple velocity taper. The curve labeled "output" is that which would be obtained from a circuit of identical cavities of the final length L_2, and the same coupling aperture dimensions as that of the last cavity of the tapered chain. In the actual taper several intermediate cavities will exist, having lengths and aperture dimensions between those of the two extremities. These lengths and aperture dimensions are all slightly different and the curves for structures comprised of identical cavities of these intermediate lengths would lie somewhere between the two limiting curves shown. The lower cutoff frequency of the amplification passband for this particular taper as well as for other types of tapers considered in this chapter will be assumed to have a fixed value throughout the taper. The reason for this assumption is simply that tapering of the lower cutoff region will not affect the pulse-edge oscillations which generally exist at the opposite end of the passband. Any alteration of other tube characteristics to bring about changes at the lower cutoff will increase the difficulty in identifying the effects of circuit tapering on the pulse-edge oscillations. Therefore, it is preferable to have a relatively small amount of circuit tapering in the forward-wave region by keeping the lower cutoff frequency unchanged. Besides, the following discussions of pulse-edge oscillations will not lose their generality with this assumption of fixed lower cutoff frequency. It can be noted from Fig. 2.3 that the upper cutoff frequency, or the π-mode frequency, of the passband remains unchanged for this scheme of straight velocity taper. It will be shown later that such a scheme is

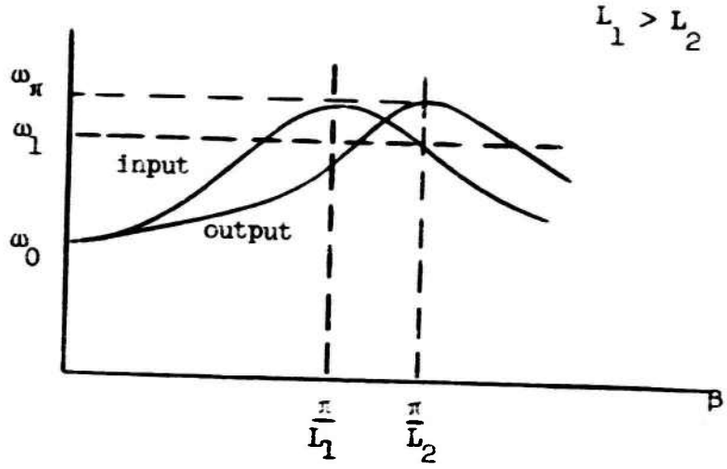

FIG. 2.3--ω-β diagram showing straight velocity taper.

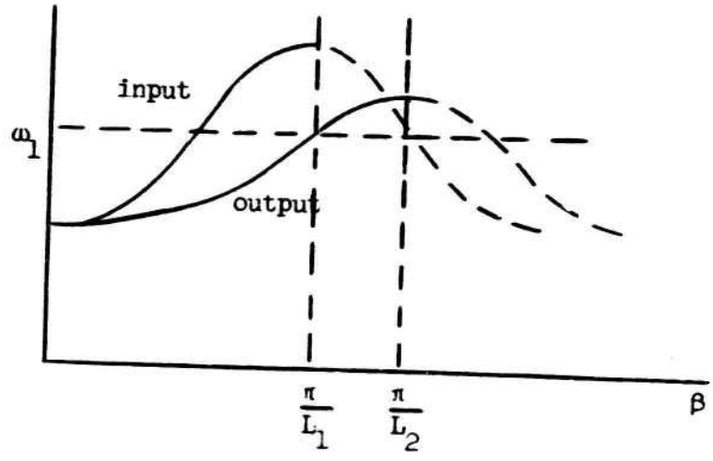

FIG. 2.4--ω-β diagrams showing velocity and frequency taper with upper cutoff frequency decreasing with velocity decrease.

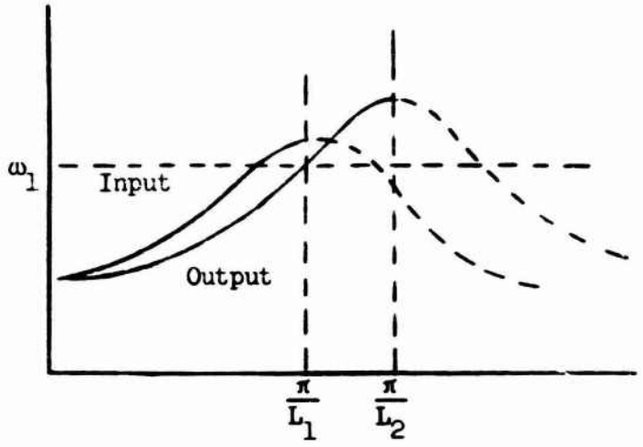

FIG. 2.5--ω-β diagram showing velocity and inverse frequency taper.

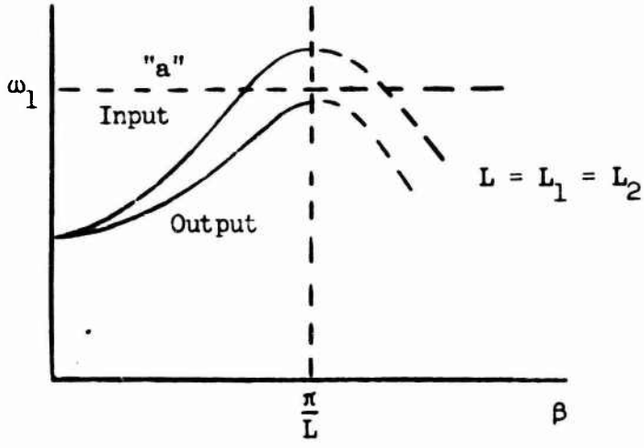

FIG. 2.6--ω-β diagram with frequency taper only. The cavity height remains constant.

not effective in suppressing the type of pulse-edge oscillation due to forward-wave interaction and high reflection. Also, if the cavity lengths are not varied drastically, the tapering in phase velocity for the backward-wave spatial harmonic region is not as large as with other types of circuit tapering, such as the one shown in Fig. 2.5. Obviously, then, this scheme is not the most desirable one.

If tapering is achieved by varying the upper cutoff frequency of the passband as well as the section lengths, then two other types of taper can be obtained, such as shown in Figs. 2.4 and 2.5. In Fig. 2.4, the "output" curve has a lower upper cutoff frequency than that of the "input" curve. If the output coupler is matched to the last cavity of the taper, this means that the usable bandwidth of the tapered circuit will be less than that of the untapered one. Such a change certainly is not desirable as far as the amplification bandwidth is concerned. Furthermore, for the same length of L_2, it can be seen that the phase velocity tapering in the backward-wave region is even smaller than that shown in Fig. 2.3. On the other hand, the tapering scheme shown in Fig. 2.5 has an upper cutoff frequency for the "output" curve higher than that of the "input" curve. This type of taper not only has a usable bandwidth equal to that of the untapered circuit, but also has a larger velocity tapering in the backward-wave region than that of Fig. 2.3. In addition, it is capable of suppressing pulse-edge oscillation due to forward-wave interaction and high reflections. The reason for this effect will be shown in detail in a later section. It is therefore believed that this type of tapering will be the most effective one for suppressing pulse-edge oscillations; there are also possibilities that it will enhance the forward-wave amplification.

Another type of circuit tapering can be obtained by decreasing the upper cutoff frequency of the passband, but keeping the cavity lengths of each cavity in the taper constant. The ω-β diagram of this type of tapering is shown in Fig. 2.6. It can be readily seen that the velocity change with the tapered circuit in the backward-wave region is in the opposite direction compared to that of other tapering schemes. Hence, as far as backward-wave oscillation is concerned, this type of taper

could be effective since the circuit phase velocity can be changed rapidly enough in this region to prevent synchronism between it and the electron beam. However, this scheme has two serious shortcomings which exclude it from being useful in a tapered amplifier. Firstly, for frequencies lying between the upper cutoff of the "input" and "output" curves in Fig. 2.6 such as indicated by the straight line marked "a," complete reflection exists in the taper. Therefore, forward-wave oscillation may still exist if the net loop gain is greater than unity. Secondly, in the same way as the scheme shown in Fig. 2.4, the "output" curve possesses less bandwidth than that of the "input" curve. Therefore, a tube with such a tapered circuit will have less usable bandwidth for amplification than the untapered tube, thereby rendering the circuit less desirable.

The effects of the above types of circuit tapering on the pulse-edge oscillations, which are classed according to the mechanisms which might possibly cause them, will be discussed in more detail in the following sections.

1. Effect of Circuit Tapering on Pulse-edge Oscillations due to Forward-wave Interaction and High Reflections

In studies of the uniform circuit traveling-wave tube, Gould[2] suggested that by considering the presence of two spatial harmonics near the edge of the amplification passband, a gain peak can be found to occur near the upper cutoff frequency for beam voltages lower than those for normal maximum bandwidth operation. This phenomenon, as can be seen from the dispersion characteristics of the slow-wave structure, is due to the fact that the electron beam at these voltages is more nearly in synchronism with the wave at those frequencies than it is at higher beam voltages, and that the circuit interaction impedance is very high at these frequencies. Under normal operation conditions, if the beam voltage of the tube is pulsed, the flat top of the pulse corresponds to the operating voltage too high for synchronism at these frequencies, whereas at the pulse-edges, the beam voltage sweeps through this frequency region, giving rise to high peaks of tube gain. On the other hand, the reflection coefficients from the junctions between the slow-wave structure and the uniform wave-guiding

system, such as coaxial line, waveguide, etc., are necessarily approaching unity at these frequencies. Because of the rapidly changing characteristic impedance of the slow-wave structure as a function of frequency near the cutoff frequencies of the passband, it is in general impossible to match this impedance well to the slowly-varying impedance of the uniform wave-guiding system except at spot frequencies. Due to the peak of the tube gain and the high reflections at the junctions, oscillation at these frequencies is inevitable for tubes with reasonable amounts of mid-band frequency amplification.

The starting condition for such oscillations is that the loop gain should be greater than unity, viz.,

$$G_f G_b \rho_{in}^2 \rho_{out}^2 > 1 \quad , \qquad (2.1)$$

where G_f is the net gain in the forward direction, i.e., in the direction of electron motion; G_b is the net attenuation of the reflected wave in the backward direction, i.e., in the direction opposite to that of electron motion; ρ_{in} is the reflection coefficient at the input end of the tube, or, if only the output section of a severed tube is considered, it is the reflection coefficient from the sever; and ρ_{out} is the reflection at the output end of the tube, or from the sever if only the input section of the tube is considered. Therefore, for a tapered tube to be effective in suppressing this type of oscillation, the left hand side of Eq. (2.1) must be reduced to less than unity; and, at the same time, the mid-band frequency amplification should be of the same order as the untapered tube of the same length.

The tapering scheme shown in Fig. 2.5 will first be considered. The "output" dispersion characteristic of this scheme has an upper cutoff frequency higher than that of the "input" characteristic, as well as larger values of propagation phase constant, β, for constant frequencies. A realistic example of this scheme is shown in Fig. 2.7 which is actually measured from a six-cavity linear taper built for empirical evaluation of circuit tapering, as discussed in Chapter III. For such a tapering of the dispersion characteristic, the corresponding change in interaction impedance

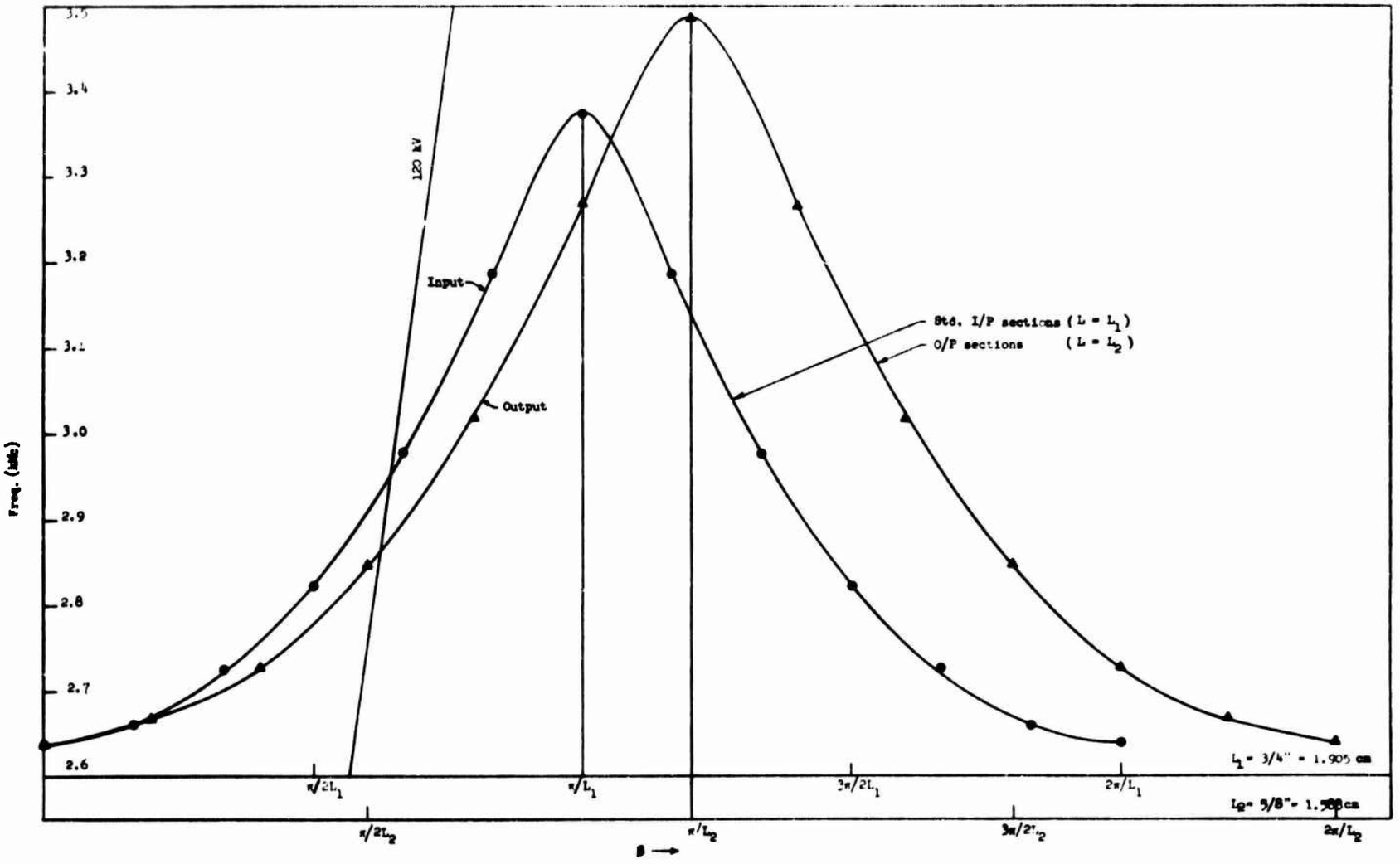

FIG. 2.7--Measured frequency vs circuit propagation constant, β of the first and the last cavities of the linear taper.

can also be obtained from "cold" circuit measurements. Figure 2.8 shows the values of the cube root of Pierce's interaction impedance,[8] $(E^2/2\beta^2 P)^{1/3}$, computed from frequency perturbation results described in Chapter III as a function of phase constant, β. This factor is directly proportional to Pierce's small signal parameter "C" given by

$$C = \left(\frac{E^2}{2\beta^2 P}\right)^{1/3} \left(\frac{I_0}{4V_0}\right)^{1/3} = \left(\frac{E^2}{2\beta^2 W v_g}\right)^{1/3} \left(\frac{I_0}{4V_0}\right)^{1/3} , \quad (2.2)$$

where E is the axial E-field, P is the power flow, i.e., $P = Wv_g$, W is the stored energy per unit length, v_g is the group velocity, and I_0, V_0 are the dc beam current and voltage, respectively. It can be seen from Fig. 2.8 that for this particular taper, the value of $(E^2/2\beta^2 P)^{1/3}$, and therefore "C" for a given beam, is changed only by a small fraction for mid-band amplification frequencies. However, near the upper cutoff frequency of the untapered cavities where the pulse-edge oscillation generally exists in uniform circuit tubes, the values of these parameters are decreased drastically in the tapered cavities for both forward and backward spatial harmonics. In addition to this, the propagation constant, β, as can be seen from Fig. 2.7, is increased successively in the taper from the "input" to the "output" values. This means, for certain beam voltages, the synchronism condition prevails only at frequencies near the upper cutoff of the "input" curve, and the gain becomes less and less as one proceeds toward the output end of the tube along the taper. Therefore, the net tube gain, G_f, which is usually high in the uniform circuit case at frequencies near the upper cutoff will be low if the taper is properly designed.

In other words, due to the small value of G_f, the left hand side of Eq. (2.1) can be made to be less than unity over the entire amplification band. This is, of course, impossible to achieve in a uniform circuit tube with the same order of mid-band frequency amplification.

When the tube is tapered in the fashion described in the previous paragraphs, and the taper is located at the output end of the tube, the output coupler is connected directly to the last cavity of the taper

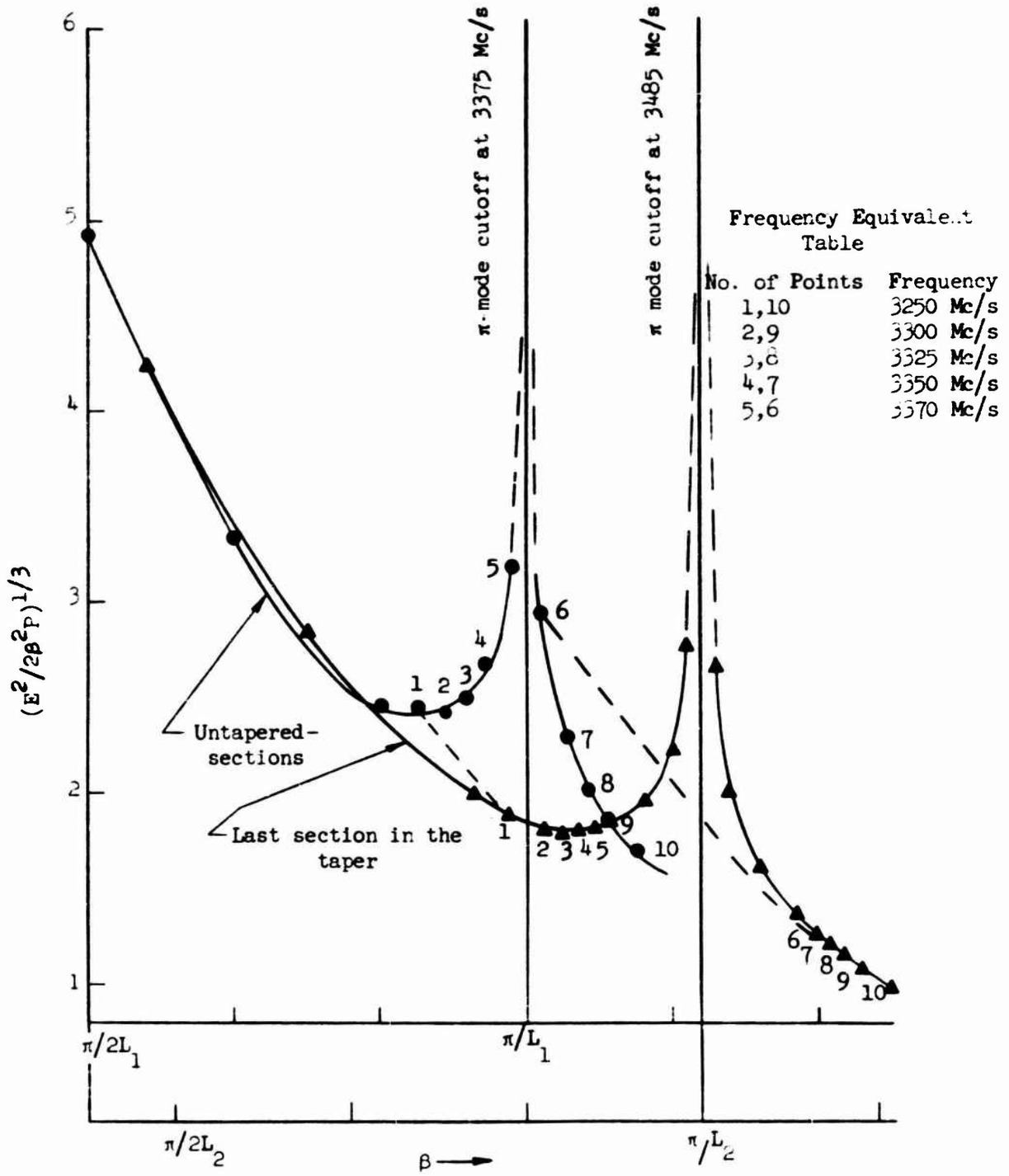

FIG. 2.8--Cube root of Pierce impedance, $(E^2/2\beta^2P)^{1/3}$ vs circuit propagation constant β of the first and the last cavities of the linear taper where $C = (E^2/2\beta^2P)^{1/3} \cdot (I_0/4V_0)^{1/3}$ and $L_1 > L_2$

which has a dispersion characteristic as the "output" curve shown in Fig. 2.7. At frequencies near or at the untapered upper cutoff, i.e., the upper cutoff of the "input" curve, the matching of circuit impedance between the output coupler and the slow-wave structure can be improved. This is because the variation with frequency of the characteristic impedance of the last tapered cavity at these frequencies is now a more slowly varying function than that of the untapered cavities, and more nearly matches the slow variation with frequency of the output waveguide impedance. In other words, the taper behaves like an impedance transformer. Hence, the value of the left hand side of Eq. (2.1) can be further reduced due to this decrease of reflection coefficient from the output coupler, i.e., the factor ρ_{out}^2 is reduced.

The simultaneous reduction of both G_f and ρ_{out}^2 is the unique feature of this particular tapering scheme. Physically this is due to the simultaneous increase of the upper cutoff frequency and the decrease of the cavity length as one proceeds from the beginning to the end of the taper. Therefore, for frequencies near that of the upper cutoff of the "input" curve, one can see from Fig. 2.5 that in addition to the increase of β in the tapered cavity, the group velocity will increase successively from the "input" to the "output" curve. Furthermore, due to the change of the circuit dimension, the E^2/W will also decrease slightly from the E^2/W value of the untapered cavities. Then, from Eq. (2.2), it follows immediately that C for the tapered cavities will be less than that of the original untapered cavities for these frequencies and since other tube parameters change only moderately, the small signal forward-wave gain at these frequencies for a properly designed taper will be smaller.

For other tapering schemes, the capability of suppressing this type of pulse-edge oscillation is considerably less than that considered above. The main reason is that the upper cutoff frequency of these types of tapers is either kept unchanged throughout the taper, or is changed to values lower than that of the untapered case. Therefore, at frequencies where the gain peak usually exists in the untapered tube, the reduction in interaction impedance is much less than in the scheme

discussed above, and the reflections from the output coupler are either the same or worse than in the uniform circuit case

For instance, one can easily observe from Fig 2.3 that any frequency on the untapered dispersion characteristic or the "input" curve in the figure will maintain its relative value with respect to the upper cutoff frequency throughout the taper In other words, frequencies corresponding to the high interaction impedance points near the upper cutoff frequency will always correspond to high impedance points in the successive tapered cavities. The only difference between this and an untapered circuit is the change in phase constant, β . For a given frequency, this also means a change in circuit phase velocity Even if such a taper could be made to suppress oscillation at small signal levels by drastically changing the phase constant, such that the circuit wave and the beam fall out of synchronism, the tube might still oscillate at high rf levels, because at high level operation a large portion of the electrons in the beam will have lower velocities near the output end of the tube than at the input end, and the taper at the output end of the tube provides high interaction impedance with successively slower phase velocities. Therefore, synchronism may always be good at high levels, and reflection from the output coupler is always high since, as can be seen from earlier discussions, nothing has been done to improve matching by this tapering method

It can also be seen from Fig. 2.3 that the group velocity for frequencies near the upper cutoff is essentially the same for all tapered cavities. Hence, the only possible way to reduce the interaction impedance, viz $E^2/(2\beta^2 W v_g)$, near the upper cutoff frequency, is by reducing E^2/W and increasing β , both of which require changes in cavity dimensions Upon comparing this scheme to the one shown in Fig. 2.5, it is seen that for the same frequency range, the group velocity v_g increases with distance along the taper in Fig. 2.5, instead of just remaining unchanged throughout the taper as in Fig. 2.3. Therefore, for the same amount of impedance reduction, the circuit dimensions must be changed much more in the scheme shown in Fig. 2.3 than in that shown in Fig 2.5 Changing the circuit dimensions to provide a large increase in the value of β will normally reduce the quantity E^2/W This reduction in the value of E^2/W in the

high frequency range will also result in a reduction of this quantity at mid-frequency, and so deteriorate amplification. This deterioration is, of course, undesirable. Therefore, for the same amount of circuit tapering in the mid-band frequency, the scheme shown in Fig. 2.5 is more effective than the one shown in Fig. 2.3.

Other tapering schemes such as shown in Figs. 2.4 and 2.6 can readily be seen to be deleterious to the forward-wave amplification in addition to their ineffectiveness in suppressing pulse-edge oscillations. This is because both of these types of tapers have an upper cutoff frequency for the "output" curve less than that of the "input" curve. Therefore, contrary to the situation in the taper of Fig. 2.5 discussed earlier, the output coupler in these cases can only be matched to the slow-wave structure in a narrower frequency interval than that of the untapered case, or the usable bandwidth for amplification of the tapered slow-wave structure is decreased to that of the "output" curve shown in these figures.

The effect of these tapers on pulse-edge oscillations can be readily seen from the ω-β diagrams of Figs. 2.4 and 2.6. For frequencies lying between the upper cutoff of the "input" and that of the "output" curves, complete reflection exists somewhere in the middle of the taper since the upper cutoff frequency of the tapered cavities is decreased successively along the taper. When this complete reflection exists at the beginning of the taper, such as for frequencies very near the "input" upper cutoff frequency, the tube may not oscillate, if the gain prior to the reflection is sufficiently small to insure that the left hand side of Eq. (2.1) is less than unity. However, if the complete reflection exists near the output end of the taper, such as for the frequency range just above the upper cutoff frequency of the "output" curve, the interaction impedance will also become higher as one approaches the position of complete reflection, and oscillations may exist. The reason for this increase in interaction impedance can easily be seen from the following consideration. Let us compare these schemes shown in Figs. 2.4 and 2.6 with those shown in Fig. 2.5 which is the same as in Figs. 2.7 and 2.8. In the former methods, the upper cutoff frequency is decreased gradually and so is the group velocity. Hence, for the schemes given in Figs. 2.4 and 2.6, one

starts from a low impedance point and proceeds gradually to the high impedance points when approaching the high reflection. This is contrary to the situation shown in Fig. 2.5. Therefore, even though β is increased, one would still expect the forward-wave gain prior to the reflection to be high. The oscillation situation in the tube, or in the output section if only this section is under consideration, will be as bad as in the untapered tube case. Furthermore, at lower frequencies just below the upper cutoff frequency of the "output" curve, the tube may also oscillate, since at these frequencies, the interaction impedance increases rapidly when one proceeds from the first to the last cavity in the taper, and the reflection at the output coupler is also high. Nevertheless, in a uniform circuit amplifier, the tube is expected to be stable at this frequency, so, in this respect, the tapered tube is even worse than the untapered one. Therefore, it is concluded that to suppress pulse-edge oscillations which might be due to a combination of forward-wave interaction and high reflections, the tapering scheme shown in Fig. 2.5 will be most effective.

2. Effect of Circuit Tapering on Pulse-edge Oscillation due to Backward-wave Interaction

As mentioned previously, a severed tube may consist of several isolated sections. Since the input section, or sections, of a tube can be made short enough to prevent backward-wave oscillation in itself, the problem is reduced to considering the stability of the output section of the tube only. In a tapered tube, the output section consists of a portion of uniform cavities and a taper at the output end connected directly to the output coupler of the tube. Therefore, as far as backward-wave oscillations, which have an inherent feedback mechanism, are concerned, the portion of untapered cavities, if sufficiently long, may oscillate independently from the tapered region. For this case, the situation is no different from that of a uniform circuit tube, and the analysis for uniform circuit backward-wave oscillators can be applied directly. However, the entire output section may also oscillate compositely; then the uniform circuit analysis can provide no usable results since the periodicity requirements necessary for the analysis are no longer fulfilled in the tapered region.

It can be seen from the simplified picture shown in Fig. 2.9, which is an analog to the one cited in Heffner's[9] article, that for backward-wave oscillation to exist the following basic conditions must hold, namely: 1) the total phase shift around the loop should be an integral number of cycles, i.e.,

$$\theta - \beta_e L = (2n + 1)\pi \quad , \tag{2.3}$$

where θ is the total phase shift along the tapered circuit, β_e is the electron phase constant, L is the length of the interaction region, and n is an integer, i.e., $n = 1,2,3,\ldots$; and 2) the loop gain must exceed unity. Because of circuit loss and the inefficiency of the energy conversion process, a certain amount of gain is necessary, since the gain per electron wavelength is proportional to C; this means

$$CN = \text{Constant}, \tag{2.4}$$

where N is the total number of electron wavelengths in the tube.

In the slow-wave circuit generally used in a high-power traveling-wave amplifier, strong coupling exists between cavities. Hence, when the circuit is tapered, the change in field quantities will be a nearly continuous function of distance along the taper, although the dimensions of cavities are changed in discrete steps. In any differential distance, dz, along the taper, all dynamic equations used in the uniform circuit case still apply, but the solutions can no longer be assumed to have the form of $e^{-\gamma z}$ since the circuit is no longer periodic. Instead of considering the field in the taper to be changed continuously, one can approximate it by a field varying in a step fashion, such as that shown in Fig. 2.10. Then, in the region of each step, one can apply the uniform circuit analysis as if it were a section of uniform circuit tube and sum these individual results to obtain an approximation to the actual solution of the tapered tube.

The validity of this approximation will depend largely on the manner in which the slow-wave circuit is tapered. For a small and gradual taper,

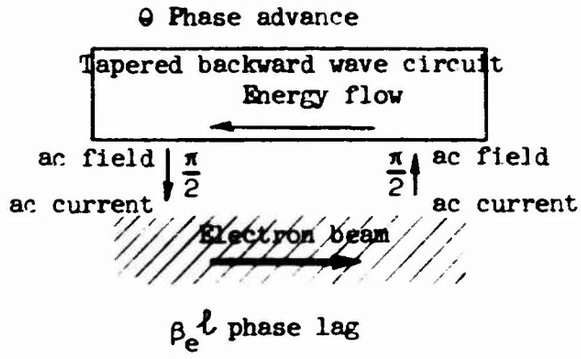

FIG. 2.9--The feedback loop of a tapered backward-wave tube.

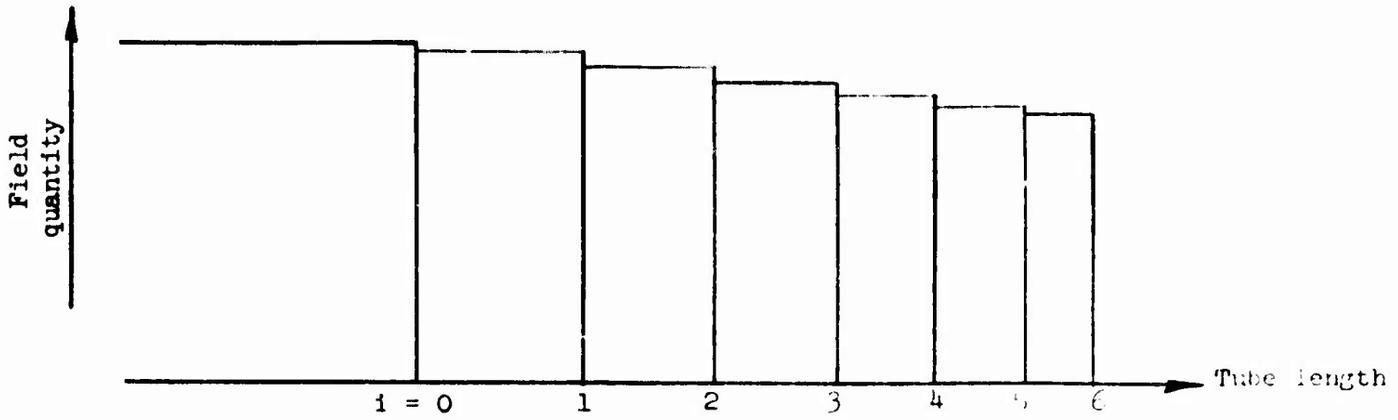

FIG. 2.10--Schematic diagram of step approximation process, where i indicates the step number.

this approximation will certainly be a close one, and the results of uniform circuit analysis can be used without giving serious error.

The six-cavity linear taper cited in Section 1 with characteristics shown in Figs. 2.7 and 2.8 will again be used to illustrate this approximation process. A tapered output section of the tube is assumed to consist of an untapered portion of five untapered cavities in addition to the above-mentioned six-cavity linear taper. Since the total increase in cutoff frequency through the six tapered cavities is only 100 Mc/s for a mid-band frequency of 3000 Mc/s, and total section length decrease is 1/8 inch, which is only 16.7% of the original value, the taper is considered to be sufficiently small and gradual for the approximate analysis to hold. To make the above step approximation, the length of each step can be arbitrarily chosen; however, for convenience, the length of each step is assumed to be the same as the length of each tapered cavity.

In order to compare with the untapered case, a uniform output section consisting of untapered cavities having the same total length as the output section of the tapered amplifier is first considered. By employing Johnson's[10] numerical results, and assuming an electron beam with a microperveance of 2, the actual value of CN of the untapered output section is normalized to the start oscillation value, CN_{st}, computed for the actual amount of phase difference, $(\beta - \beta_e)L$, along the circuit, where β is the circuit phase constant and L is the length of the output section. The normalized results are plotted in Fig. 2.11, which shows that an untapered output section with the same length as the tapered output section will oscillate at frequencies above 3255 Mc/s, since CN/CN_{st} is larger than unity for those frequencies. It can also be seen from this figure that for the six-cavity linear taper, this value is reduced to below 0.75 for these frequencies. Therefore, the tube will be stable after tapering.

The starting condition for the tapered output section is obtained from the approximation process outlined above, which is equivalent to defining

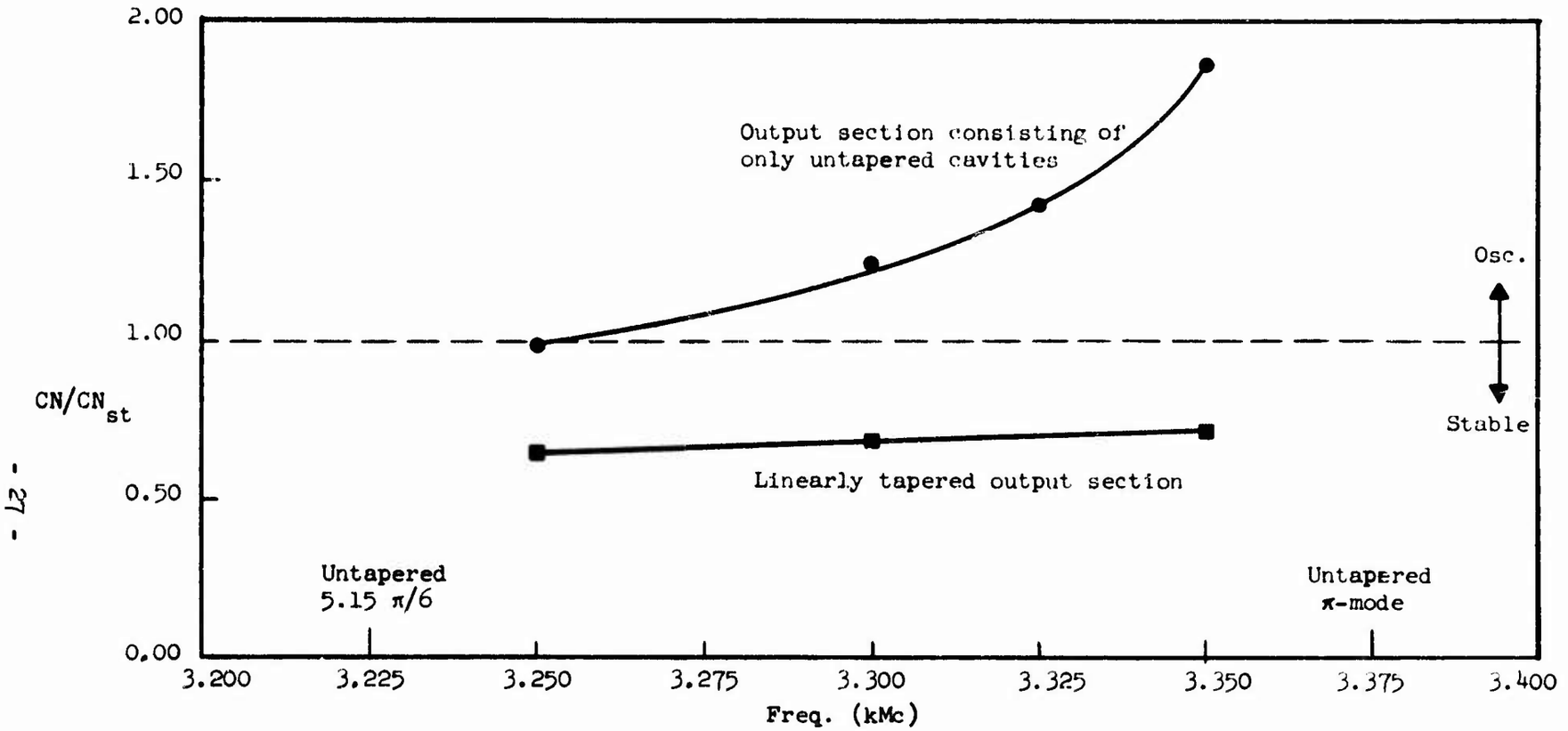

FIG. 2.11--Normalized CN of an output section consisting only of an untapered section and a tapered output section with respect to the start oscillation value as a function of frequency.

an equivalent uniform circuit to have

$$CN = \sum_{i} C_i N_i$$

$$(\beta_{eq} - \beta_e)L = \sum_{1}^{11} \beta_i \ell_i - \beta_e L \quad , \tag{2.5}$$

where $i = 1,2,3,\ldots 11$ indicates the step number, or in the present case, the cavity number in the eleven-cavity output section, ℓ_i is the length of each step, and L is the total length:

$$L = \sum_{1}^{11} \ell_i$$

$$\beta_{eq} = \frac{1}{L}\sum \beta_i \ell_i \quad . \tag{2.6}$$

Therefore, one can find the value of CN_{st} from the actual value of phase difference. In this example, the CN_{st} was found from the phase difference.

During this approximation process it was found that the relatively low value of CN for the tapered output section is achieved in part by the decrease in C and in part by the change in circuit phase velocity in the tapered chain. These changes, as discussed in Section 1, are the largest when the tapering scheme shown in Fig. 2.5 is used for a fixed amount of phase velocity tapering in the forward-wave region at the mid-band frequency. If other tapering schemes are used, either the forward-wave amplification of the tube will deteriorate or the amplification bandwidth will be decreased in order to achieve the same purpose, even if such schemes are possible.

3 Pulse-edge Oscillation due to Simultaneous Interaction of Forward wave and Backward wave with the Beam

In the studies of the uniform circuit tube, it has been found[2,3,4] that at the frequencies corresponding to the transition between the forward-wave and backward-wave regions of the ω-β diagram, oscillation due to simultaneous interaction of the forward and backward spatial harmonics with the electron beam is possible. This is because at this transition region, which is located at the upper cutoff, both waves have nearly the same value of phase velocity as well as the same absolute value of group velocity. At cutoff the values of both are identical, so we are considering a small region in the vicinity of and including the cutoff point. Furthermore, the interaction impedances, as discussed previously in Section 1, are very high for both the fundamental and first backward wave in this region; that is, interaction is strong in both cases.

We shall now discuss how oscillations arising from this type of interaction can be avoided by circuit tapering. By referring to Fig. 2.5, for example, we see that the upper cutoff frequency is gradually increased toward the output end of the taper. In other words, the region in which the forward- and backward-space harmonics have nearly the same phase and group velocities is gradually increased in frequency as the output end is approached along the taper. Therefore, for frequencies slightly less than or equal to the untapered upper cutoff frequency, the tapered slow-wave structure has much lower interaction impedance at the output end of the taper than at the untapered input end. The reason for this reduction is the same as that given in Section 1, and can easily be seen from the subsequent example. Hence, when the beam is synchronized with the untapered cavities in the tapered tube at these frequencies, the tapered cavities will contribute little to this type of oscillation because: 1) the interaction impedance in the tapered cavities is low, and 2) the waves and the electron beam are out of synchronism due to the increase of phase constant, β, as one proceeds toward the output end of the taper. In a tapered tube, the uniform portion of the output section should always be made short enough to avoid oscillation in this region. Then the entire output section should not oscillate because the taper does not contribute significantly to the growth of oscillations in this frequency range.

For a taper which does not have a change in upper cutoff frequency such as the one shown in Fig. 2.2, however, the build-up of such oscillations is possible when the tube is driven. The tube can also support oscillations due to high forward-wave gain and large reflections at the ends of the section as previously described in Section 1. In either case, the electron velocity will reach a lower value at the output end of the taper than at the input end; furthermore, the circuit phase velocity is also decreased in the same fashion, due to the change of cavity lengths. Therefore, the synchronism condition between the circuit wave and the beam is always maintained. Because the upper cutoff frequency is kept unchanged throughout the taper, the interaction impedance for frequencies in the neighborhood of the upper cutoff is always high for all the cavities. Hence, strong interactions exist in the entire length of the output section and the tube will likely oscillate.

For other tapering schemes, the upper cutoff frequency is changed to a lower value in the tapered cavities. Therefore, in addition to the simultaneous interaction of both the forward and backward waves with the beam, one also expects high reflections in the tapered region for frequencies close to the untapered upper cutoff. This will increase the possibility of tube oscillation. Furthermore, it has already been shown in Sections 1 and 2 that these tapering schemes are also poor in suppressing other types of pulse-edge oscillations.

The taper which has an increased upper cutoff frequency along its length as shown in Fig. 2.5 appears to be most effective in suppressing all three types of the pulse-edge oscillations discussed above, which exist near, or at, the upper cutoff frequency of the fundamental passband. The realistic example cited in the above sections will be shown further in later chapters to be effective in suppressing these oscillations in an experimental tube.

In the operation of uniform circuit traveling-wave tubes, another kind of oscillation is often found. This oscillation does not belong to the category of pulse-edge oscillations considered above, but exists with frequencies of the second higher passband near or on the flat top of the beam voltage pulse. Such oscillations are often referred to as higher

passband oscillations. An ω-β diagram of the second higher passband obtained from a tapered clover-leaf structure is shown in Fig. 2.12. For the circuit cited, such oscillations usually exist near the lower cutoff frequency of the second higher passband. The beam voltage necessary for synchronism with this frequency region, as can be seen from Fig. 2.12, is nearly the same as that required for synchronism with the mid-band frequencies of the amplification passband.

There are many possible causes of these oscillations including those previously discussed, depending on where the voltage line intersects the propagation characteristic. A tapered circuit designed to suppress pulse-edge oscillations may not be effective in suppressing upper passband oscillations. For instance, the tapered circuit whose dispersion characteristics are shown in Fig. 2.12 is effective in suppressing the pulse-edge oscillations as mentioned in the preceding sections. However, for beam voltages below 130 kV, the tapered tube may still oscillate in the frequency range from 5400 Mc/s to 5600 Mc/s, since in this frequency region, the interaction impedance of the circuit is relatively high. Thus, oscillations which result from simultaneous forward-wave and backward-wave amplification together with high reflections from the output coupler which is poorly matched in the higher passband are likely to occur.

Methods for suppressing the higher passband oscillations have been studied in this laboratory.[11] The one adopted for the experimental tapered tube is that of selective attenuation. As the name suggests, this method applies attenuation in such a way that the loss provided for the higher passband is much higher than that provided for the amplification passband. Sufficient attenuation in the higher passband can therefore be obtained to suppress most oscillations while allowing little attenuation of the amplification passband. An alternative method is that of using an external high-pass coupling system with a cutoff frequency above the frequencies of the amplification passband. With this coupling, the external system can couple a large amount of loss into the slow-wave structure at the higher passband frequencies when the external system is properly loaded with lossy materials. However, in the amplification

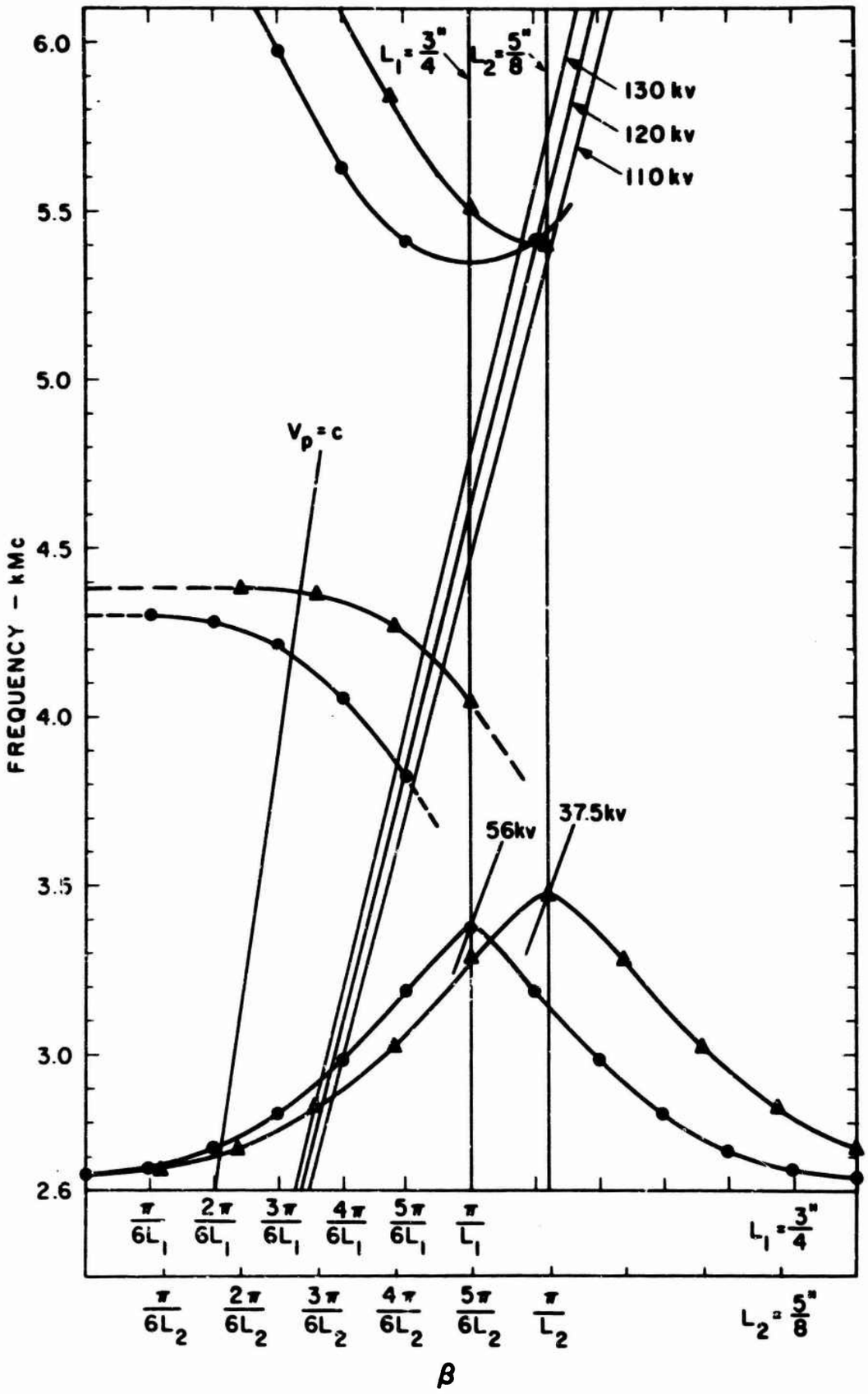

FIG. 2.12--The ω-β characteristics for tapered cloverleaf TWT.

passband no appreciable loss is coupled to the circuit because of the cutoff property of this coupling system. Hence, the building up of higher passband oscillations can be precluded by sufficiently loading it to the nonoscillation point without appreciably affecting the amplification properties of the tube.

C EFFECT OF CIRCUIT TAPERING ON AMPLIFICATION

We have discussed the effects of tapering on pulse-edge oscillation. In this section we shall discuss another aspect of circuit-tapering, viz., the effects of tapering on amplification; an approximate method of predicting performance will be introduced.

For a tapered amplifier consisting of a uniform circuit portion and a taper at its output end, the total small-signal gain will be less than that of a uniform circuit tube having the same length and operating under the same conditions if the uniform cavities used in both tubes are designed to provide optimum small-signal gain. This is because the tapering achieved by gradually changing the cavity dimensions near the output end of the tube will change both the interaction impedance and the synchronism condition. Therefore the total gain is reduced. Nevertheless, if the tapering is small, such reduction in total gain will not be serious, and can be predicted approximately by a method to be shown later.

When the input signal power increases beyond strictly small-signal operating values, the single beam velocity picture in the tube breaks down, and more and more electrons in the beam reach a final velocity at the output end of the tube less than the original value at the input end of the tube. If, for a certain input signal level, the circuit phase velocity is also decreased gradually in the region of the taper in the same manner as that of the electron velocity, then the synchronism condition between the circuit and the beam will be improved in this region, so the total gain of the tube will be higher than that computed by the standard small-signal theories. On the other hand, a uniform circuit tube at the similar increased input level will have less total

gain than the small-signal value because at this level most electrons in the beam slow down near the output end of the tube, but the cavities in that region are designed to give optimum gain when synchronizing with the original beam velocity. In other words, the small-signal gain is the highest gain obtainable in the uniform circuit tube case, whereas in the tapered tube case, this is no longer true.

Such nonlinear dynamics in a uniform circuit tube have been studied thoroughly in a series of experiments by Cutler.[5] In an example of a typical uniform circuit tube given in his paper, he showed that when the input level increases from strictly small-signal operating values corresponding to an output power level less than -22 db below saturation, most of the electrons in the beam start to consolidate into a "main bunch" in the decelerating phase region and at the same time experience a rather rapid decrease in velocity. As the input level was increased corresponding to an output power level -12 db below saturation, the final velocity spread was reached. At this level, most of the electrons were in the "main bunch" with reduced velocities. However, a second "spur" was just starting to grow. Beyond this level, more and more electrons shifted into the second "spur" and moved into the accelerating phase region. Ultimately, almost all the electrons in the beam consolidated into two groups, both containing the same number of electrons. One group was located in the decelerating phase of the rf circuit fields, while the other was in the accelerating phase, so there was no further net power transfer from the beam to the circuit and the tube reached saturation.

In the above experiment it was noted that most electrons in the beam experienced a maximum change in velocity and consolidation into a main bunch in the decelerating phase when the input power had values corresponding to the onset of the nonlinear operation region of the tube. It is the region corresponding to the output power between -22 db to -12 db below saturation. Since the variation of power output in a traveling-wave tube with respect to the input levels is related to the variation with respect to distance along the tube, this means that when the power output at the end of the tube reaches a level of -12 db below

saturation, the electron velocity will start to spread at a distance corresponding to 10 db power gain toward the input end of the tube as measured from the output end. If the phase velocity of the slow-wave circuit starts to decrease at the same distance from the output end, the synchronism condition between the circuit and the beam can be improved.

To evaluate this effect analytically, one may either perform nonlinear numerical analysis, which undoubtedly will be more involved than that in the uniform circuit case to obtain a precise solution, or extend the small-signal analysis to give an approximate result. In the following paragraphs, an extended small-signal analysis will be developed and a practical example of a tapered amplifier with a six-cavity linearly tapered cloverleaf structure will also be given.

The approximation process employed here is essentially the same as that used previously in considering the case of backward-wave oscillations, except that the average electron velocity is also varied from section to section. In other words, the tapered portion of the tube is now considered as composed of a series of "sub-tubes", each having different circuit dimensions and beam velocities. The term "sub-tube" is used here to indicate that each cavity of the taper is considered as a small section of a uniform circuit tube built with cavities of the same dimensions operating at a beam velocity equal to the average electron velocity at the position of the particular cavity in the taper. Since in this process only the beginning of the nonlinear operation region is of interest, the approximation should be good if the circuit tapering is small and the input signal level is not too far from the small-signal operating values. Unfortunately, the average electron velocity change in a tapered tube is unknown due to the lack of a suitable nonlinear computation, or experiments similar to those Cutler did for the uniform circuit tube case. But, if one considers the problem slightly differently, one may obtain an upper bound for the expected increase in gain without knowing this information. From knowledge of the type of circuit tapering it can be seen that the phase velocity of the circuit is decreased successively when one proceeds toward the output end of the taper, and, if

the tapering is small, the final electron velocity spread in the beam will not differ drastically from that of a uniform circuit tube with the same tube parameters. Hence, one may choose a series of average electron velocities between the initial velocity and the final average electron velocity which, as mentioned above, could be found roughly from the uniform circuit tube results, and compute the gain for each of the "sub-tubes" mentioned above. From these results one can find that the position corresponding to the optimum gain, which is chosen to be at the beginning of the taper at the initial electron velocity, will shift toward the output end of the taper, when the average electron velocity decreases. For a schematic example of this process, Fig. 2.13 shows a six-section taper with eight assumed averaged electron velocities. The g's in the table may represent any of the tube parameters. Each column represents the value changes for each "sub-tube" parameter when the average electron velocity changes. Each row indicates the parameter change for a certain electron velocity. For instance, the g's may represent the gain of each "sub-tube." Then each column indicates the gain variation when the average electron velocity changes. On the other hand, each row indicates the gain change when the average electron velocity is kept constant. For instance, the first row in the table gives the values for initial electron velocity. If the g's represent the gain, then the sum of $g_{11}, g_{12} \cdots g_{16}$, i.e.,

$$G_T = \sum_{j=1,\ldots,6}^{i=1} g_{ij} \quad , \tag{2.7}$$

will give the total small-signal gain in the tapered portion of the tube. The total gain of the tube will be $n \times g_{10}$, plus the sum shown above, where n indicates the number of untapered cavities in the tube. If the circled g's represent the optimum gain obtainable for each electron velocity, and if at a certain input level the average electron velocity decreases along the taper with values corresponding to those of the circled g's, the total gain of the tube will have the highest value.

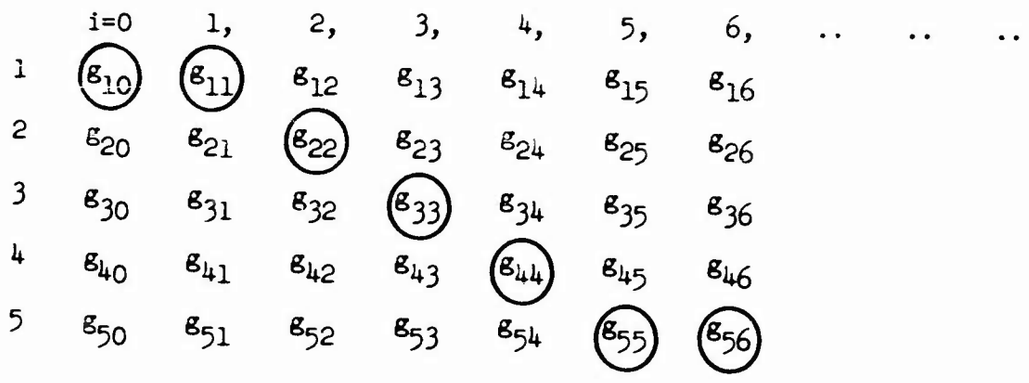

i = 0 the untapered cavity.

i = 1, 2, ...6, tapered cavities.

FIG. 2.13--Schematic example of a six section taper with eight assumed electron velocities.

In other words, the sum of circled g's will form the upper bound for the possible improved tube gain. For other input levels, the average electron velocity will start to decrease either before reaching the taper or inside the taper; these, as can be seen from Fig. 2.13, will all give less total gain in the tube than the summation of circled g's.

The example of a six-cavity linearly tapered clover-leaf structure previously discussed will again be used here to illustrate the approximation method. The amplification at a mid-band frequency of 3060 Mc/s will first be considered. From the circuit parameters of the untapered cavities, it is found from Cutler's results that a tube constructed from identical cavities has a final beam velocity at this frequency of the order of 0.42×10^8 m/s with an initial beam velocity of 1.76×10^8 m/s at 120 kV beam voltage. Therefore, eight intermediate electron velocities are assumed in computing the gain for each "sub-tube." The ω-β diagram for the taper obtained from the measurement described in Chapter III has already been shown in Fig. 2.7; however, a more detailed one for the amplification passband is shown in Fig. 2.14. The abscissa in the later figure is plotted in the propagation constant, β , and the phase shift per section, βL , is also indicated. In the figure, L_{in} is the length of untapered cavity. The $L_1, L_2, \ldots L_{out}$, are the length of the tapered cavities from number one to the last cavity which is indicated as L_{out} . The interaction impedance of the taper is then computed from frequency perturbation results given in Chapter III and is plotted vs cavity number as shown in Fig. 2.15. Since the interaction impedance is independent of the beam parameter, it is a single value for each "sub-tube." The results shown in the figure are coincidently linear for this frequency; however, they are not necessarily linear for other frequencies. The reason for it being a decreasing function of cavity number can be easily seen from Pierce's argument.[8] The dimension change due to circuit tapering will, of course, decrease the value. The values of the modified "C" parameter are shown in Fig. 2.16 as a function of cavity number in the taper with beam velocity as a parameter. The modification is made by considering the beam voltage V_0 in Eq. (2.2) as the equivalent beam voltage corresponding to the reduced average electron velocity in each "sub-tube." However, the

of the tapered wave amplifier.

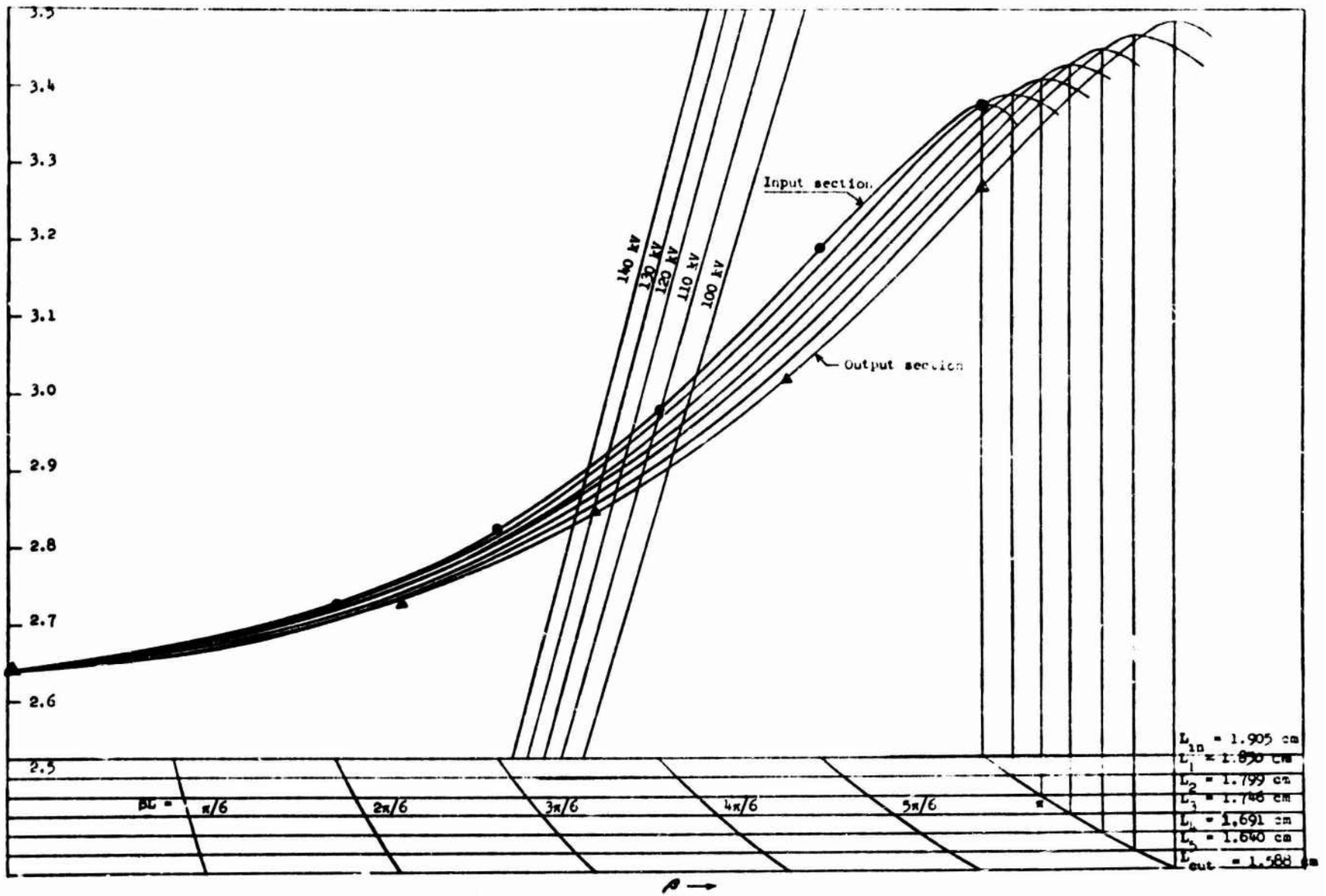

FIG. 2.14--An ω-β diagram for the lower passband forward wave of the tapered wave amplifier.

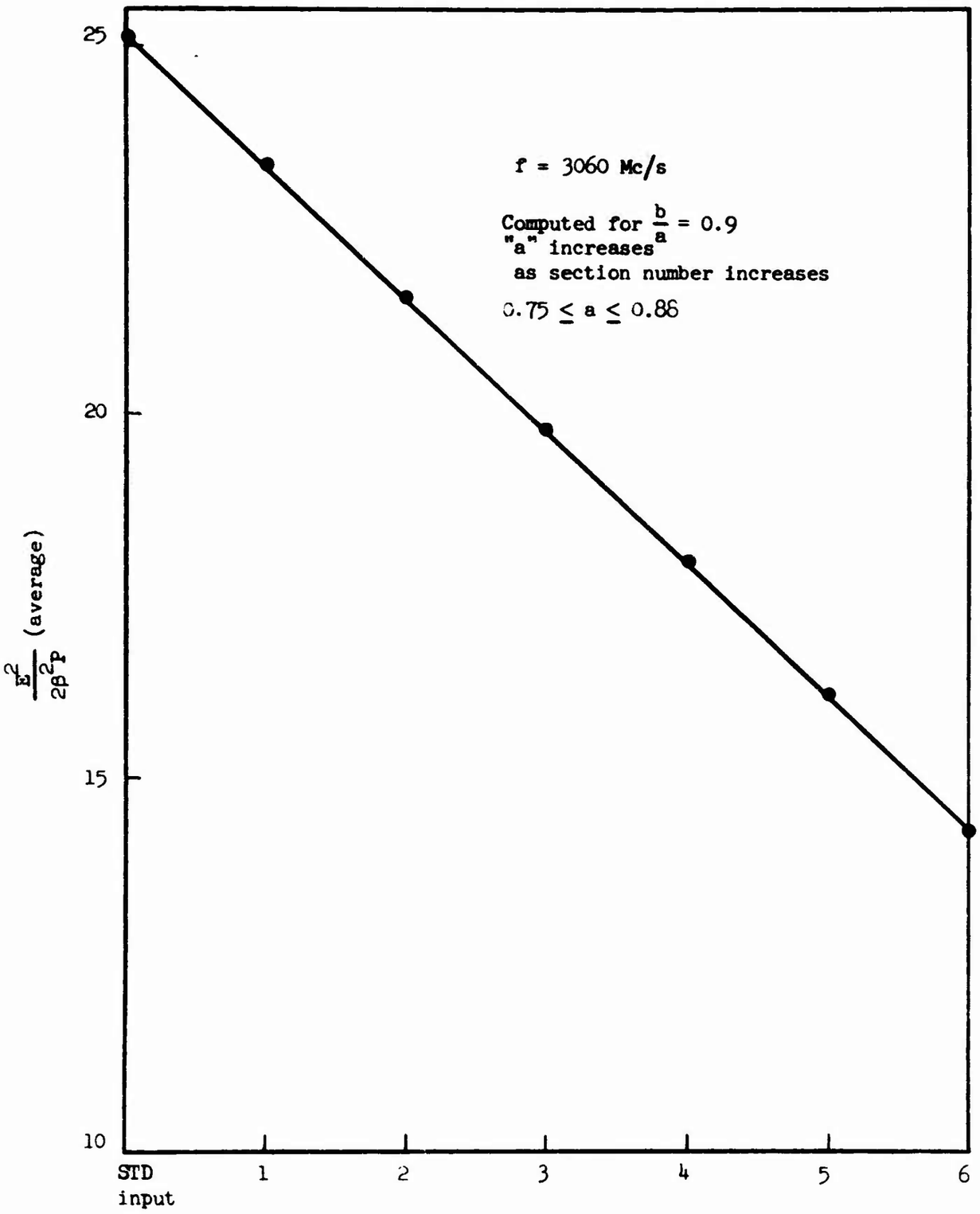

FIG. 2.15--Pierce Impedance vs section numbers.

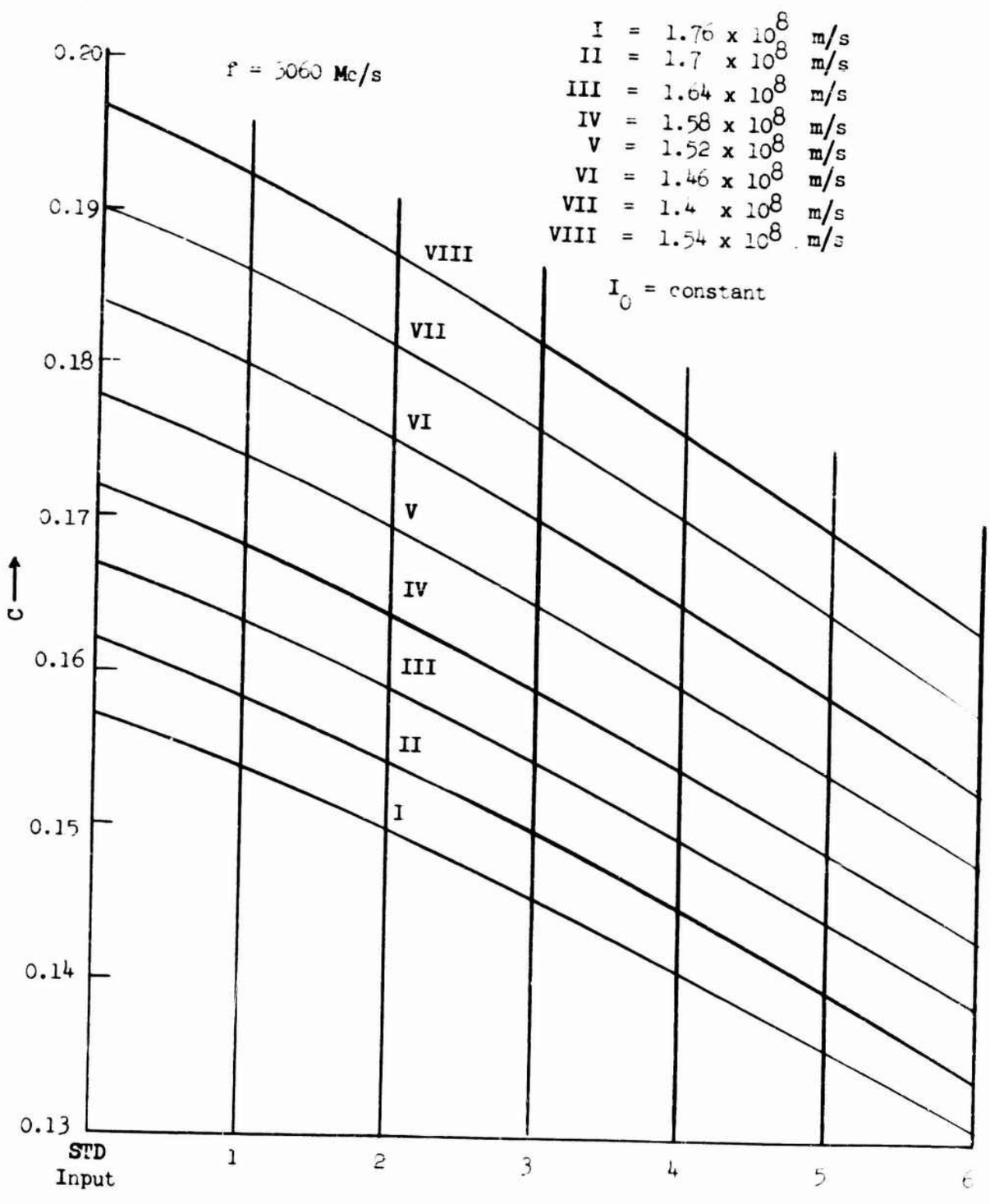

FIG. 2.16--C vs section number.

original value for dc current, I_0 , is used in computing the C's , since even though the electron velocity is reduced, the electron density may increase in the region of the taper.

Figure 2.17 shows the change of velocity parameter, b , with respect to the change in cavity number, and with the electron velocity again as a parameter.

The space-charge parameters, QC , are shown in Fig. 2.18 as a function of the number of cavities with beam velocity as a parameter. In evaluating this parameter, the reduced plasma frequency is assumed to change with the electron velocity, and the beam diameter is assumed to be always 90 percent of the cavity central aperture diameter, which is nearly the actual case.

The above parameters are tabulated in Table II.1. From these parameters, a set of x_1 parameters are obtained from Birdsall and Brewer's computations,[12] and are plotted in Fig. 2.19a, b. It is interesting to note from the curves of Fig. 2.19a, b that the peak value of x_1 shifts toward the output end of the taper as the average electron velocity decreases.

From the value of the x_1's, the gain of each "sub-tube" for each reduced electron velocity can be calculated. However, the total gain of a tube with an input section of eleven untapered cavities and an output section consisting of five untapered cavities and a six-cavity linear taper mentioned previously, is shown in Fig. 2.20 for three different cases. The curve marked "optimum case" is obtained by considering each "sub-tube" as having its maximum gain, which gives the highest gain obtainable in a tapered tube, and corresponds to the case of the circled g's mentioned earlier. The middle curve denoted by $b = 0$ is obtained by assuming that the electron velocity is always the same as the circuit phase velocity. The total gain of the tube which can be seen from the figure is less than the optimum case, but still can be 2.1 db higher than the strictly small-signal case. The lowest curve in the figure is the strictly small-signal case, that is the case by considering that the electron velocity is the same throughout the tube, and that the total gain is the lowest compared with the other two cases shown in Fig. 2.20.

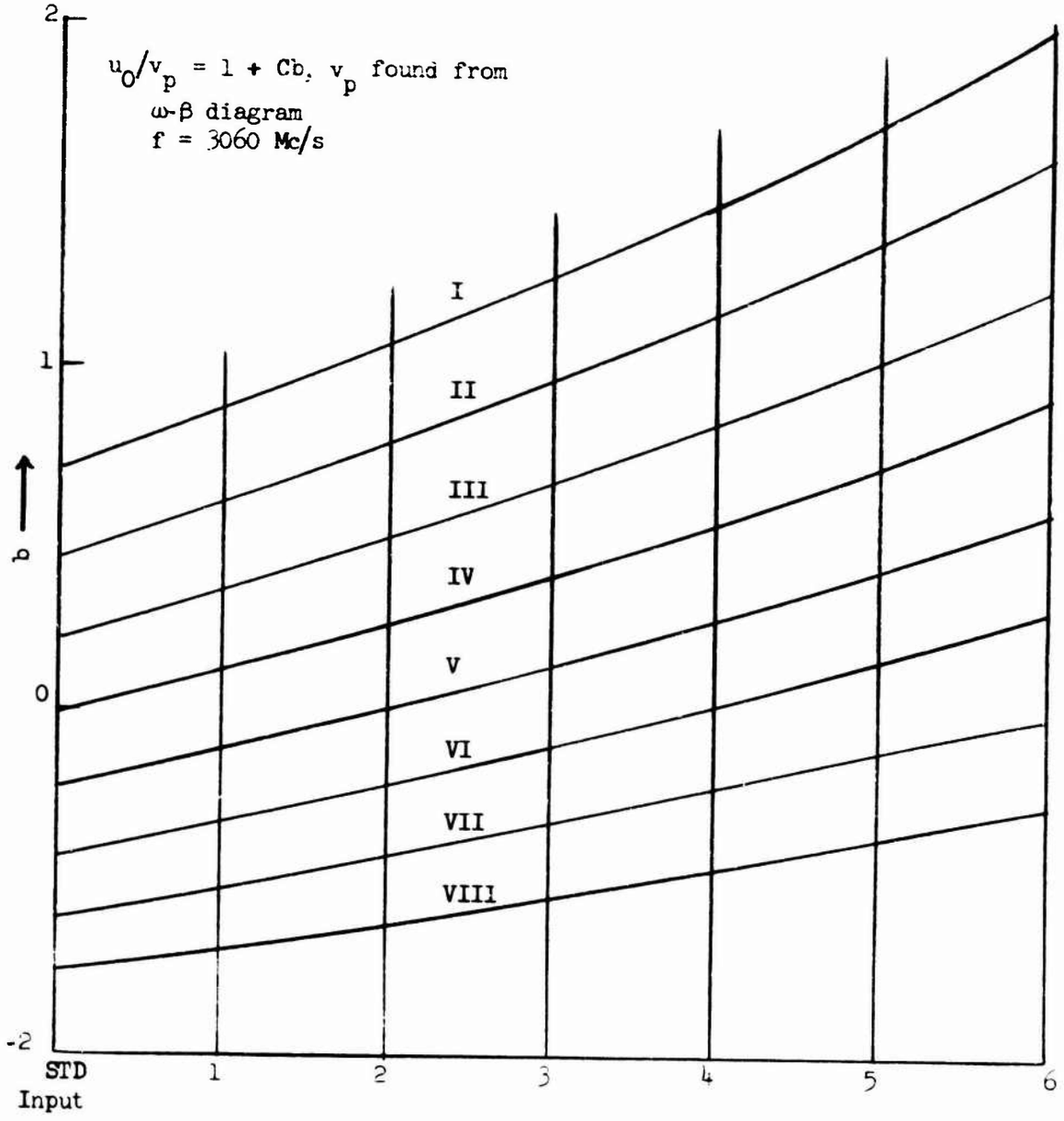

FIG. 2.17--b vs section number for values of C found from Fig. 2.2.

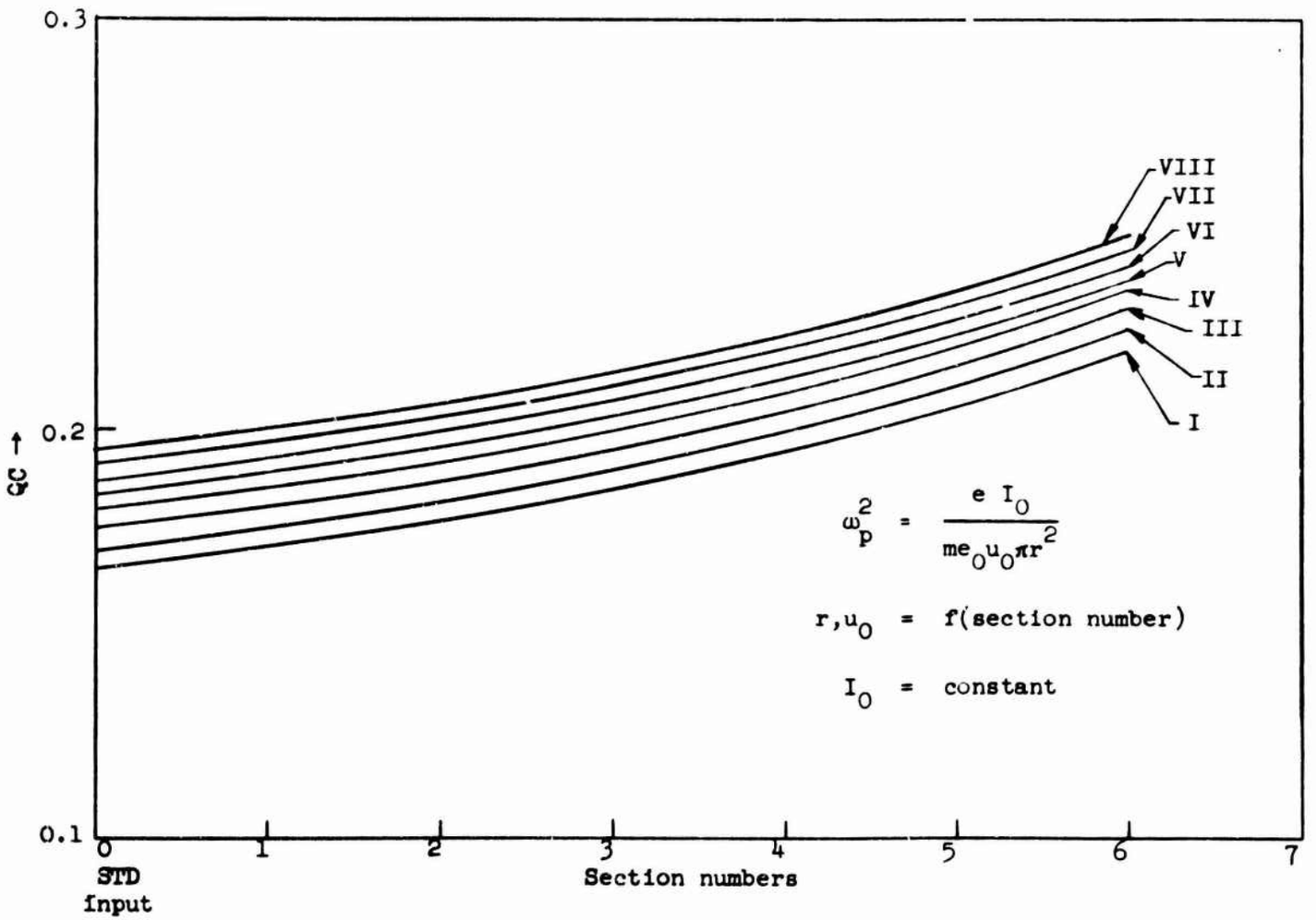

FIG. 2.18--QC vs section numbers from data of Fig. 2.2.

TABLE II.1

PARAMETERS OF TAPERED SECTIONS

FOR

DIFFERENT ELECTRON VELOCITIES

f = 3060 Mc

$\frac{U_0}{x10^8}$		STD Input	No. 1	No. 2	No 3	No. 4	No. 5	No. 6
1.76	QC =	.166	.172	.179	.186	.195	.207	.219
	b =	+.700	+.864	-1.08	+1.274	+1.475	+1.71	+1.97
	C =	.157	.154	.150	.146	.141	.136	.131
	x_1 =	.813	.81	.803	.79	.756	.69	.62
1.7	QC =	.171	.1768	.184	.191	.201	.212	224
	b =	+.438	+.610	+.780	+.960	+1.15	+1.35	+1.60
	C =	.162	.158	.154	.150	.145	.140	.134
	x_1 =	.79	.81	.81	.81	.79	.77	.72
1.64	QC =	.176	.180	.187	.196	.205	.217	.228
	b =	+.204	+.362	+.506	+.678	+.834	+1.04	+1.22
	C =	.167	.163	.159	.154	.150	.144	.139
	x_1 =	.76	.78	.79	.80	.79	.79	.77
1.58	QC =	.181	.185	.192	.1995	.210	.220	.233
	b =	-.017	+.118	+.246	+.400	+.530	+.725	+.902
	C =	.172	.168	.164	.159	.154	.149	.143
	x_1 =	.69	.73	.734	.76	.77	.77	.77
1.52	QC =	.184	.188	.196	.204	.213	.224	.237
	b =	-.224	-.115	.0	+.139	+.262	+.415	+.575
	C =	.178	.174	.169	.164	.159	.154	.148
	x_1 =	.61	.65	.68	.69	.71	.73	.76
1.46	QC =	.188	.192	.200	.207	.216	.226	.240
	b =	-.432	-.328	-.212	-.0905	0	+.138	+.274
	C =	.184	.180	.175	.170	.165	.159	.153
	x_1 =	.533	.566	.594	.625	.65	.66	.69
1.4	QC =	.193	.197	.203	.210	.220	.231	.244
	b =	-.615	-.516	-.422	-.318	-.234	-.121	0
	C =	.190	.186	.181	.176	.170	.164	.158
	x_1 =	.393	.437	.499	.534	.537	.566	.60
1.34	QC =	.195	.200	.206	.213	.223	.234	.247
	b =	-.761	-.704	-.620	-.534	-.464	-.357	-.270
	C =	.197	.192	.187	.182	.176	.170	.163
	x_1 =	.271	.28	.35	.396	.414	.442	.46

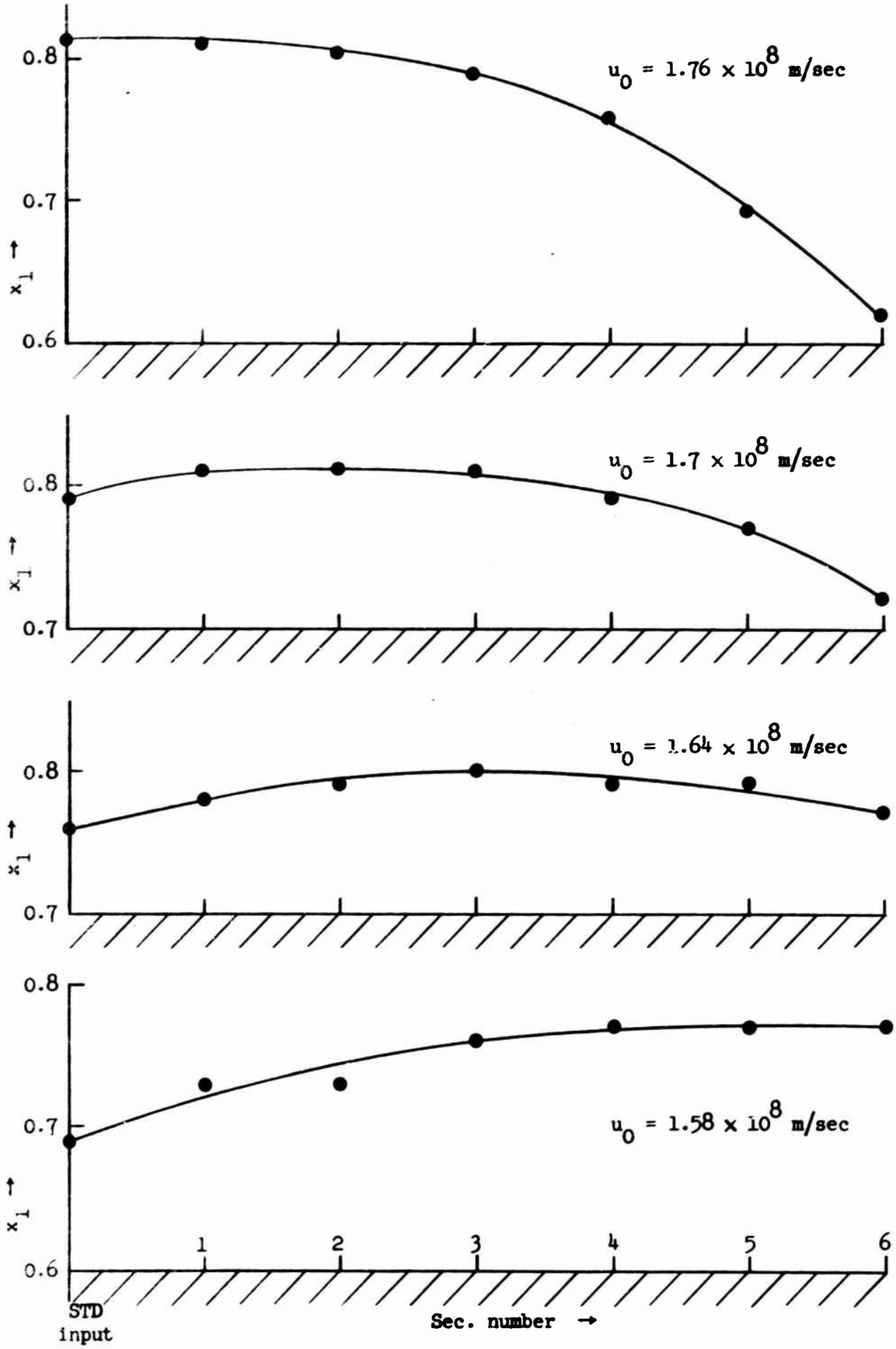

FIG. 2.19a--Forward growing wave gain parameter, x_1, vs section number of the taper for reduced beam velocities.

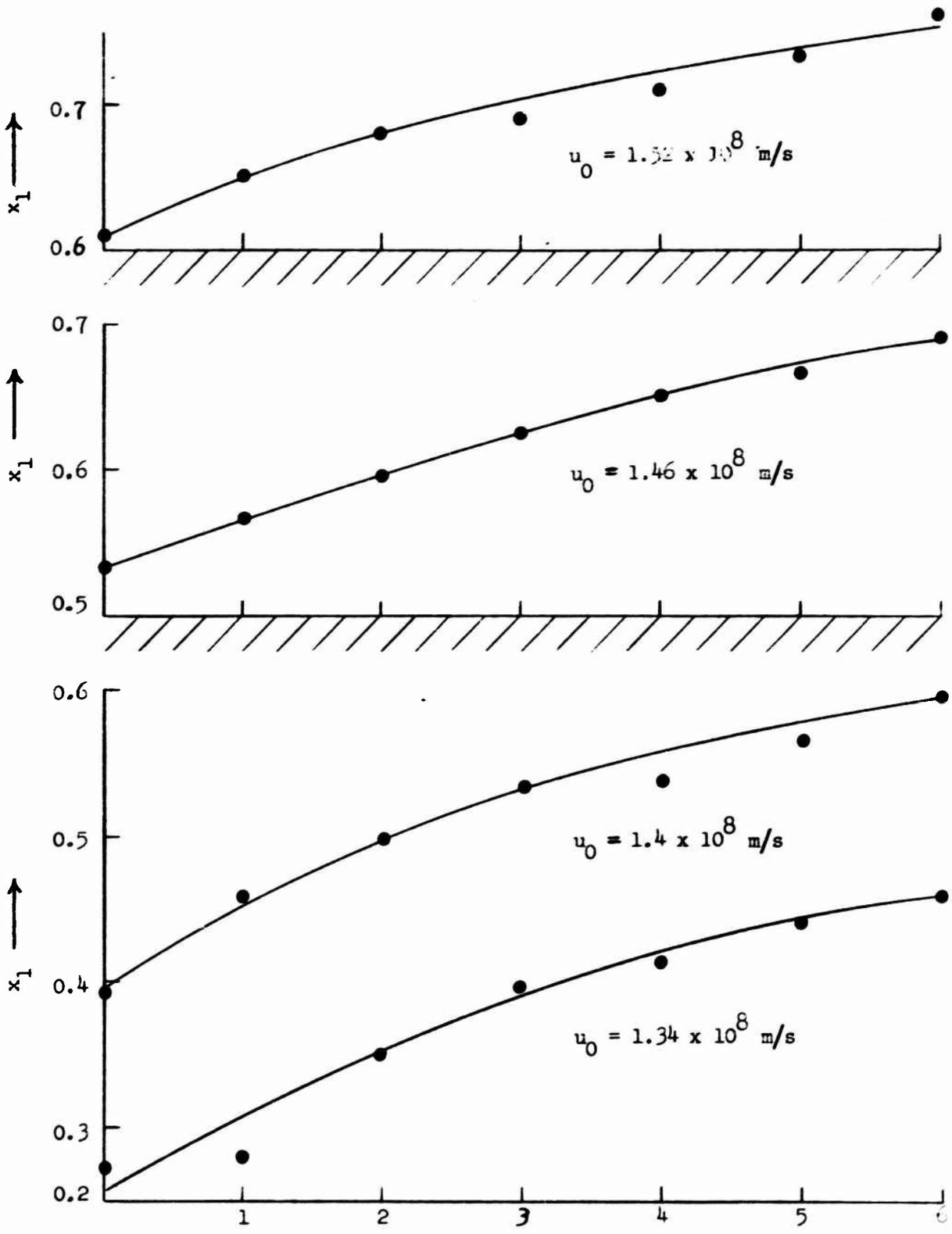

FIG. 2.19b--Forward growing wave gain parameter, x_1, vs section number of the taper for reduced beam velocities.

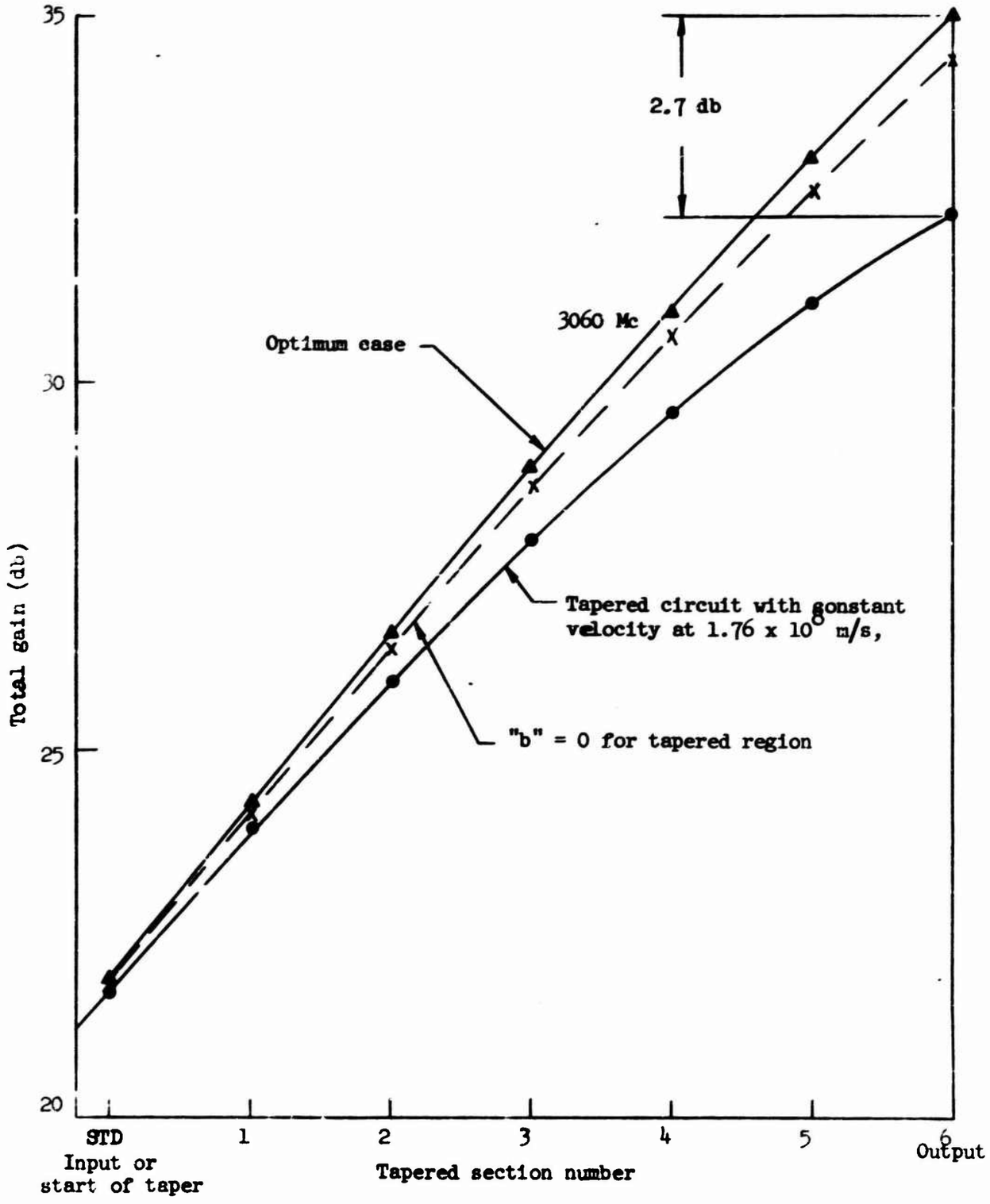

FIG. 2.20--Total gain vs tapered section numbers at 120 kV for f = 3060 Mc/s.

It can be seen from these results that for an observer at the output end of the tube, a 2.7 db gain increase may be observed when the input signal level is increased beyond the small-signal operating values. This means that in the transition region between the strictly small-signal operating and saturation regions the gain of the tube may increase beyond the small-signal value.

The power-in vs power-out curve may have the shape shown in Fig. 2.21. This gain increase property also occurs at other frequencies, though the amount of increase will vary with frequency. At 2920 Mc/s, for example, the same tapered tube gives only a small optimum calculated gain increase of 0.9 db when the input signal level increases beyond the small-signal levels. The results for this frequency are plotted in Fig. 2.22. The total gain of the tube is higher than that at 3060 Mc/s; however, on a graph similar to that of Fig. 2.21, such a small increase may be difficult to notice. One would notice, however, that the linear region extends to within a few db of the saturated output power instead of the usual 10-15 db in an untapered tube.

D. EFFECT OF CIRCUIT TAPERING ON EFFICIENCY

It has been shown in the last section that the improvement on the forward-wave amplification due to circuit tapering when the tube is driven can be approximated reasonably well by direct application of the small-signal theory. However, when studying the efficiency of the tapered tube, such an approach can hardly provide any useful results since the efficiency is measured when the tube is driven to saturation, an entirely large-signal phenomenon. One approach to this problem of estimating the efficiency is to extend the large-signal analysis of the uniform circuit tube to account for the variation of circuit phase velocity in a tapered amplifier.[13,14] But, when dealing with a solid beam untapered tube, the existing large-signal theories[15-20] all show some common deficiencies.

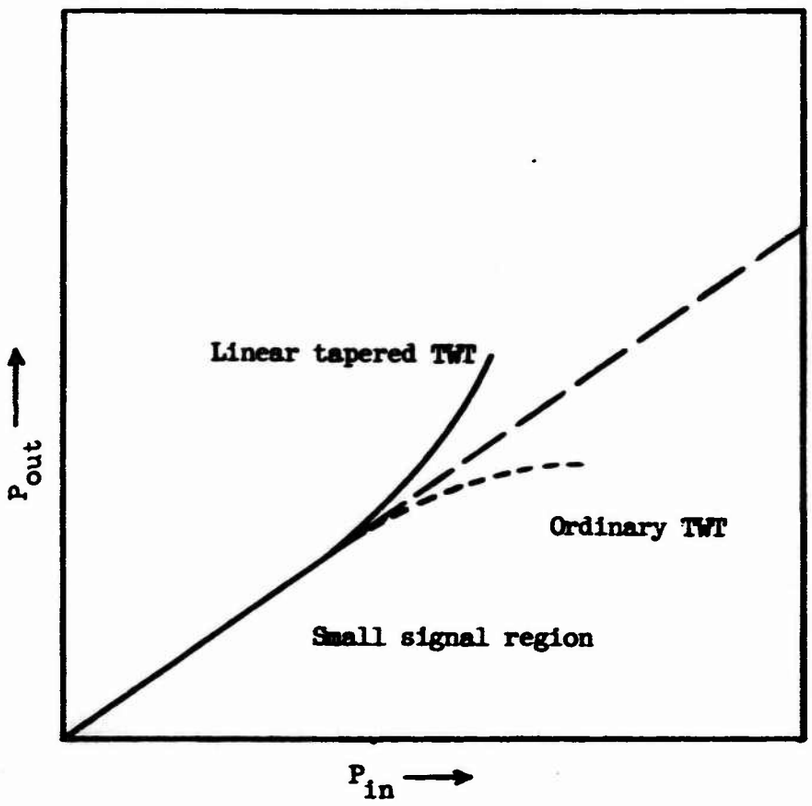

FIG. 2.21--Expected power-out vs power-in curve for the tapered tube as compared with the untapered tube at input power level below saturation.

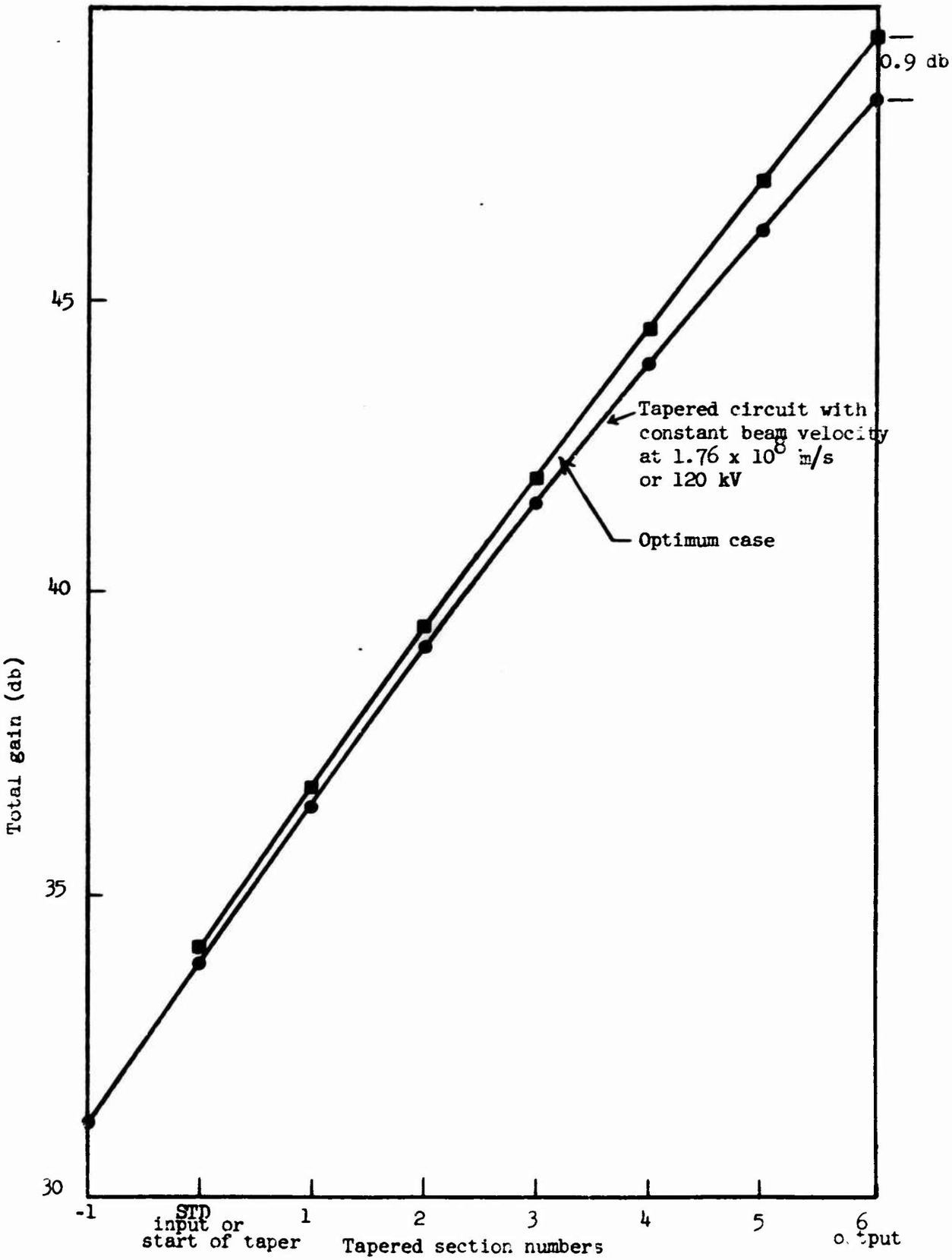

FIG. 2.22--Total gain vs tapered section number at 120 kV for f = 2092 Mc/s.

For instance, as pointed out by Cutler,[5] the calculated efficiency values are, in general, higher than what can be obtained from the experiment. It is mainly because all the large-signal theories are essentially dealing with one dimension only, and consider the circuit field and space-charge force to be constant across the beam. Hence, except for a small beam, or a hollow beam case, all the large-signal theories, though in agreement with each other,[21] can hardly give correct results. In some cases, an error of 25 percent has been observed.[22] Furthermore, for high-power traveling-wave tubes, such as the S-band clover-leaf tube,[23] S-band centipede tube,[7] etc., operating in the megawatt power range, the electron velocity in the tube is comparable with the velocity of light. The relativistic effect can no longer be neglected. But the large-signal theories to date are all based upon a low power as well as low electron velocity tube model, and the relativistic effect is, in general, neglected.(1) To deal with tapered high-power tubes, some modifications to the large-signal theories are inevitable, and more assumptions must be added in order to describe the variation of the circuit tapering. Even if such a modification can be made, it is doubtful whether the results would justify the effort since the results would be only as good as the assumptions.

Fortunately, an empirical study of large-signal behavior of the uniform circuit traveling-wave tube has been successfully carried out. From the results of this study, a qualitative understanding of the effect of circuit tapering on the tube efficiency can be readily derived. On the spent-beam study of a scale model tube, Cutler[22] revealed the nature of tube saturation by interpreting the experimental results in the form of a velocity-phase pattern. A set of such velocity-phase patterns for the small QC case is shown in Fig. 2.23, which is the same as that of Cutler's, except that only six input level cases are presented here. A brief description of these patterns will be given in the following paragraph. However, it is suggested that the readers refer to the original paper by Cutler, since the following paragraph is intended only to refresh the memory of those who are already familiar with the original literature.

---

(1) Exception: J. E. Rowe made some modification to his theory.

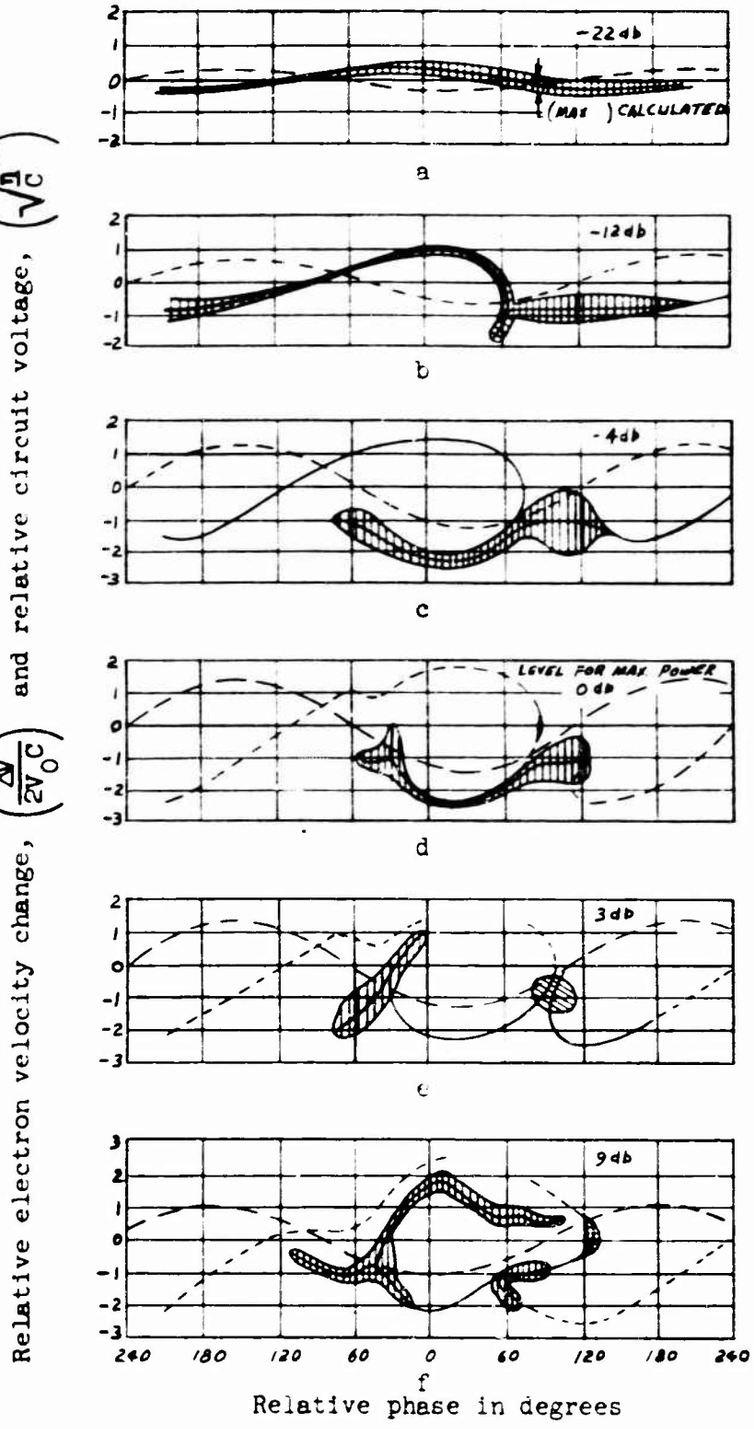

FIG. 2.23--Curves of current and velocity as a function of phase for various input levels. The velocity becomes multivalued at a very low level, a tail forming a nucleus for a second electron bunch which eventually caused saturation in the output. For this run C = 0.1, QC = 0.06, γr_0 = 0.4 and b = 0.26

In Fig. 2.23, the corresponding change in voltage of the relative electron velocity change and the inverted relative circuit voltage (i.e., dashed sinusoidal-like curve in the figure) were plotted against the relative phase angle. The solid line patterns represent the ac velocity, and the shaded area represents the charge density corresponding to that velocity. Thus in each pattern one can get a complete story of electron velocity, current density and circuit voltage as a function of phase, for a particular signal input level. The case shown in Fig. 2.23 is for a tube with $C = 0.1$, $QC = 0.06$, $\gamma r_0 = 0.4$ and $b = 0.26$. An unmodulated electron beam enters the circuit field at the input end of the tube, and the electrons are accelerated or decelerated according to their phase relative to the wave. Figure 2.23a shows a typical low level or linear case with input power 22 db below the input power for saturation output. Although this velocity-phase pattern was measured at the output end of the scale model tube, it can also be considered as that existing somewhere near the input end when the output end of the tube is at saturation. This is because in a traveling-wave tube the power gain is a function of the length along the tube. Therefore, velocity-phase patterns for different drive levels can be considered as the velocity-phase patterns in different locations along the tube. After the beam travels a distance from the input end of the circuit, the electrons in the beam consolidate into a short phase interval in the decelerating phase region, as shown in Fig. 2.23b which corresponds to an input drive level of +12 db below saturation drive. At this location, or corresponding drive level, the nonlinearity in the beam is evident, and the velocity and current are no longer sinusoidal. Furthermore, a spur in the velocity curve is clearly shown, and a definite nonsinusoidal bunching exists in the retarding field region. As the beam is traveling further toward the output end of the tube, such as shown in Fig. 2.23c, which corresponds to a drive level 4 db below the saturation drive level, the electrons in the retarding field region consolidate into even shorter phase intervals. However, more electrons bleed into the spur which, in turn, has penetrated into the accelerating phase region. It is interesting to note that the electron velocity in the phase region between 60° to 180° has not changed significantly. This can be true only if the space-charge field just compensates

for the circuit field, such that the total decelerating field is zero. However, near the spur, the space-charge field is apparently reversed according to the evidence of the sharp deceleration and the forming of the spur. As the beam travels further down the tube, more electrons are bled into the acceleration phase and form another electron bunch in the accelerating phase region. Evidently, a few electrons in the right-hand tip of the electron bunch in the decelerating phase region can no longer find the space-charge field sufficient to balance the circuit field, and they are decelerated into a second low velocity loop. As the beam reaches a location corresponding to saturation drive level, i.e., 0 db, as shown in Fig. 2.23d, more than 95 percent of the total electrons are consolidated into two equal bunches with opposite phases, such that the energy given up to the circuit wave at the decelerating phase region is at the same rate as the energy absorbed by the electrons from the circuit wave at the accelerating phase region. Therefore, a power balance is actually formed in the tube. At even higher drive levels, such as shown in Figs. 2.23e and f, electrons continue to bleed from the decelerating phase bunch to the accelerating phase bunch. The bunch in the accelerating phase region develops further into two parts. One part is accelerated ahead into a new spur, and another falls further back in phase. For an even higher drive level, the pattern becomes too complicated and is utterly indescribable.

At the saturation level, most electrons are in two bunches in the opposite phases. Thus the efficiency of the tube can be determined very closely by the velocities of the electrons in the two bunches provided that all the kinetic energy lost by the electrons is converted into rf energy in the circuit wave. For instance, in the example cited in Fig. 2.23, the two bunches have nearly the same velocity change of -1.1 at saturation level, i.e.,

$$\frac{\Delta v}{2V_0 C} = -1.1$$

Then the efficiency of the tube should be nearly

$$\eta = \frac{\text{RF Power Output}}{\text{DC Power Input}} = \frac{\Delta V}{V_0} = -2.2C \quad ,$$

where C is Pierce's gain parameter.

Therefore, if a taper is properly designed to increase the efficiency, then at saturation the velocity-phase pattern at the output end of the circuit will have a much larger value of $\Delta V/2V_0C$ for the two bunches with opposite phases than that obtainable from the corresponding untapered tube, that is, a uniform circuit tube built with a circuit identical to that used in the untapered portion of the tapered tube.

In order to understand the effect of the circuit tapering on the efficiency, or equivalently on the velocity-phase pattern, let us consider the change in the phase angle due to circuit phase velocity tapering. Figure 2.24 shows a time vs distance plot. The phase velocity is represented by dz/dt in the figure. For a constant phase velocity, such as in a uniform circuit tube, or in the untapered part of a tapered tube, the phase velocity can be represented by a straight line with constant slope, as v_{p1} in Fig. 2.24, which represents the phase velocity of the untapered part of the circuit. When reaching the tapered part of the circuit, the phase velocity changes to a lower value; therefore, the slope of the line will also be changed, such as the change in the v_{p2} line shown in the figure.[1] Since $v_{p1} > v_{p2}$, the new line will lie below that of the v_{p1} line. When the phase velocity is going through a further decrease in value, the slope of the line in Fig. 2.24 will have additional changes. For $v_{p1} > v_{p2} > v_{p3} > v_{p4}$, the changes are represented in Fig. 2.24, respectively.

Due to the decrease in phase velocity, Pierce's velocity parameter b and the axial phase constant β will also have consequential changes.

---

[1] In an actual tapered tube, the phase velocity in the tapered region will not have the abrupt changes as shown in Fig. 2.24. This is because the clover-leaf cavities are closely coupled together. Hence the change in phase velocity should be smooth. The purpose of Fig. 2.24, however, is only intended to serve as a qualitative illustration. Therefore, by representing the changes as shown in the figure it does not deteriorate the generality.

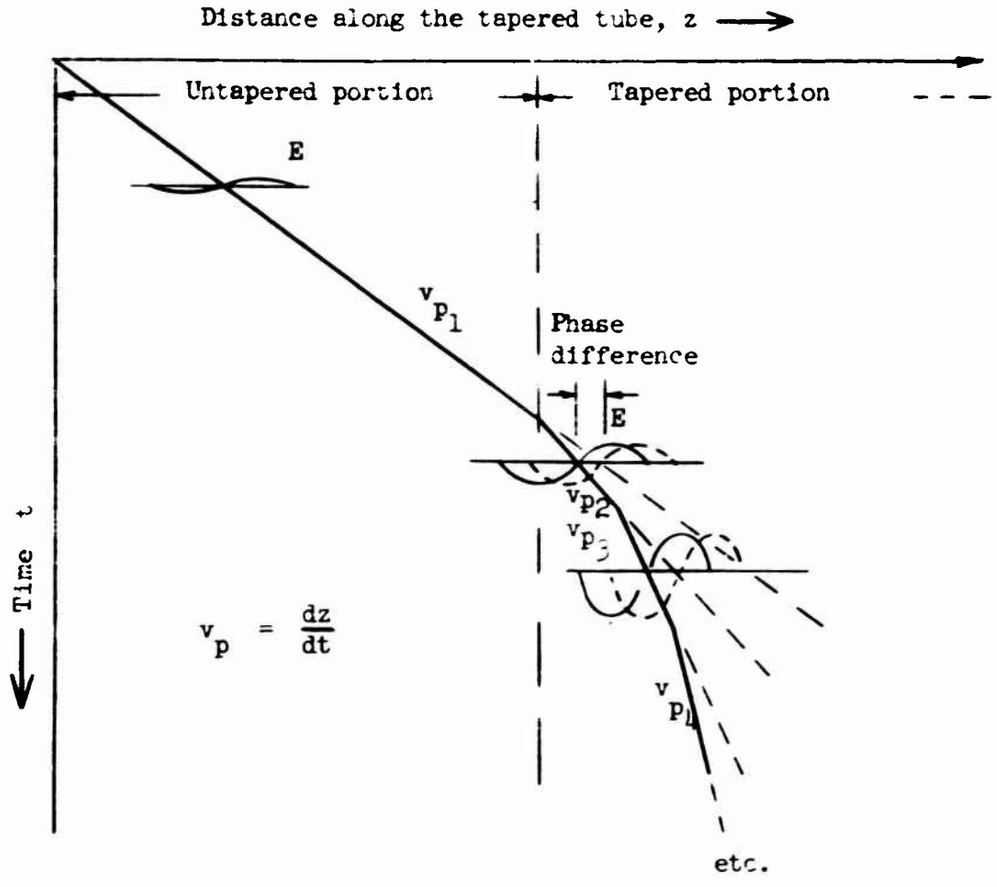

FIG. 2.24--Time-distance plot along a tapered TWT where $v_{p_1} > v_{p_2} > v_{p_3} > v_{p_4}$ ..., etc.

Hence, to an observer in the original phase velocity frame, the change in phase velocity corresponds to a shift in phase angle. This is also represented conceptually by the small waveforms superimposed on the phase velocity line in Fig. 2.24. It can be seen from the figure that as the phase velocity is decreased, the waveform will shift to the left in the original phase velocity frame. In the velocity-phase diagram, a decrease in circuit phase velocity also corresponds to a shift of circuit field to the left. A typical example is shown in Fig. 2.25, which represents a velocity phase diagram viewed at the junction between the uniform and tapered portions of a tube at a certain input drive level. However, instead of circuit voltage, circuit field intensity is plotted. The solid line denoted by E is the field intensity in the original phase velocity frame. In other words, it forms the pattern in a uniform circuit tube at the same location with the same input drive level. In a tapered tube, the electrons can only see a retarded field shifted to the left of the pattern of the original phase velocity frame, indicated by the broken line marked E′ in the figure. Hence, the field situation in the beam will be altered. For instance, at the phase angle just to the right of the spur, the retardation field is increased due to the shift of the field as shown in Fig. 2.25. Therefore, the aforementioned balance between the circuit field and the space-charge force can no longer be held, and a net decelerating field will result. Consequently, the velocity line at this phase interval will be moved into a lower velocity region. If a taper is properly designed, the electrons in the main bunch will be decelerated into lower and lower velocity regions when the beam travels closer and closer to the end of the tapered tube. Finally, when reaching saturation, the two bunches of electrons in opposite phases will have a much higher value of $\Delta V/2V_0C$, and therefore will have higher efficiency.

However, a proper taper is very difficult to obtain. In the following paragraphs we will consider several factors which complicate the design of the taper.

Cutler showed in his paper[5] that when the space-charge factor QC increases, the electrons in the beam will not consolidate into a short phase interval, such as in the case shown in Fig. 2.26 for $QC = 0.48$ at saturation. Thus, when the beam enters the taper, we encounter a

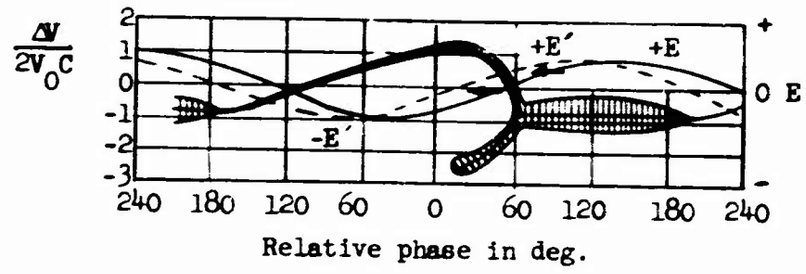

FIG. 2.25--Velocity as function of relative phase, where E is uniform circuit field, E′ is tapered circuit field, and $\Delta V/2V_0C$ is relative electron velocity change.

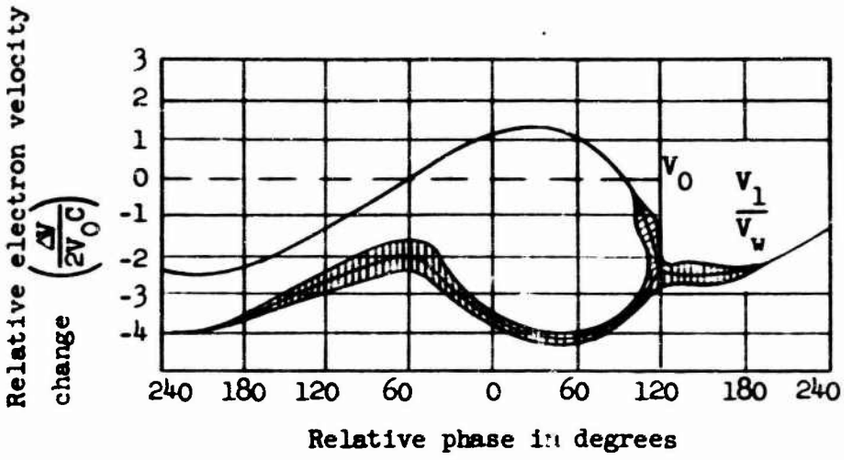

FIG. 2.26--Phase-velocity for QC = 0.48.

serious problem immediately That is, even he electrons near the spur are decelerated into a lower velocity region and the right hand tip of the main bunch may be accelerated into a higher velocity region. In other words, even though some of the electrons lose much more kinetic energy to the circuit wave than in the untapered case, other electrons will again take it back from the circuit. Consequently, the efficiency may not be improved but the velocity-phase pattern will be much disturbed.

In addition to the space-charge parameter QC , the starting position of the taper, the rate of tapering, and the length of the taper all play vital parts in the successfulness of a taper Let us refer back to Fig. 2.23 If a taper starts too soon, for instance as in Fig 2.23b, we will run into a similar difficulty as in the high QC case. And if the taper starts too late, such as in Fig. 2.23c, too many electrons are already in the accelerating phase region Then the saturation will soon be reached, when the velocity of the electron bunch in the decelerating phase region is only decreased a small amount. The efficiency, therefore, can only be improved by a small amount. As mentioned earlier, a properly designed taper should be able to decelerate the electrons into lower and lower velocity regions. In other words, each cavity in the taper should have an additive effect to the preceding cavity In order to achieve such a taper, the rate of circuit tapering must be proper. If the circuit tapering is too slow, the balance between the circuit field and the space-charge force is disturbed so little that hardly any improvement on the efficiency can be accomplished. If the tapering is too fast the E-field is decreased so much for the part of the main bunch in the decelerating phase that the space-charge force can no longer be balanced out. This means that the electrons in this region may be speeded to a higher velocity, thus deteriorating the efficiency. The rate of tapering may need to change from cavity to cavity, since the velocity-phase pattern will be changed due to both the power gain and the circuit tapering The effect of the length of the taper is essentially the same as the starting point of the taper, but in some cases, it is different, for instance, in the case of a taper designed to serve more than one purpose, such as to improve the efficiency and the stability

Circuit tapering for improved efficiency has been studied experimentally by several authors.[13,24,25] However, to the knowledge of the author, no optimum design has been achieved.

The experimental tapered tube studied in this paper is used mainly for eliminating the pulse-edge oscillations, and the tapering in the forward-wave interaction region is purposely made small, so no efficiency improvement is expected from this tube.

CHAPTER III

DESIGN OF A LINEARLY-TAPERED TUBE

A. INTRODUCTION

In the previous chapters various types of circuit tapering have been discussed, and their effects on the tube performance have been predicted from a theoretical point of view. In order to verify these predictions empirically, a tapered tube with a six-cavity linearly-tapered chain was used. In this chapter, the design of this tapered circuit as well as the design of other components of the tapered tube are given in more detail. The methods used to measure and to evaluate various parameters are also described and the results are presented. The properties of this tapered circuit have been cited in earlier sections to illustrate various effects of circuit tapering, and in some cases, such as in the study of backward-wave oscillations, and in forward-wave amplifications, quantitative estimates have been obtained.

B. TAPERED CIRCUIT DESIGN

There are many high-power TWT circuits which could be used in constructing a tapered tube to evaluate the effects of circuit tapering on tube performance. However, after comparing various properties of these circuits, it is found that the well-known clover-leaf structure has several advantages over the other circuits. An obvious one is that this circuit has a comparatively simple construction and a very simple relationship exists between its electrical characteristics and its physical dimensions. In addition, cold circuit characteristics as well as test results from an untapered tube built with such circuits are available for comparison.[26]

In an earlier work of Craig,[26] it was found that the π-mode cutoff frequency f_π of the clover-leaf fundamental passband is related to the

central aperture diameter of the structure by a simple cubic equation

$$f_{\pi} = k + qd^3 \quad , \tag{3.1}$$

where d is the central aperture diameter, q is the dimension conversion factor, and k is an empirical constant with dimension of frequency. This is consistent with the predictions of Bethe.[27] For circuit dimensions shown in Fig. 3.1, k was found to be 3280 Mc/s. On the other hand, the 0-mode cutoff frequency of the passband is related to the slot length S.L. in a linear manner, shown in the figure, provided the change is made at the inner end of the slot. A general example of such a variation is shown in Fig. 3.2 which was measured from a structure consisting of several clover-leaf cavities. If a change is made on the section length, then both the π-mode and 0-mode cutoff frequencies will be varied. An example of such a variation is shown in Fig. 3.3 where the section length is decreased successively from L_1 to L_5, and the 0-mode and π-mode frequencies are pushed further apart. Hence, by varying these three dimensions properly, a prescribed tapered circuit could be obtained.

The first problem encountered in the course of designing the experimental tapered tube is to determine the kind and the amount of circuit tapering needed. Since the main purpose of this tube is to evaluate the effect of circuit tapering on the pulse-edge oscillations, the tapering scheme shown in Fig. 2.5 (which provides both upper cutoff frequency tapering and phase velocity tapering) appears to be an adequate one. For ease of identifying the effect of circuit tapering from tube test results, a tapered circuit with linear changes in both upper cutoff frequency and cavity heights with the manner shown in Fig. 2.5 is desirable.

In the study of electron distribution in a spent beam at saturation level, Yadavalli[28] showed that, for a uniform circuit TWT built with cavities identical to the untapered cavities used in the linearly tapered tube, the electrons in a saturated electron beam have a distribution in velocity as shown in Fig. 3.4. The electron velocities in the figure are indicated by beam voltages which are normalized to the injection beam voltage, V_0, which is 125 kV in this case.

From this distribution one can see easily that at the saturation level most of the electrons in the beam possess a velocity corresponding to $0.63\ V_0$.

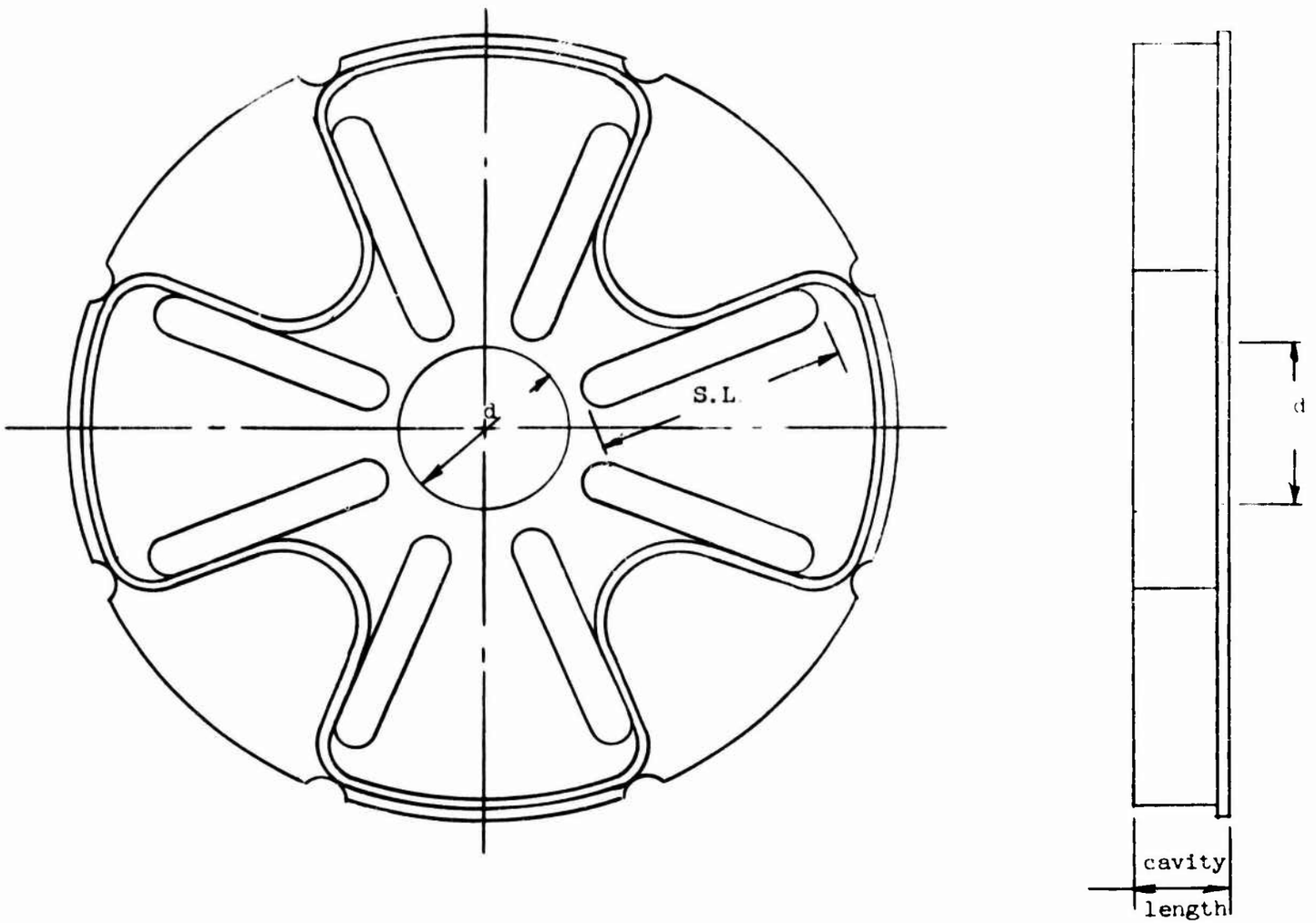

FIG. 3.1--Typical untapered cavity for linear tapered TWT, with S L = $1\frac{1}{2}$ in., d = 3/4 in., cavity length = 3/4 in.

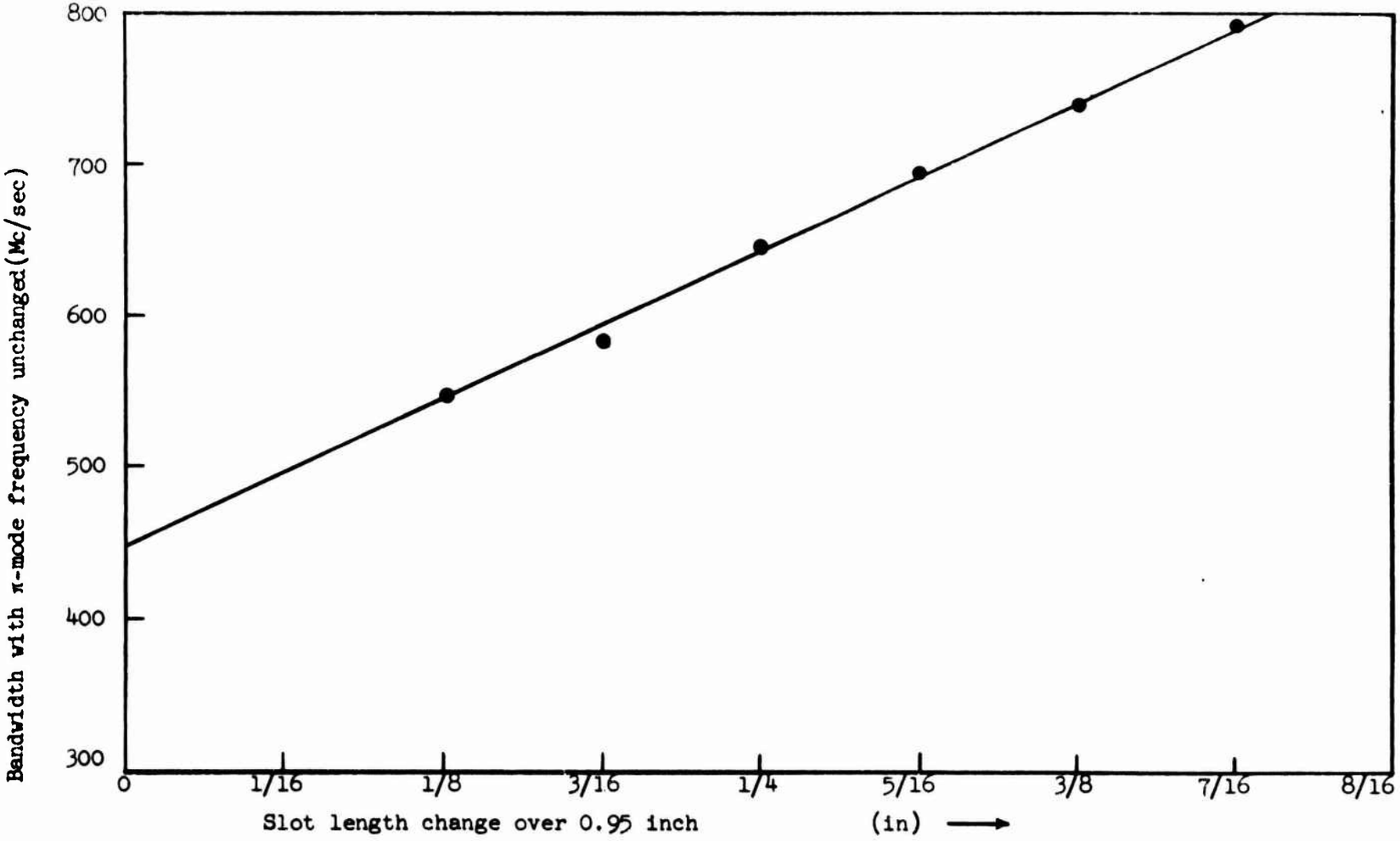

FIG. 3.2--0-mode cutoff frequency as a function of slot length change at the inner end.

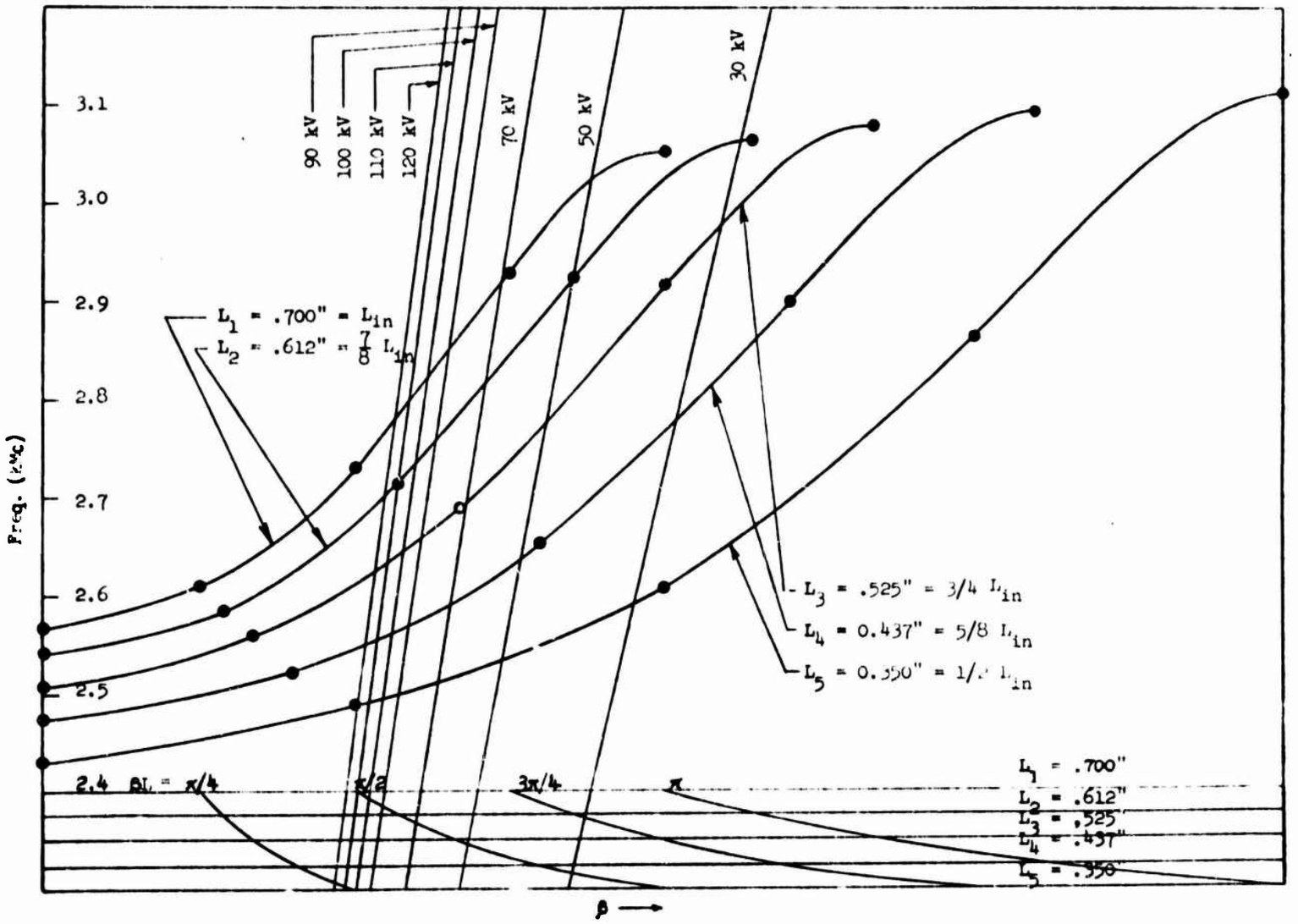

FIG. 3.3--Variation in ω-β diagram as cavity length changes.

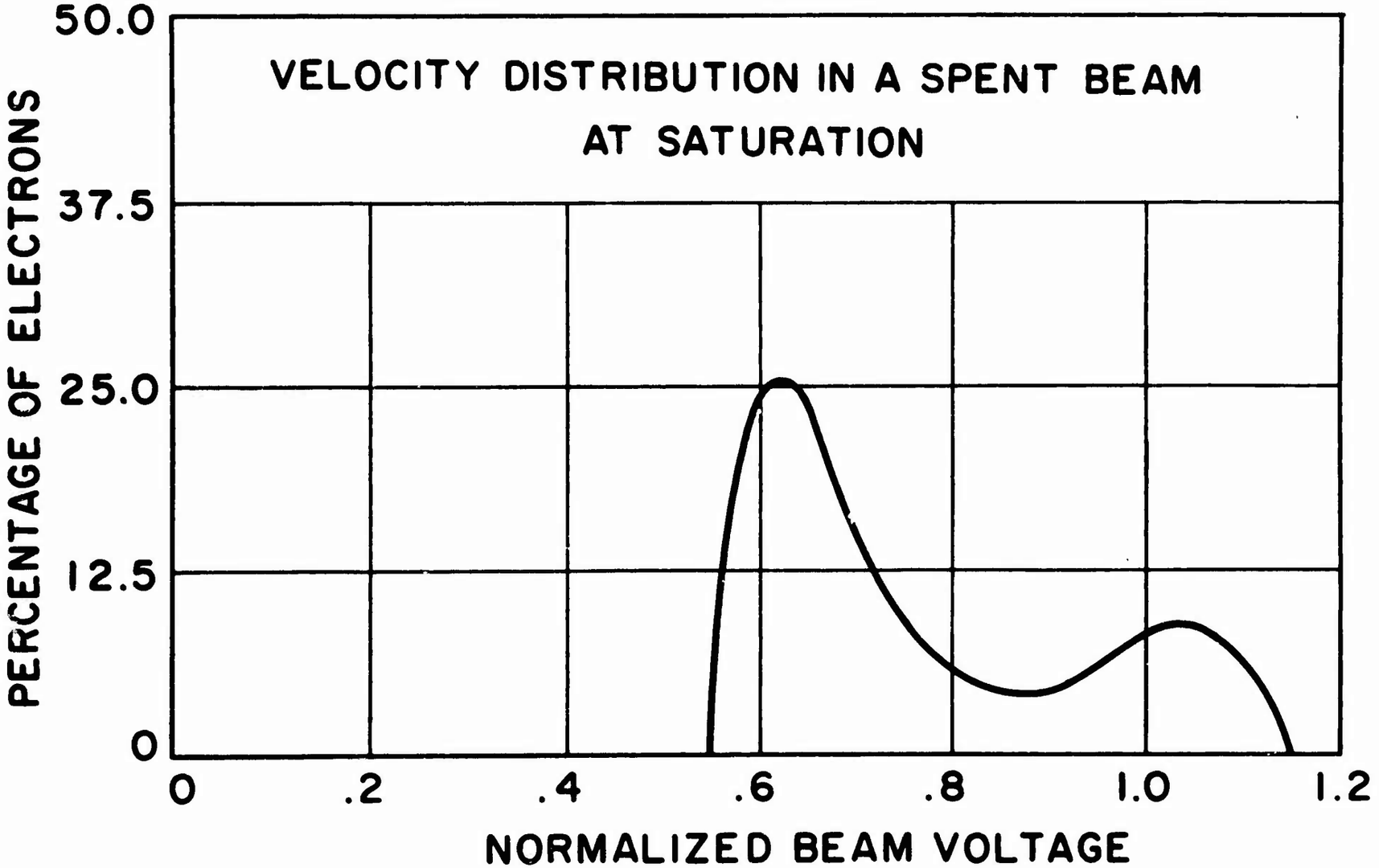

FIG. 3.4--Velocity distribtuion in a spent beam at saturation. All beam voltages in the figure are normalized to the operating beam voltage at 125 kV.

If a similar situation exists in the tapered tube and the velocity spread of nearly the same order is maintained, then by tapering the phase velocity in the forward-wave region of the clover-leaf structure down to this value at synchronous frequency, the forward-wave interaction could be enhanced due to the improvement of synchronism conditions near saturation. But, at the pulse-edge oscillation frequencies, the circuit phase velocity should be tapered more, such that the circuit wave is slowed more than the beam, and the interaction for pulse-edge oscillations becomes so weak that oscillation can not be built up as discussed in Chapter II.

In the actual linearly tapered circuit design, the desired circuit tapering is achieved by changing the dimensions of the central aperture, the cavity height, and the slot length of the clover-leaf structure. By enlarging the central aperture successively, the upper cutoff frequency of the fundamental passband is increased by a total amount of 100 Mc/s for the six-cavity linear taper, at a constant rate of increase of 16.67 Mc/s per cavity. The cavity height is decreased from the untapered value of 3/4 in. successively to a final value of 5/8 in. as shown in Fig. 3.5. The total decrease is about 16.7 percent of the original cavity height. At the same time, the slot length is decreased successively in order to maintain the lower cutoff, or the 0-mode frequency at the same value for all cavities in the taper, for the reasons already stated in Chapter II. By making the above dimension changes, a six-cavity taper with a dispersion in Fig. 2.5 is achieved. The measured ω-β diagram and the cube root of interaction impedance, $E^2/2\beta_p^2$, are shown in Figs. 2.7 and 2.8, respectively.

C. "COLD" CIRCUIT MEASUREMENTS[29] AND EVALUATION OF PARAMETERS

In the measurement of the "cold" circuit characteristic of a tapered slow-wave structure, the conventional cold test measurement techniques can no longer be used because the periodicity requirement necessary for the application of these techniques is not fulfilled any more in the tapered circuit case. However, for a smooth and gradually tapered circuit, a good approximation can be obtained by interpolating the results from the measurements made by considering each cavity of the tapered circuit discretely. In practice, such results can be obtained by measuring the characteristics of structures consisting of cavities identical to each of

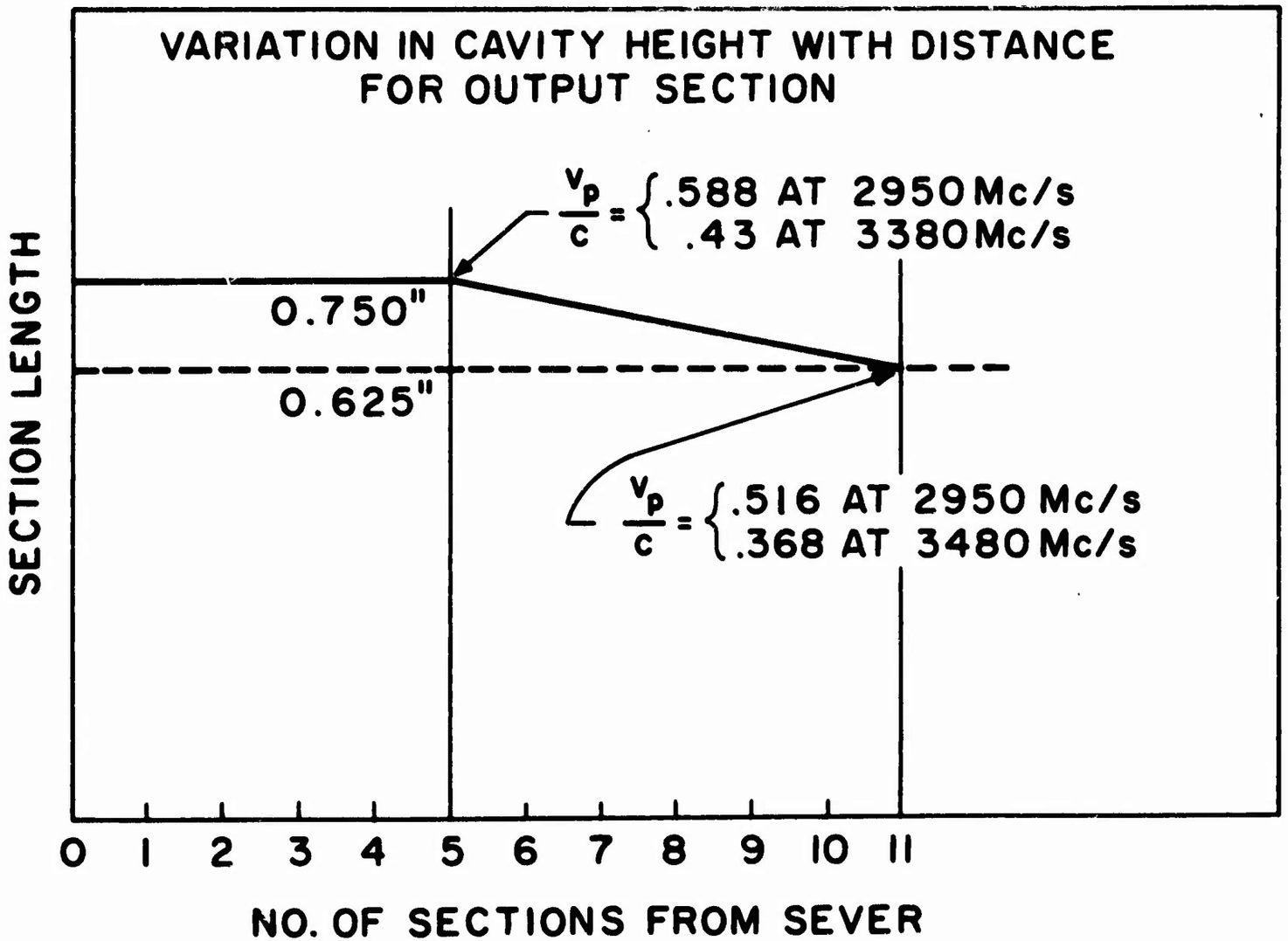
VARIATION IN CAVITY HEIGHT WITH DISTANCE
FOR OUTPUT SECTION
$\frac{V_p}{c}$ = {.588 AT 2950 Mc/s
.43 AT 3380 Mc/s
0.750"
0.625"
$\frac{V_p}{c}$ = {.516 AT 2950 Mc/s
.368 AT 3480 Mc/s
SECTION LENGTH
0 1 2 3 4 5 6 7 8 9 10 11
NO. OF SECTIONS FROM SEVER

FIGURE 3.5

the tapered cavities by the usual uniform circuit techniques. Figure 2.12 shows such measurement for the linearly tapered circuit herein proposed. The ω-β diagram marked "input" is measured from a structure consisting of six cavities identical with the untapered cavities of the tube, whereas the "output" curves are obtained from another structure consisting of six cavities identical to the last cavity in the tapered circuit. These two sets of curves form the upper and lower bounds for the characteristics of all the tapered cavities. In other words, any intermediate cavity should have a similar dispersion curve lying somewhere between these two extremes. In order to check the linearity of the tapered circuit, structures made of identical intermediate tapered cavities have been measured. The results from such measurements showed good linearity of this taper.

The phase velocity normalized to the electron velocity at the normal operating voltage of 125 kV of the forward-wave and the backward-wave of the "input" and "output" curve as a function of frequency in the fundamental passband is shown in Fig. 3.6. The velocity distribution curve of Fig. 3.4 is also reproduced and superimposed on the figure, so that one can easily compare the electron velocity spread in the saturated beam with the phase velocity at the synchronous frequency corresponding to 125 kV. However, attention must be given to making the comparison in the figure, since the abscissa represents different things for these two families of curves. For a quantitative comparison of the phase velocity in the forward-wave and the backward-wave regions of the fundamental passband, the total change of phase velocity through the tapered circuit as a percentage of the phase velocity in the uniform circuit for both waves is plotted as a function of frequency in Fig. 3.7. It can be seen from this figure that the phase-velocity tapering for the backward-wave increases linearly as the frequency approaches the π-mode cutoff frequency of the uniform circuit. Such an increase in phase velocity tapering, as analyzed in Chapter II, should have a pronounced effect on the backward-wave oscillations which usually exist in this frequency region in a uniform circuit case. In the mid-band frequencies of the forward-wave fundamental passband, the phase-velocity tapering is nearly constant with frequency, consistent with the design value previously discussed. This result indicates that the forward-wave interaction of the tube may be enhanced in this band of frequencies by the tapered circuit.

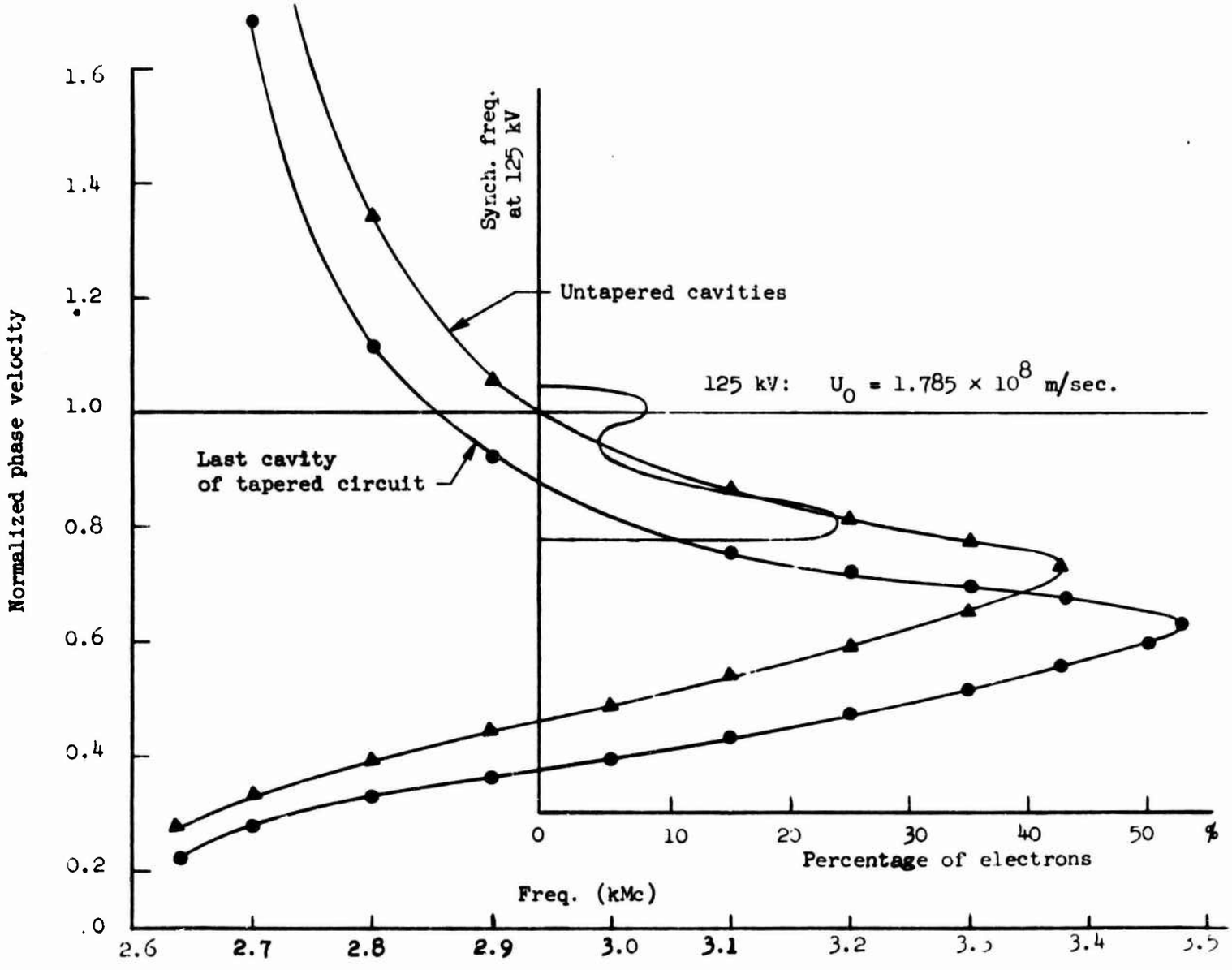

FIG. 3.6--Frequency and electron percentage at saturation as functions of normalized phase velocity. All the phase velocities are normalized to beam velocity at 125 kV.

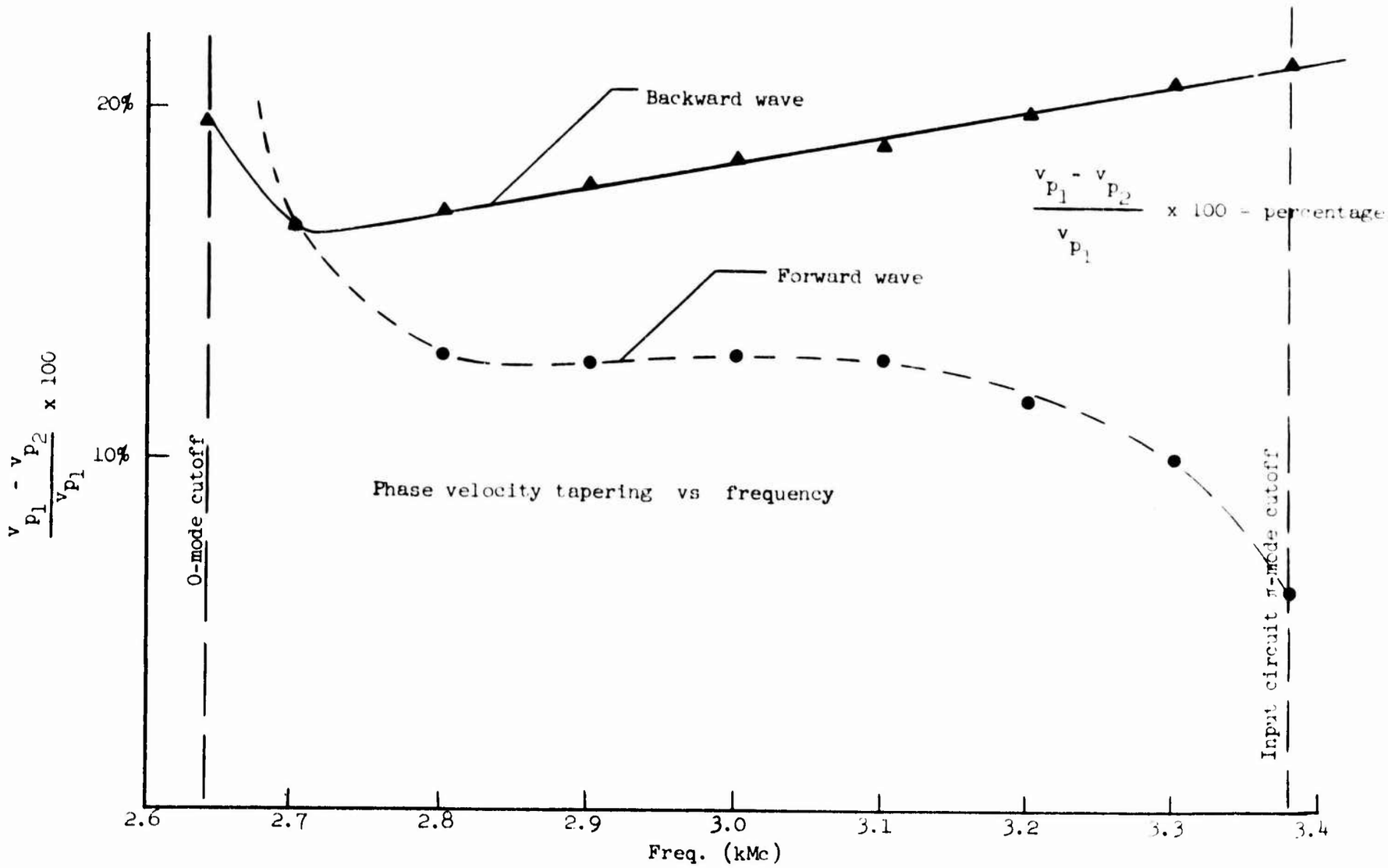

FIG. 3.7--Phase velocity tapering for both the forward and the backward wave as a function of frequency.

The frequency perturbations measured in structures consisting of identical untapered cavities and of identical cavities the same as the last cavity in the tapered circuit are shown in Fig. 3.8. These results are obtained by the usual perturbation techniques.[29,30,31]

A uniform sapphire rod of 0.100 in. diameter was used to perturb the axial E-field in a structure consisting of several identical cavities. The frequency perturbation Δf so obtained and the values calculated at the edge of the central aperture of the clover-leaf circuit are normalized to the corresponding mode resonant frequencies f, and are plotted vs frequency in the figure. These two sets of curves, marked "input" and "output," respectively, again form the upper and lower bounds of all the values obtainable from the intermediate cavities in the taper. The calculation of the frequency perturbation at the edge of the central aperture is made because the diameters of these apertures are progressively increased as one proceeds toward the end of the tapered tube. It is more reasonable to compare the fields at this position because the electron beam normally spreads at high modulation levels and will always nearly fill the holes. One may note from this figure that the difference in frequency perturbation between "input" and "output" curves is not great. Therefore the effect on the gain parameter, C, is small since the cube roots of $\Delta f/f$ are involved in obtaining this parameter.

From these frequency perturbation measurements, and the ω-β diagrams shown in Fig. 2.12, various TWT small-signal parameters can be deduced for the untapered cavities and the last cavity in the tapered circuit. These two sets of parameters will again form the lower and upper bounds for the parameters of the intermediate cavities in the taper. The detailed procedure for evaluating these parameters will be presented in the Appendix. A summary of the computational results is given in Table III.1, where b is the velocity parameter which is defined as

$$\frac{u_0}{v_p} = 1 + Cb \quad ,$$

where u_0 is the beam velocity, and v_p is the circuit velocity. The

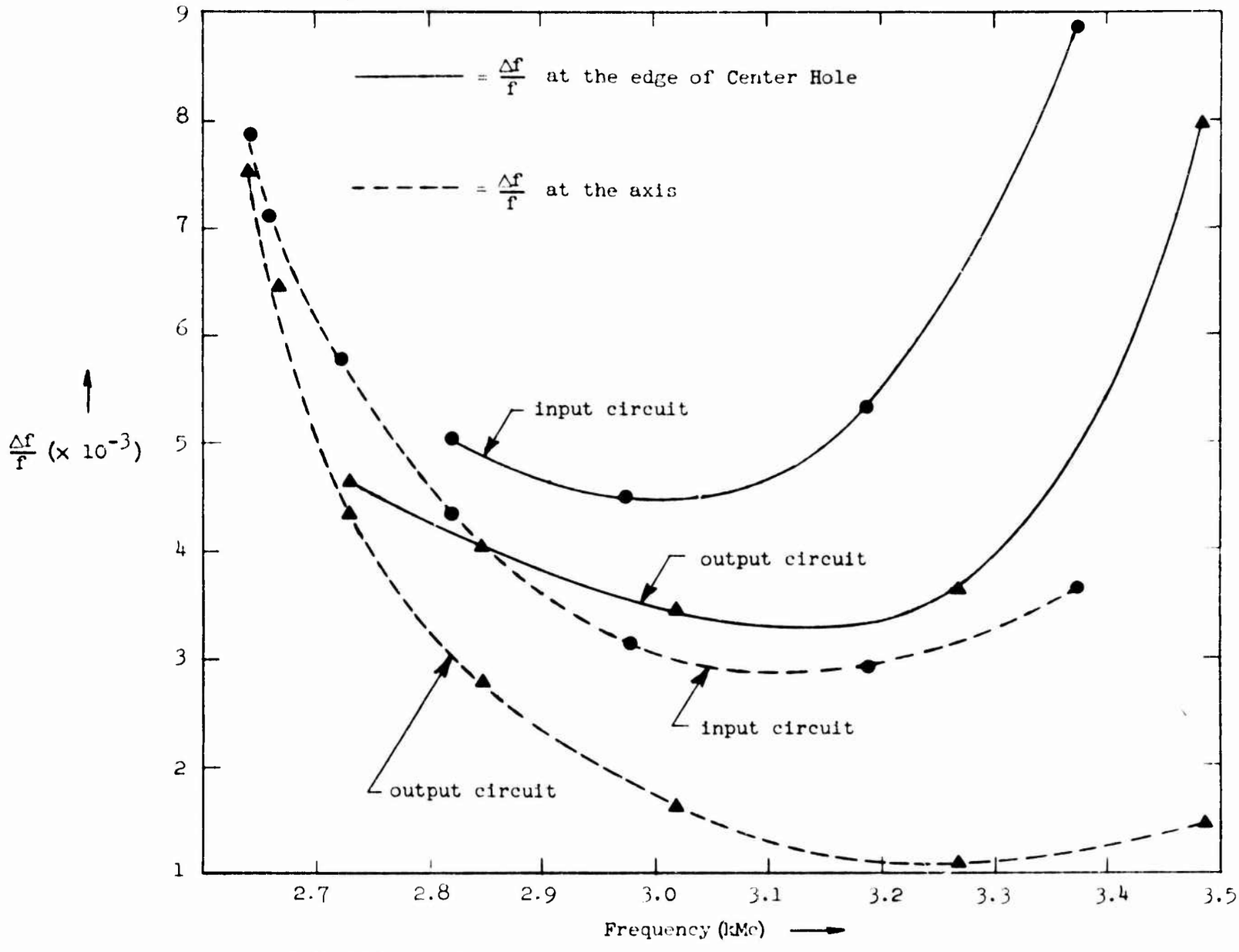

FIG. 3.8--$\Delta f/f$ vs frequency for tapered sections

TABLE III.1

SMALL-SIGNAL CIRCUIT PARAMETERS
OF LINEARLY TAPERED CIRCUIT
AT BEAM VOLTAGE 120 kV
(Constant beam velocity)

A. Untapered Cavities

f	C	QC	b	BC/section
2822	0.27	0.065	-0.72	3.46
2977	0.18	0.19	0.12	2.50
3187	0.14	0.24	1.55	1.96
3295	0.13	0.22	1.92	1.55

B. Cavities Identical to the Last Cavity of the Tapered Circuit

f	C	QC	b	BC/section
2822	0.283	0.04	0.265	3.8
2977	0.15	0.136	-1.03	0.94
3187	0.107	0.255	-2.52	0
3295	0.1	0.28	-3	0

QC is the space charge-parameter defined as

$$\sqrt{4QC^3} = \frac{\omega_q/\omega}{1 + \omega_q/\omega} \quad ,$$

where ω_q is the modified plasma frequency, and BC is the gain parameter defined as

$$B = 54.6\, x_1 \quad .$$

D. TAPERED TUBE COMPONENTS DESIGN

Two versions of a linearly tapered tube have been tested. The first version consisted of sixteen untapered cavities and six linearly tapered cavities. The slow-wave structure was severed at the middle by means of an attenuator and decoupling plate as shown in Fig. 3.9. The attenuator disks were made from carbonized ceramics and when used in conjunction with a special housing provided a good termination to the circuit over a broad frequency range. The structure on the left in Fig. 3.10 is one of the two matching structures, or the housings at each side of the sever. The one shown on the right is the carbonized ceramic disk and decoupling plate assemblage. The drift tube shown in the center of the structure is also used to prevent direct beam bombardment on the ceramic disks. This sever and network divides the tube circuit into two isolated parts as shown in Fig. 3.9; the input part consists of eleven untapered cavities and the output part consists of five untapered and six linearly tapered cavities. Also indicated in the figure are the cavities attenuated by lossy rods and Kanthal, a lossy metal, which has been sprayed on the inner surfaces. The lossy rod provides more attenuation in the higher passbands than in the fundamental. For the second higher passband near 5400 Mc/s, a cavity loaded by four of these rods provides 1.7 db loss as compared to 0.4 db loss in the amplification band. The construction of such a cavity is shown in Fig 3.11. In addition, Kanthal is sprayed over cavities to minimize any reflection from either the rods or from the disk termination

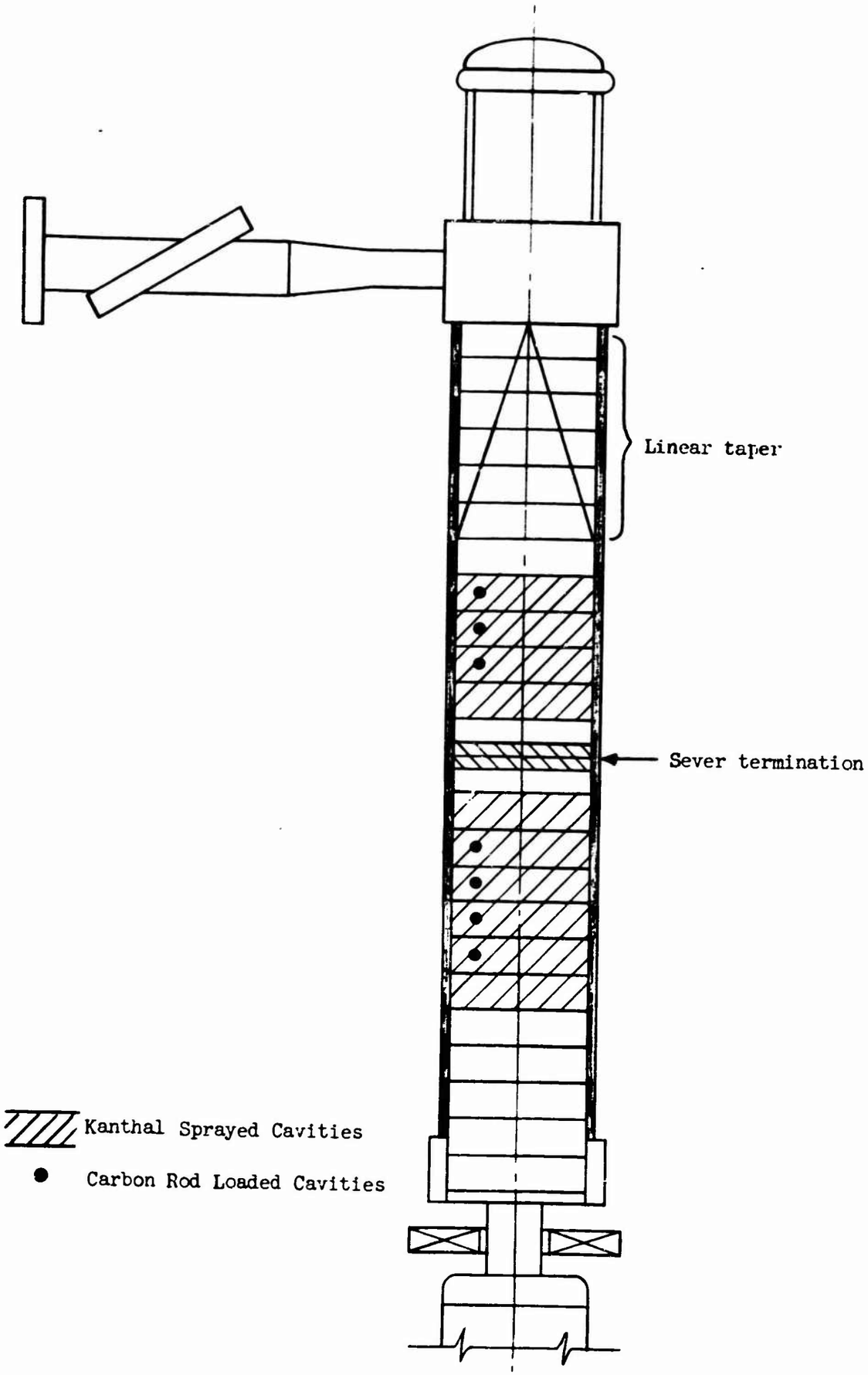

FIG. 3.9--Distribution of loss in tapered TWT.

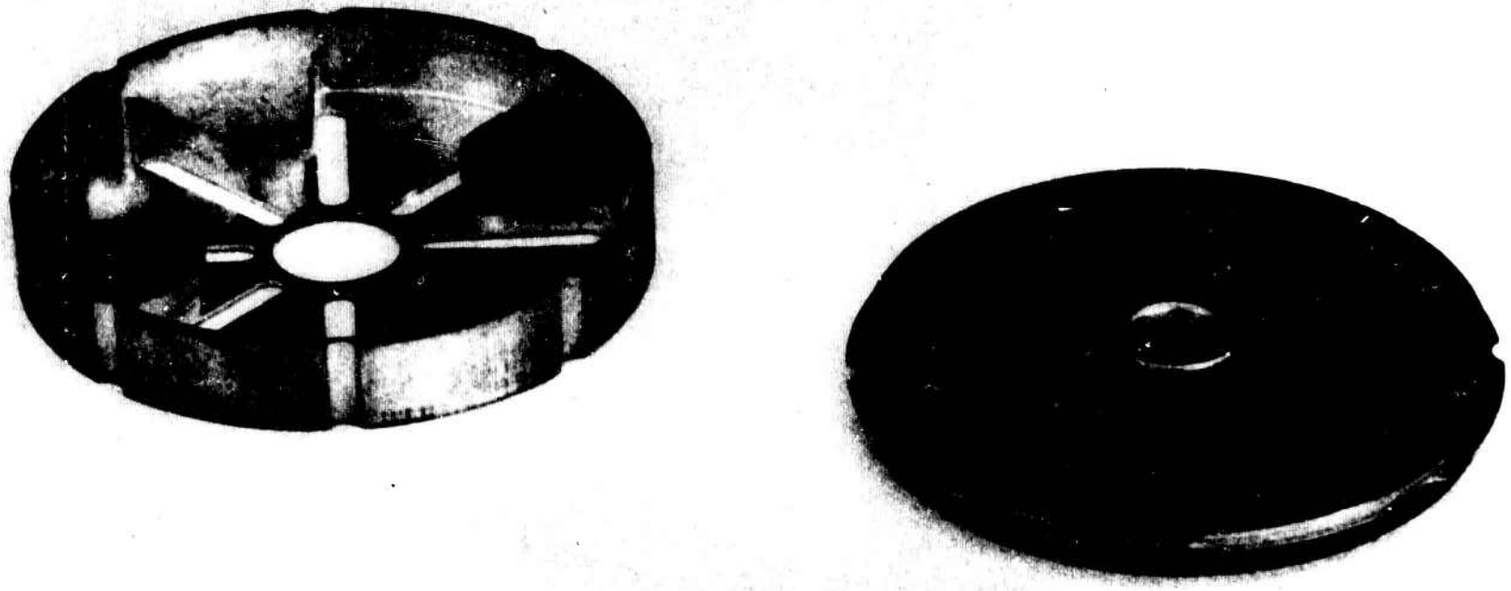

FIG. 3.10--Cloverleaf termination and housing. (10 MW TWT)

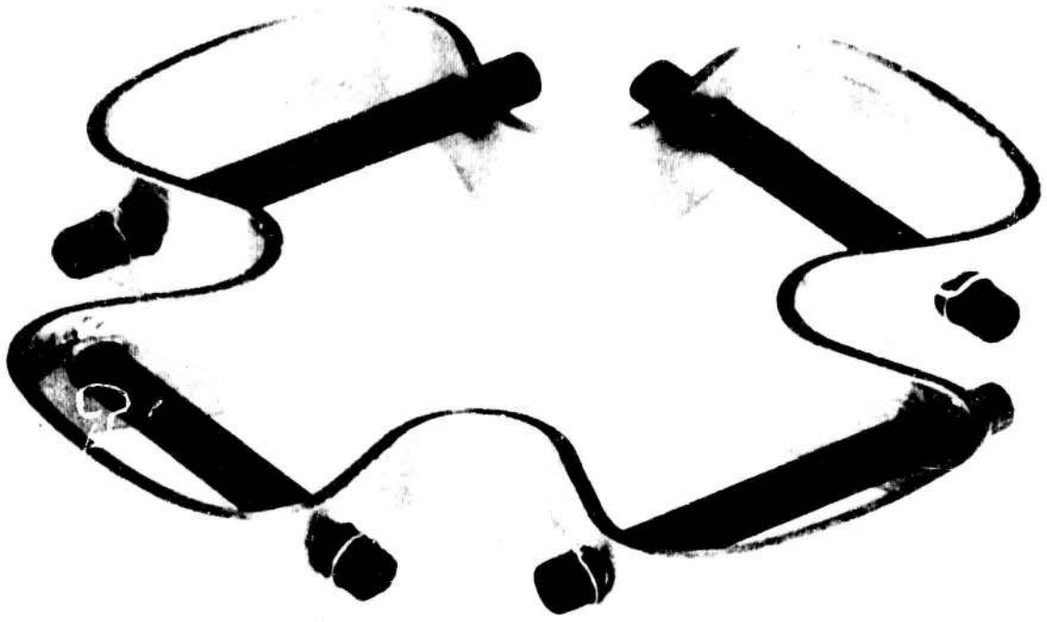

FIG. 3.11--Mode loading ceramic rods 10 mW TWT.

at the sever. The first version of this amplifier was later modified by the addition of eight more untapered cavities. The original model was demountable so the modification was achieved simply by inserting a middle section, consisting of eight cavities identical to those comprising the input section, and an additional sever section between this and the output section of the original tube. However, the input section was one cavity less than the original because the input coupler was replaced in the second version. The purpose of the additional eight-cavity section was simply to boost the small-signal gain of the amplifier, and hence there was no need to change in the tapered circuit. A schematic diagram of the modified version is shown in Fig. 3.12 with relevant attenuators indicated.

Different parts of the slow-wave circuit in the tube are joined by demountable junctions at the severs. That is, instead of brazing together the different parts of the tapered tube, they are joined together by compression only, which is provided by four tension bars outside the circuit. These junctions were expected to be no different from that or ordinary brazing joints from an electrical point of view because they are located at the sever sections, so little, if any, rf current appears across them. In order to secure good vacuum pressure, a stainless steel envelope was provided which enclosed the slow-wave circuit and was heliarc-welded to each end of the circuit. The demountable construction permitted the taking apart and re-assembly of the tube with ease, such that any modification of one part of the circuit could be made easily without disturbing the rest of the circuit. Furthermore, the collector and the electron gun were also joined to the slow-wave circuit by heliarc-welds, and could be easily removed and replaced.

The input coupler of the tapered tube was designed to provide a matched transition between the type-N input coaxial cable and the input section of the tube circuit over the entire fundamental passband of the untapered cavities which comprises the input part of the tube circuit. It was made small enough to pass through the focusing solenoid. This coupler consists of essentially a length of symmetrical modified Y-shaped coaxial line and relevant matching beads and strips. A simplified sketch of such an input coupler is shown in Fig. 3.13, although not in the exact proportion. The

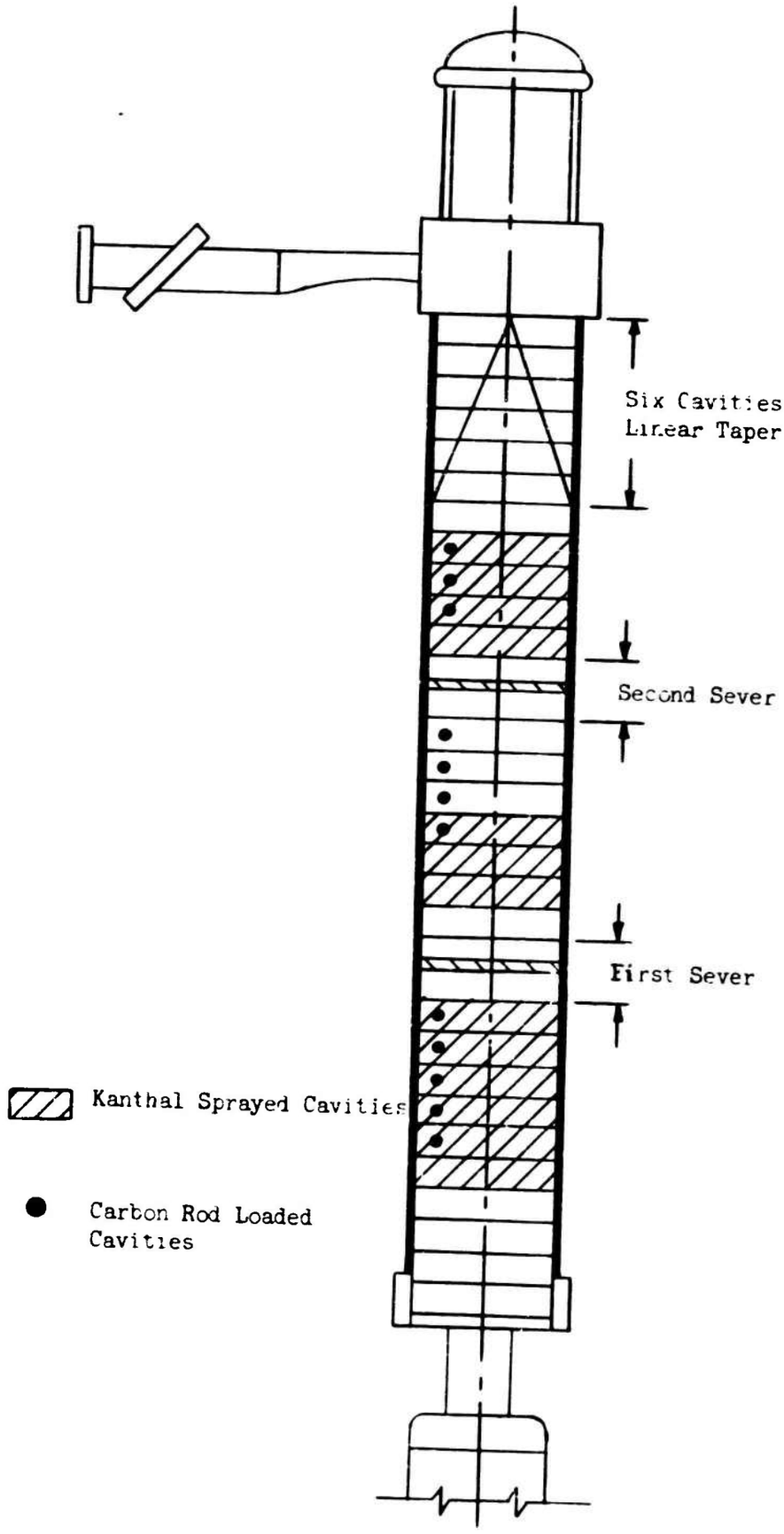

FIG. 3.12--Distribution of loss in modified linear tapered TWT .

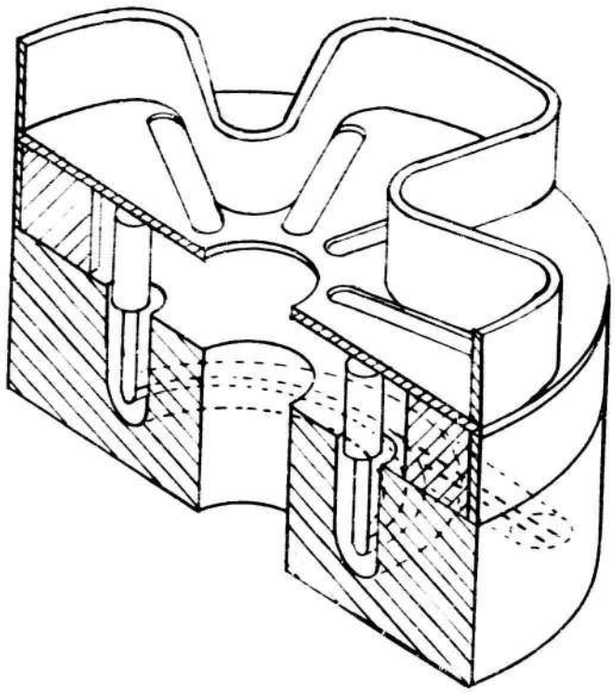

FIG. 3.13--Sketch of input coupler.

with a cutoff frequency of 4100 Mc/s. It can be seen that the higher passband oscillation at 5640 Mc/s is filtered out, and the remaining spikes are the oscillations of the lower passband. Figure 4.2c shows the waveforms obtained directly from the input end. Note that one can see both the incident rf pulse and the reflected oscillations though the directional coupler. Compared with Fig. 42a, these waveforms show some discrepancies. An obvious one is that the higher passband oscillation does not appear in the input end of the tube. This means that the oscillation exists in the output section of the tapered tube only. Another discrepancy is that the pulse-edge oscillations appear with different shapes when viewed from different ends of the tube. This is because the oscillation pulse contained many frequencies and the tube amplification is a function of frequency. That is, the beam modulation by these oscillations by the rest of the tube are both different for different frequencies. In addition, the coupling through the directional couplers is also a function of frequency. The oscillations observed from the output end, i.e., the amplified oscillations, therefore appeared with different shapes than those observed from the input end of the tube. However, when the oscillation frequencies were carefully measured, it could be found that whenever there was a frequency at the output end, the same frequency could always be found simultaneously at the input end at exactly the same relative position on the voltage pulse, i.e., at the same beam voltages. In other words, the oscillations observed from the two ends of the tube were actually the same oscillations since they were of the same frequencies at the same beam voltages and appeared at the two ends of the tube simultaneously. The middle section of the tube, as mentioned in Chapter III, was designed short enough such that no independent oscillations could build up there, as can be shown both from theoretical computations and from earlier empirical results of untapered tubes built with the same untapered cavities. Therefore, from these data and from the reasoning given in Section B of this chapter the pulse-edge oscillations could only exist in the input section of the tapered tube.

Unlike the one-sever tube case, the pulse-edge oscillations existing in the input section could no longer be stopped by adjusting the available

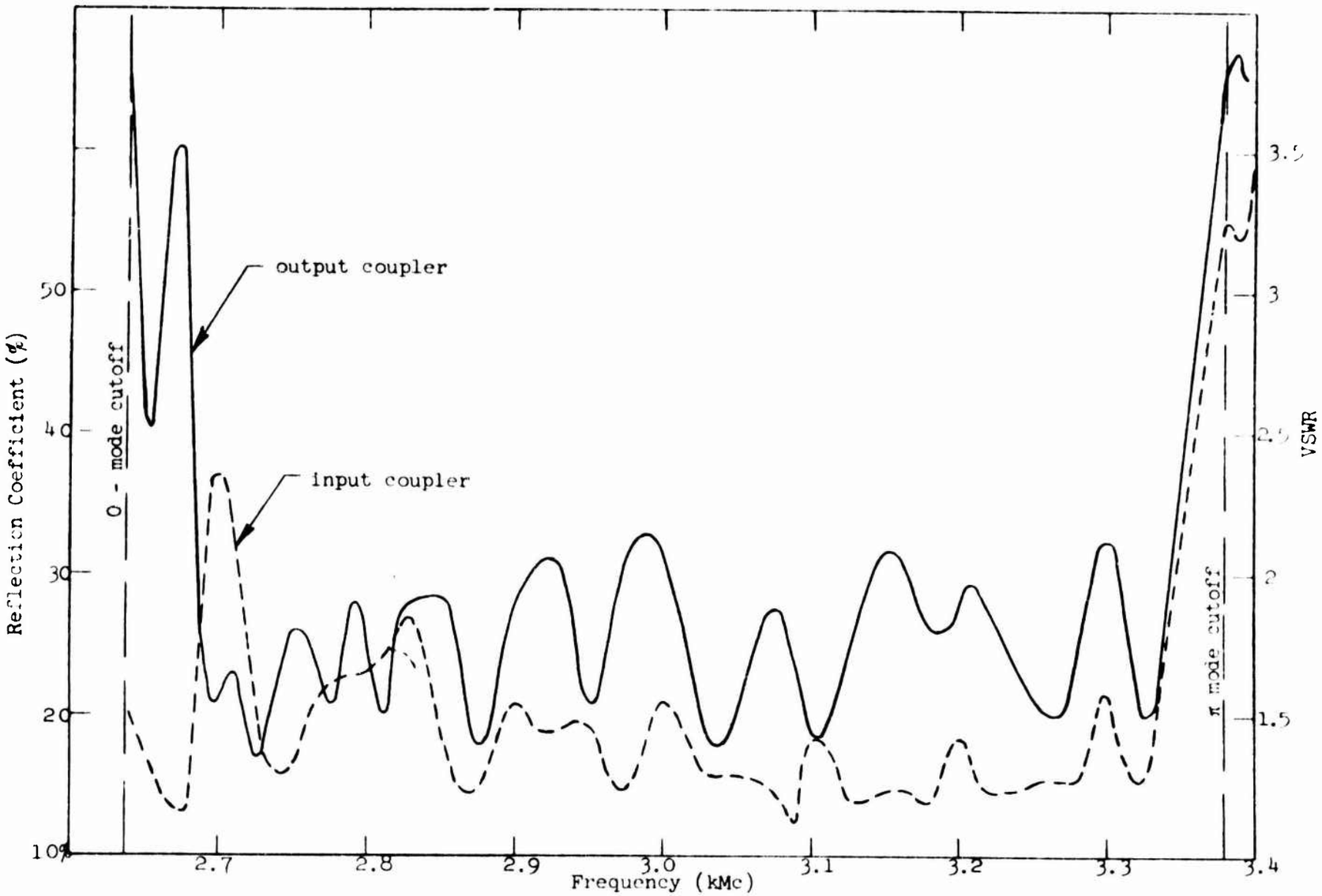

FIG. 3.14--VSWR vs frequency for input and output couplers on assembled amplifier.

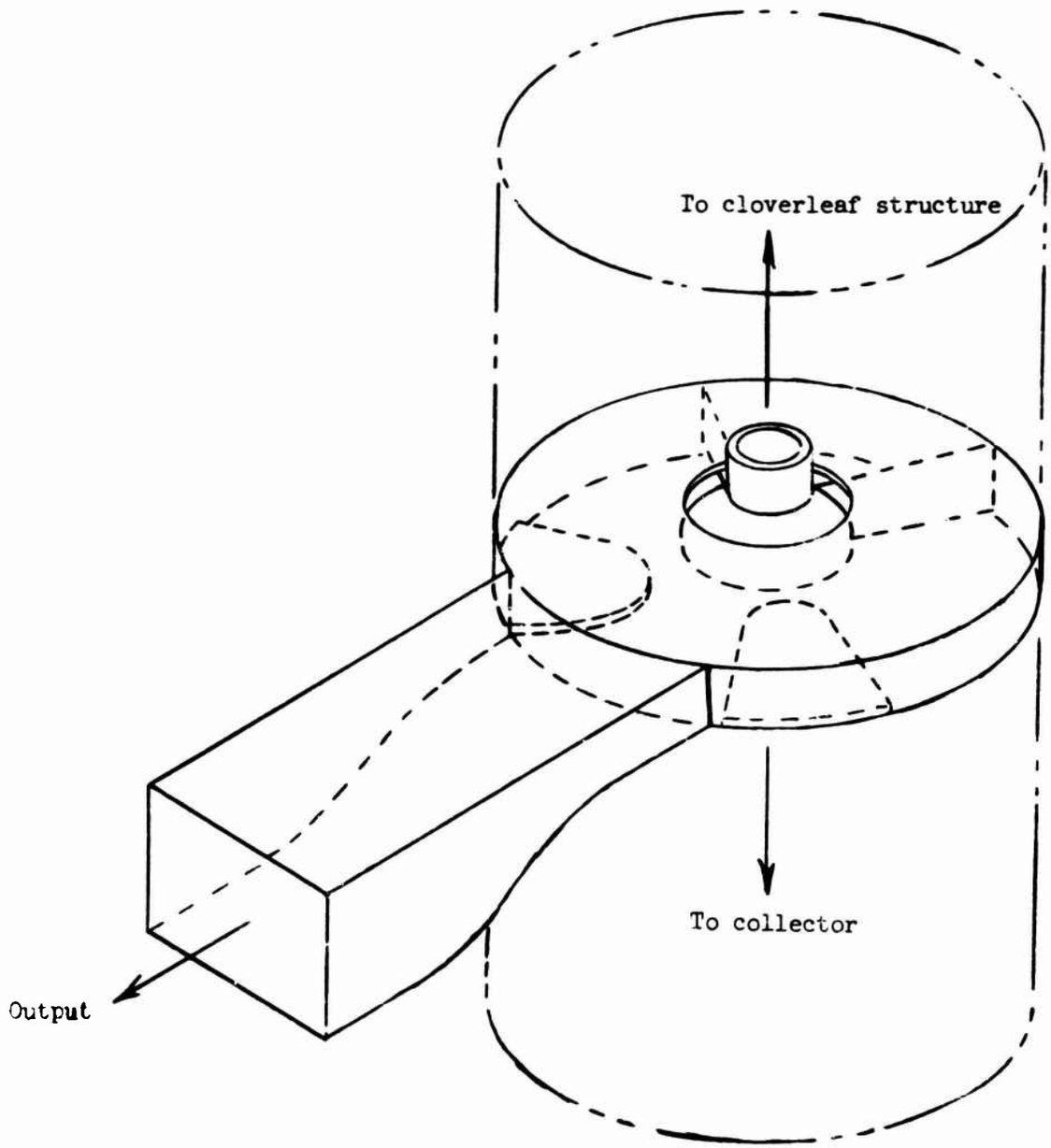

FIG. 3.15--Output coupler.

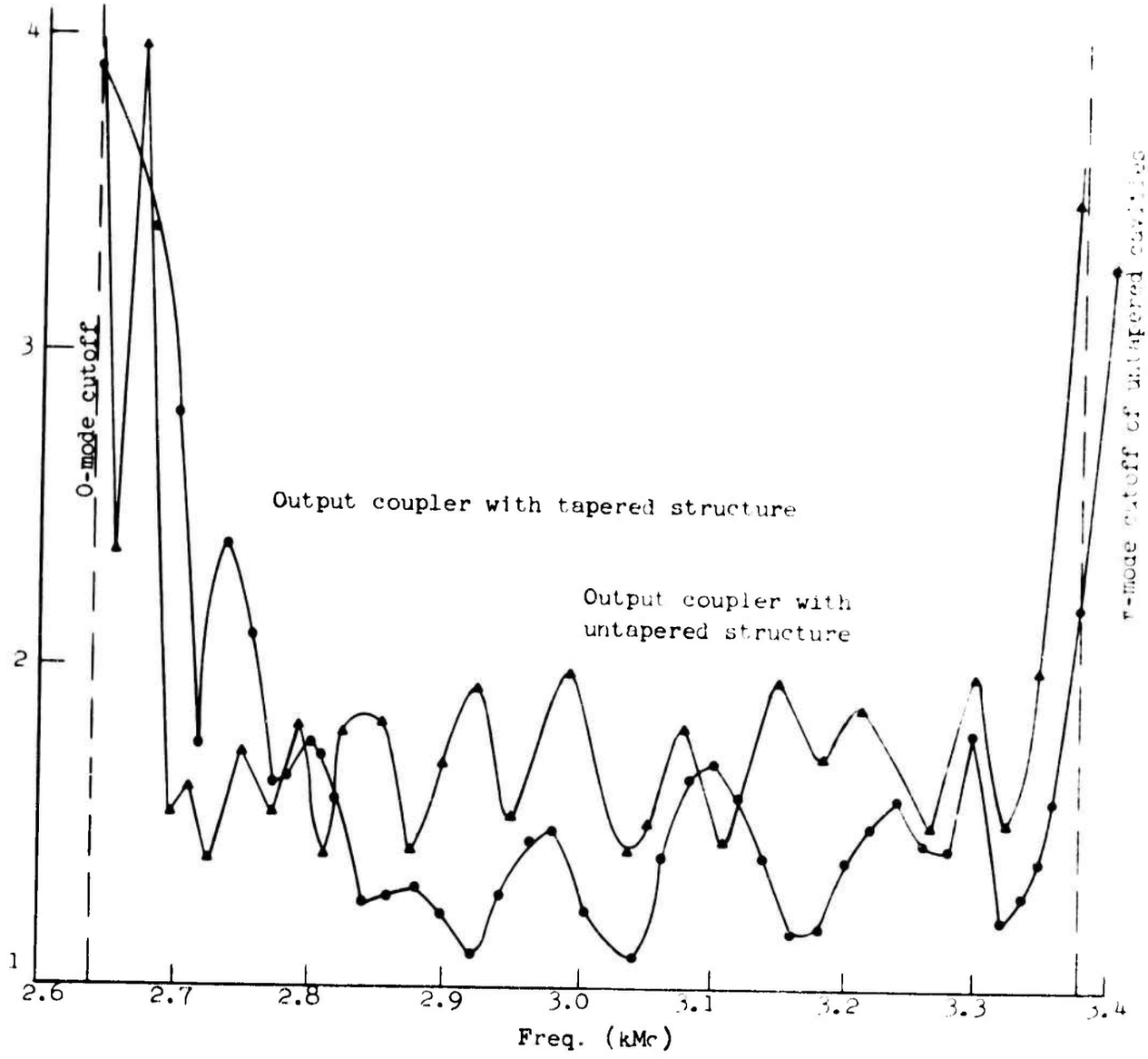

FIG. 3.16--VSWR measurements on output coupler with tapered and untapered structures.

previously. The results of the VSWR measurement are superimposed on the results obtained from step one in Fig. 3.16. It can be seen from this figure that mismatch now exists above the untapered upper cutoff frequency at 3375 Mc/s. The reason for this mismatch is that each succeeding cavity in the tapered chain has a dispersion curve cutoff at successively lower frequencies as one proceeds away from the output coupler toward the input end of the tube. Hence, at frequencies higher than that of an untapered upper cutoff frequency the rf field initiated at the output coupler can only propagate a short distance, less than or equal to the tapered circuit length toward the input end of the circuit, and the reflection, or reflections, of waves so produced inside the tapered circuit makes continuous matching impossible for more than spot frequencies. However, as mentioned in Chapter II, when the beam voltage sweeps through this frequency region each tapered cavity will synchronize at different frequencies and different beam voltages; and because of the rapid change in interaction impedance and phase constant, the tendency for oscillation at these frequencies is expected to be small although the reflections are high. These high reflection coefficients are outside the passband of the untapered cavities which comprise the major part of the tube and determine the bandwidth of amplification. Unfortunately, during the brazing process, the matching changed to some extent so that the high reflections began at 30 Mc/s below the upper cutoff frequency of the untapered cavities as shown in Fig. 3.14. Elsewhere the VSWR within the passband is below 2:1.

A slanted ceramic output window of an existing design was used in this tube. It was well-matched over the entire fundamental passband with reflection coefficient never exceeding 15 percent. Its power handling capacity was above the 2 to 3 megawatt range anticipated.

The electron gun used was purchased from Litton Industries, and provided a 3/4 in. diameter beam with a perveance of almost 2×10^{-6} .

CHAPTER IV

TAPERED TUBE PERFORMANCE

A. INTRODUCTION

As described in Chapter III, a linearly tapered tube was designed and constructed in order to evaluate the theoretical predictions made in Chapter II. In this chapter the test results of such a tube are given.

Two versions of the tapered tube were used in the test. The first was built with one sever which divides the tube at the center into two isolated sections. The input section of the tube consists of eleven untapered clover-leaf cavities, and the output section consists of five untapered cavities and the six-cavity linearly tapered circuit as mentioned previously. The second, a modification of the first, was almost identical except for the addition of another sever and an eight-cavity untapered middle section between the input and output sections. The original input section was shortened from 11 to 10 cavities, because of the replacement of the input coupler.

The test results from the one-sever tube, i.e., the first version of the tapered tube, are given in the following section, but, due to the lack of sufficient gain in this version of the tube, the effect of circuit tapering could not be clearly determined, and therefore the results are inconclusive. The addition of a middle section to this tube results in a two-sever amplifier which shows a great improvement in gain and the test results distinctly reveal the effect of circuit tapering.

Comparison of the test results with previous theoretical predictions shows close agreement. This not only proves the existence of such effects, but also validates to some extent the methods used in predicting them.

B. PERFORMANCE OF AN AMPLIFIER WITH ONE SEVER

In this first version of the linearly tapered tube, the input section was purposely designed long enough to give pulse-edge oscillations when the beam is defocused slightly so that the beam diameter is increased to more nearly fill the drift tube. Therefore, by adjusting the focusing magnetic field at the input section of the tube, the pulse-edge oscillations in this region of the tube can be started or stopped quite readily. The location of the oscillations in the tube, on the other hand, can be determined by employing the unidirectional behavior of the rf fields through the sever. That is whenever the oscillations exist in the output section of the tube, they will not propagate through the sever in any appreciable amplitude and thus they appear at the output end of the tube only. However, oscillations which occur in the input section of the tube will modulate the electron beam, and hence will induce rf fields in the output section and are amplified in the rest of the tube. Therefore, they will appear at both the input and output ends of the tube simultaneously. Although the sever terminates the rf circuit fields equally well in both directions, the propagation of the oscillations can only be stopped in the direction opposite to that of the electron flow by the sever. Therefore the location of oscillations can be clearly determined.

Unfortunately, it was found after the tube was built that a piece of porous copper was used in constructing the input window and coupler. The resulting leakage of air tended to poison the cathode; therefore, only limited observations could be made on this tube during the short period that the cathode remained active.

Under normal operating conditions, no pulse-edge oscillations could be observed from either end of the tube. However, when the beam was slightly defocused, pulse-edge oscillations of identical frequencies appeared simultaneously on both input and output ends of the tube, and always occurred at the same relative positions on the voltage pulse. Since at the edges of the voltage pulse the beam voltage sweeps through all values between zero and full operating value, each position on the pulse-edge corresponds to a particular beam voltage. This means that

oscillations with the same frequency observed from the two ends of the tube actually exist at the same beam voltage. The typical waveforms of the detected rf output from the tube are shown in Fig. 4.1. The waveform shown on top in the figure was obtained from the input end of the tube. The large square pulse shown in the center of the waveforms is the rf signal pulse, and the narrow ones on the two sides are the pulse-edge oscillations existing at the edges of the voltage pulse. By carefully examining the oscillation frequencies, one could find that these oscillations were distributed in an orderly fashion according to their frequencies, with the highest frequency of 3375 Mc/s located at the innermost position corresponding to the highest beam voltage, and the lower frequency oscillations toward the two ends of the voltage pulse corresponding to lower beam voltages. The same frequency can always be found at the same relative position on the voltage pulse on the input and output waveforms. The frequency content of the pulse-edge oscillations was found from the lowest value of 3276 Mc/s to the highest value of 3375 Mc/s. No distinct oscillation whatsoever could be made to appear at one end of the tube only, even if the beam focusing was radically changed. Therefore it appears that these oscillations exist in the input section of the tube only. Unfortunately the gain of this amplifier was somewhat lower than expected, and the tube could not be saturated with available drive power, so the lack of independent pulse-edge oscillations in the output section of the tube could be interpreted as the consequence of insufficient gain in the output section due to incorrect design of the tapered circuit equally as well as to the effect of circuit tapering. The results are therefore inconclusive.

When the electron beam was defocused, an oscillation at a fixed frequency of 5640 Mc/s could be observed from the output end of the tube. This oscillation belonged to the second highest, or TM_{02} passband, and was believed due to forward-wave interaction and high reflections at both the output coupler and the attenuator since they were, in general, well matched for the fundamental passband frequencies, but not for this higher frequency range. More discussion concerning this oscillation will be given in Section C.

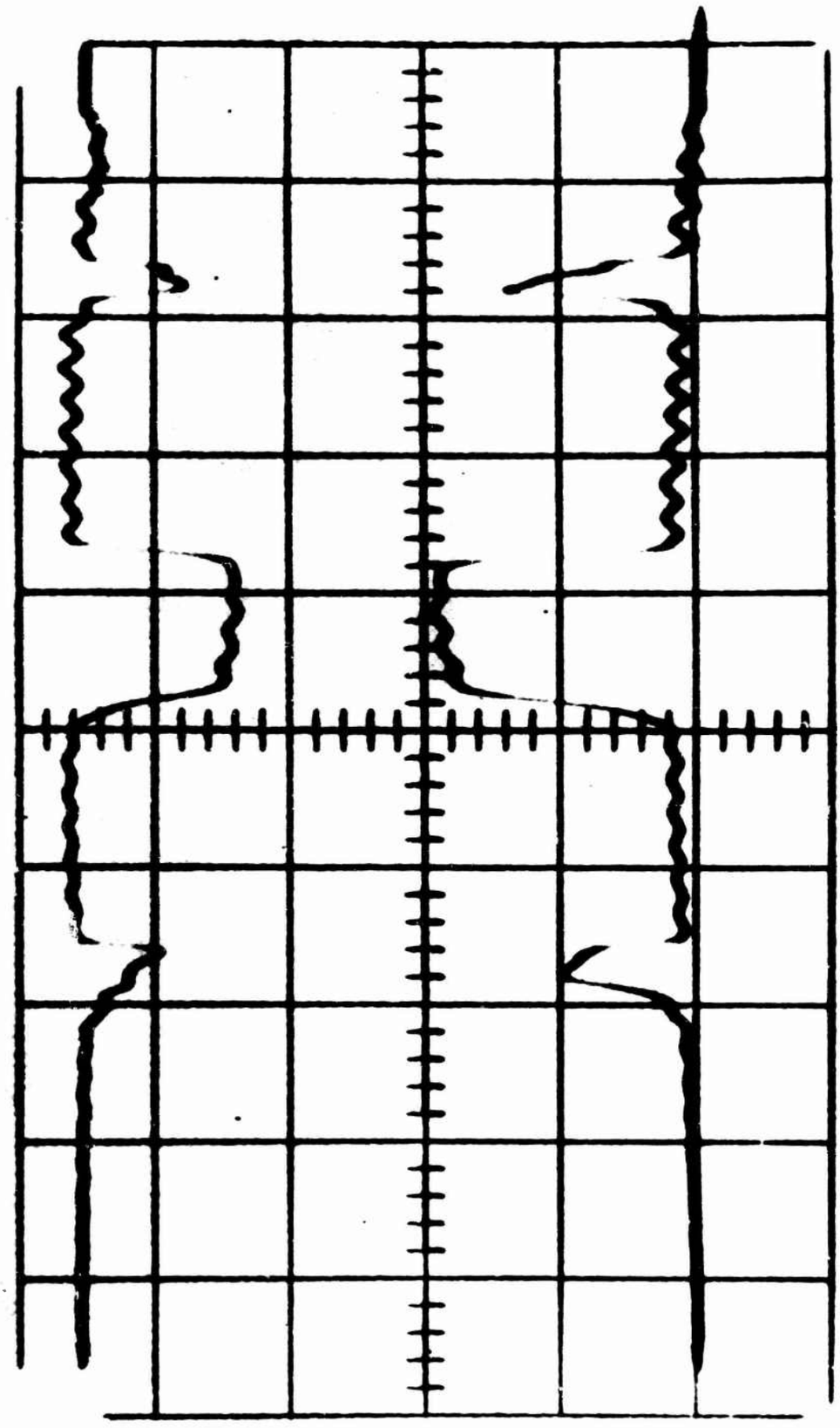

FIG. 4.1--Amplified rf pulse in tapered TWT.

During the short period that the cathode of the one sever tube remained active, the typical small-signal gain at mid-band frequencies near 3000 Mc/s was about 21 to 24 db and the peak power output for these frequencies at normal operating voltage at 120 kV was 1 1 megawatts, which corresponded to an efficiency of 20 percent. The beam transmission was about 85 percent with a magnetic focusing field of 1 5 times that required for Brillouin flow in an untapered tube.

C. TEST RESULTS FROM AN AMPLIFIER WITH TWO SEVERS

1 Observations of the Tube Oscillations

The modified version of the tapered tube showed a similar oscillation pattern as in the earlier version except that the higher passband oscillations were more serious in this version than in the first. The gain of the untapered portion of this tube was greatly increased. The effect of circuit tapering could therefore be more clearly determined.

Several methods of identifying the oscillations were tried. The most successful one was that of following the formation of each oscillation. For instance, in studying the lower passband pulse-edge oscillations, the beam voltage was increased slowly from a value low enough to insure that the tube was not oscillating. As the beam voltage increased, the first oscillation appeared at a beam voltage equal to 60 kV and beam current at 14 3 amp with oscillation frequency of 3276 Mc/s. This oscillation occupied, at first, a small portion of the top of the voltage pulse, and could be observed on both input and output ends simultaneously at the same relative position on the voltage pulse. As the beam voltage was increased, new oscillations with higher frequencies were created. The highest frequency corresponding to the highest beam voltage was always located in the center of the pulse, and the lower frequencies corresponding to lower beam voltages were pushed to the two sides and distributed in monotonically decreasing order according to their frequencies. The reason for such distribution can be easily understood from the dispersion characteristics of the slow-wave structure. This process of formation

continued until the beam voltage reached 98 kV. For beam voltages above this value, no additional oscillation frequencies in the lower passband could be obtained, and the rectified waveform was divided into two groups located symmetrically on the two edges of the voltage pulse. Each one of the two groups possessed almost the same frequency content from 3276 Mc/s to 3375 Mc/s and appeared on the pulse-edges in the form of irregular peaks. The distribution of the oscillation frequencies was still maintained, with the higher frequencies always occurring nearer the center of the voltage pulse, i.e., at higher beam voltages, as before. When the operating beam voltage was increased further, the beam voltage swept through a wider voltage range in the same transient time intervals at the pulse-edges. The frequency content in the leading edge oscillation decreased. But the frequency content in the falling edge oscillation always covered the same range. The reason for this effect is because the time for the beam voltage to sweep through the pulse-edge oscillation region was too short for some of the oscillation to build up at the leading edge. Since the transient time at the falling edge of the voltage pulse is usually long the time was still long enough to permit all the oscillations to start.

For beam voltages exceeding 100 kV a higher passband oscillation at a fixed frequency of 5640 Mc/s could be observed at the output end of the tube only. This oscillation was much stronger in this tube than it was in the single-sever tube. However, it did not exist in the presence of sufficient rf drive, and thus it did not interfere with other measurements.

Typical waveforms of tube oscillations observable from the input and output ends of the tube under normal operating conditions are shown in Fig. 4.2 a,b,c. The waveforms were photographed from an oscilloscope for a beam voltage of 140 kV. In Fig. 4.2a the waveform was obtained directly from the output end. The square pulse in the center is the amplified input rf pulse. The two strong oscillation pulses adjacent to each side of the rf pulse are the higher passband oscillations at a fixed frequency of 5640 Mc/s. Further from the two sides are the aforementioned lower passband pulse-edge oscillations. This is clearly shown in Fig. 4.2b where the rf output was filtered through a low-pass filter

Relative amplitude

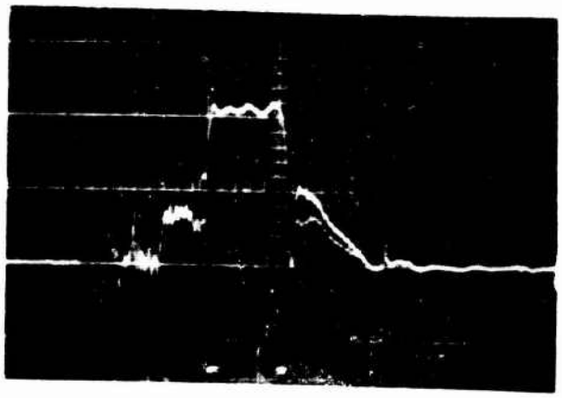

Time (1μs/Div.) →

a--RF output pulse without filter.

Relative amplitude

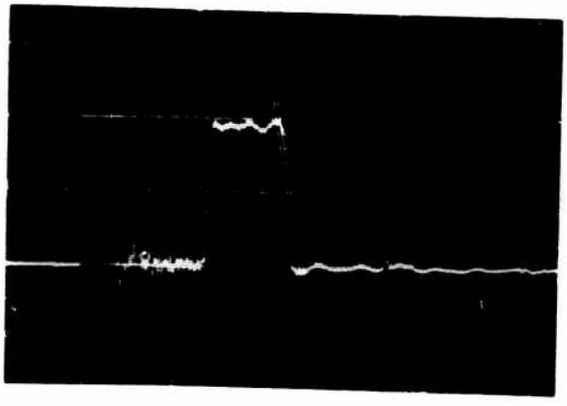

Time (1μs/Div.) →

b--RF output pulse with 4100 Mc/s low pass filter.

Relative amplitude

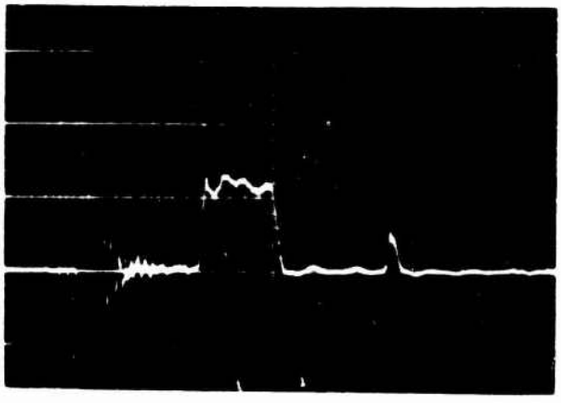

Time (1μs/Div.) →

c--Input rf pulse.

FIGURE 4.2

with a cutoff frequency of 4100 Mc/s. It can be seen that the higher passband oscillation at 5640 Mc/s is filtered out, and the remaining spikes are the oscillations of the lower passband. Figure 4.2c shows the waveform obtained directly from the input end. Note that one can see both the incident rf pulse and the reflected oscillations though the directional coupler. Compared with Fig. 42a, these waveforms show some discrepancies. An obvious one is that the higher passband oscillation does not appear in the input end of the tube. This means that the oscillation exists in the output section of the tapered tube only. Another discrepancy is that the pulse-edge oscillations appear with different shapes when viewed from different ends of the tube. This is because the oscillation pulse contained many frequencies and the tube amplification is a function of frequency. That is, the beam modulation by these oscillations by the rest of the tube are both different for different frequencies. In addition, the coupling through the directional couplers is also a function of frequency. The oscillations observed from the output end, i.e., the amplified oscillations, therefore appeared with different shapes than those observed from the input end of the tube. However, when the oscillation frequencies were carefully measured, it could be found that whenever there was a frequency at the output end, the same frequency could always be found simultaneously at the input end at exactly the same relative position on the voltage pulse, i.e., at the same beam voltages. In other words, the oscillations observed from the two ends of the tube were actually the same oscillations since they were of the same frequencies at the same beam voltages and appeared at the two ends of the tube simultaneously. The middle section of the tube, as mentioned in Chapter III, was designed short enough such that no independent oscillations could build up there, as can be shown both from theoretical computations and from earlier empirical results of untapered tubes built with the same untapered cavities. Therefore, from these data and from the reasoning given in Section B of this chapter the pulse-edge oscillations could only exist in the input section of the tapered tube.

Unlike the one-sever tube case, the pulse-edge oscillations existing in the input section could no longer be stopped by adjusting the available

focusing field. This is due to some misalignment of the cathode during assembly of the tube such that the magnetic focusing field required for the input section region was unconventionally high in order to confine the beam in the drift tube, and that no further adjustment was possible because of the limits of the available power supply. The beam transmission during normal operation was about 85 percent. A typical focusing field distribution is shown in Fig. 3.

By comparing the measured input section oscillation frequencies and their corresponding beam voltages to the ω-β diagram of untapered cavities, it was found that such oscillations appeared to be the backward-wave oscillations except for the high spike closest to the center of the pulse which is due to the forward-wave interaction nature as discussed in Chapter II.

The circuit length of the output section is nearly 1 cm longer than the input section, and the loading in the output section is also lower than that of the input section. Hence, if untapered cavities are used in the output section, the output section will certainly oscillate, simply because the input section, which is shorter, has been shown to be unstable. Such oscillations if they exist, can be easily distinguished from those of the input section. Because of the differences in circuit length and other circuit parameters as mentioned before, the starting oscillation conditions in the input and output sections are different. If the independent oscillations do exist in the two sections, they are most likely to start at different beam voltages which means they will appear at different locations on the pulse edges, and will occur at slightly different frequencies.

However, this phenomenon was not observed from the tapered tube although careful measurements were made in an effort to detect it. Hence, the only other possible cause for the lack of independent oscillations in the output section is that the gain is too low in the output section. If this were true, the starting current for oscillation would, of course, be higher. The forward-wave gain in the output section, on the contrary, is better than that in the untapered case. Therefore, it is concluded that the lack of pulse-edge oscillations in the output section of the tube is actually due to the effect of circuit tapering.

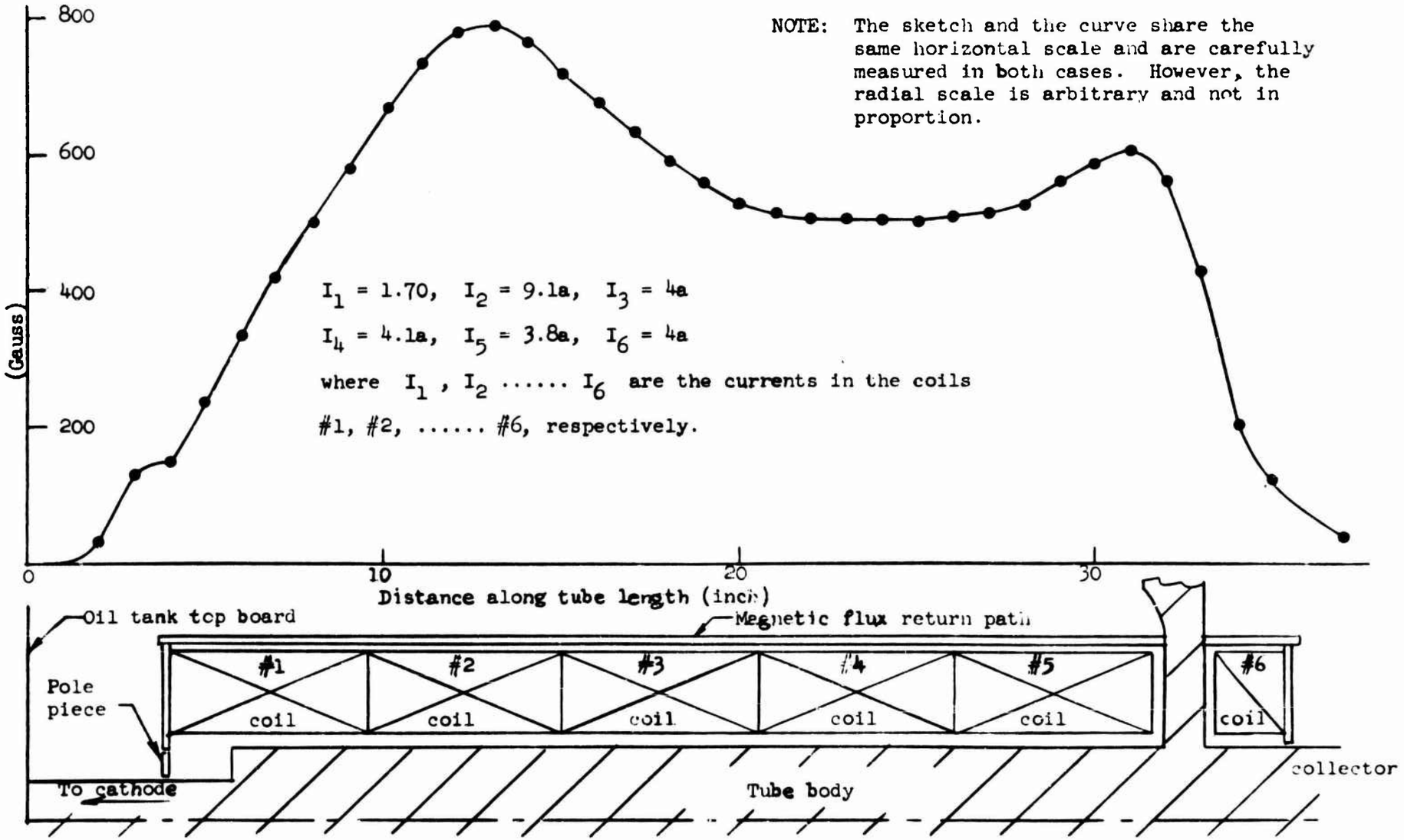

FIG. 4.3--Magnetic field along the tube length measured at the axis without tube and pole piece under the normal operation conditions of 120 kV.

Compared with the theoretical results obtained in Chapter II, it can be seen readily that the experimental results agree well with the predictions shown in that chapter. The method used to estimate the start oscillation conditions for backward-wave oscillation, though an approximate one, can be seen from the above results to be effective in predicting the stability of a tapered tube.

The higher passband oscillation at a fixed frequency of 5640 Mc/s, as mentioned earlier, was stronger in the two-sever tube than it was in the single-sever tube. This is because by the addition of the middle section the forward-wave gain in the tube at this frequency was also improved. Hence, this oscillation, which possibly was due to forward-wave interaction and reflections, could no longer, of course, be eliminated by simply adjusting the magnetic field. Fortunately such an oscillation did not exist in the presence of an rf signal pulse; it also could be filtered out by a 4100 Mc/s low-pass filter. Therefore no serious interference had been caused by such oscillations in the measurement of a low passband tube performance such as power measurement during pulse, efficiency, etc. However, this oscillation did cause some inconvenience in measuring the collector current since it loaded the beam so much that it changed the beam transmission to the collector. A typical waveform of the collector current under such a situation is shown in Fig. 4.4. The figure was drawn from a photograph taken for a beam voltage at 120 kV. The ripples indicated by 1 and that on other parts of the waveform are due to dc circuit pick-up. Those indicated by 2 and 3 are due to the pulse-edge oscillations at the input section of the tube. Those indicated by 4 and 5 are due to the higher passband oscillations. The middle one indicated by 6 is due to the input rf signal pulse, and the dotted line indicates the possible unmodulated waveform.

2. Gain and Efficiency Measurement

One of the most interesting characteristics of the linearly tapered tube is the sudden increase in slope of the power-out vs power-in characteristic as the input power was increased to what is normally the nonlinear

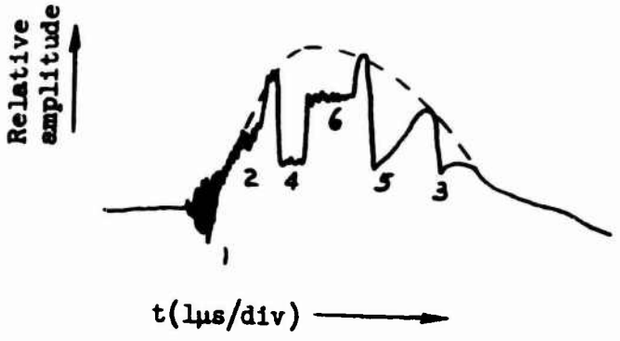

FIG. 4.4--Collector pulse waveform with beam voltage at 120 kV.

region in an untapered tube. Figure 4.5 shows a family of such characteristics obtained from the linearly tapered tube for different frequencies at a beam voltage equal to 120 kV. It can be seen from this figure that for frequencies below the synchronous frequency the tube behaves as a linear amplifier until about 1 db below saturation, where it abruptly becomes saturated as the drive increases further. For mid-band frequencies, the characteristics show a sudden increase in slope, or equivalently, an increase in gain, when the drive power is increased such that the output power is about 4 db below maximum power. For slightly higher frequencies this effect becomes more noticeable. At a typical frequency of 3060 Mc/s, as can be seen in the figure, the increase in gain has its maximum value at the point of inflection of 2.3 db above the small-signal value which is approximately 33 db. However, for higher frequencies the small-signal gain is so low that the available drive power is not enough for observing this increase, although it is expected to behave in a similar fashion. On the other hand, at lower frequencies, the small-signal gain is so high that a small increment in gain could not easily be detected. For higher beam voltages, this phenomenon is still exhibited but with higher saturation output power. For beam voltage at 130 kV and 140 kV, the power-out vs power-in characteristics obtained from the tube are shown in Figs. 4.6 and 4.7, respectively. It can be seen from this figure that the frequencies for the maximum gain increase are shifted to lower values and the magnitude of the maximum gain increase is changed slightly. For instance, at a beam voltage of 140 kV, the highest gain increase occurs at 3020 Mc/s with a magnitude of 2.7 db. The shift in frequency can be readily understood from the dispersion characteristic of the tapered circuit since at higher beam voltages the synchronous frequency shifts to lower values.

These results agree closely with the theoretical estimations shown in Section C, Chapter II. For mid-band frequency at 3060 Mc/s an optimum gain increase of 2.7 db is expected from a theoretical point of view. However, in the actual tapered tube, the maximum gain increase was measured to be 2.3 db at 120 kV beam voltage. The difference is only

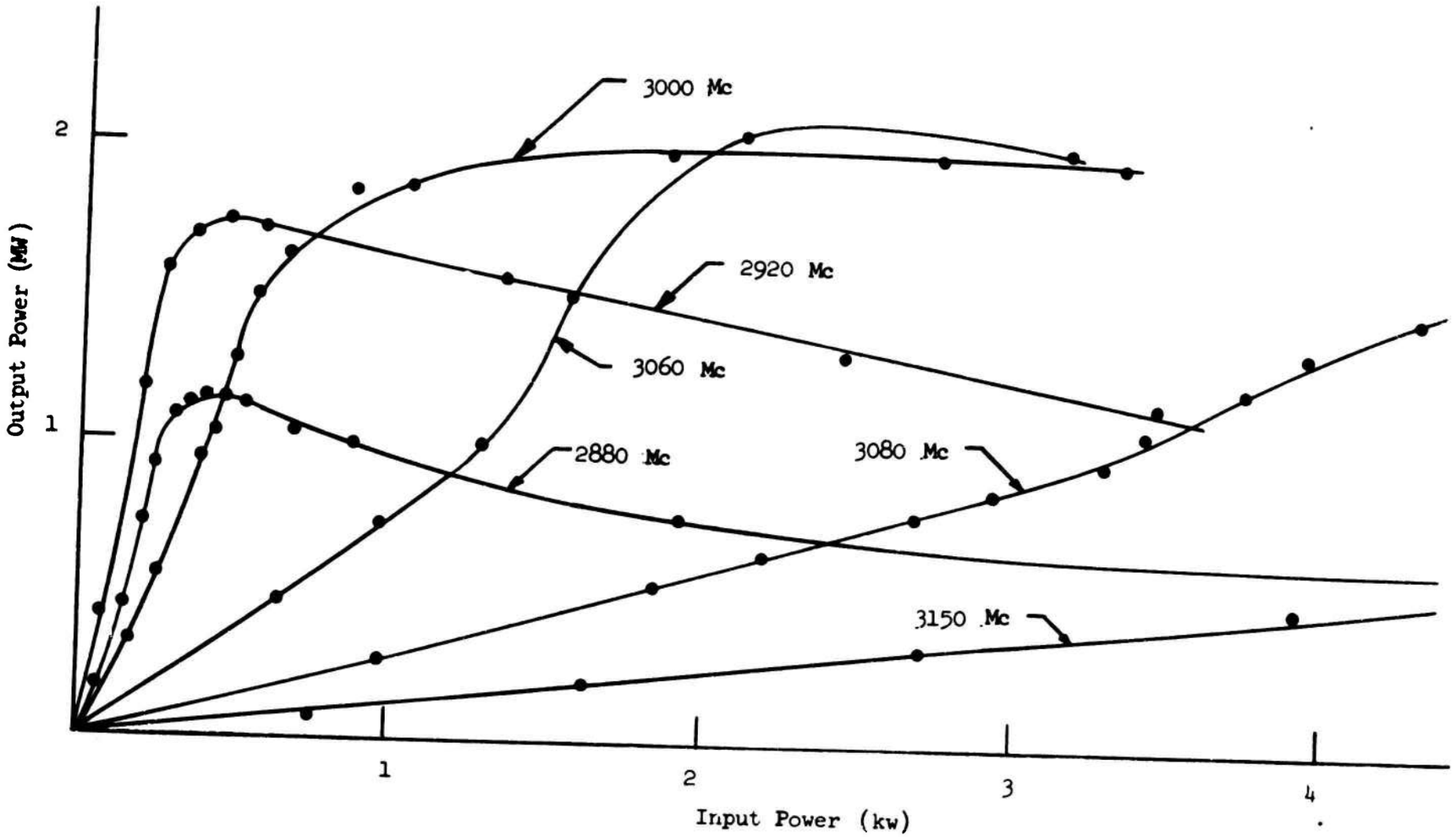

FIG. 4.5 --Output power as a function of input power with frequency as a parameter; V_0 = 120 kV .

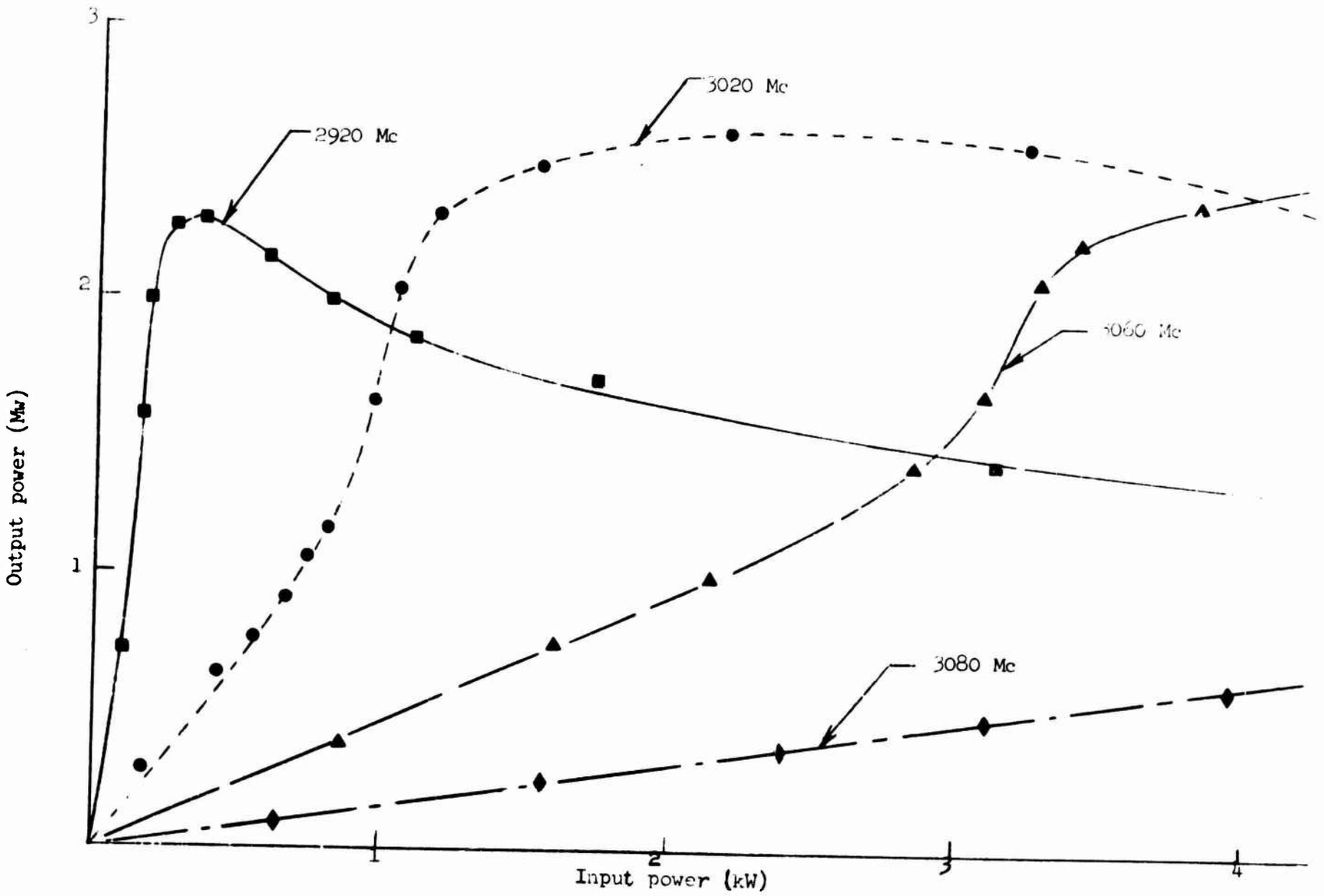

FIG. 4.6--Outpower power vs input power characteristics of linear tapered TWT with beam voltage at 130 kV.

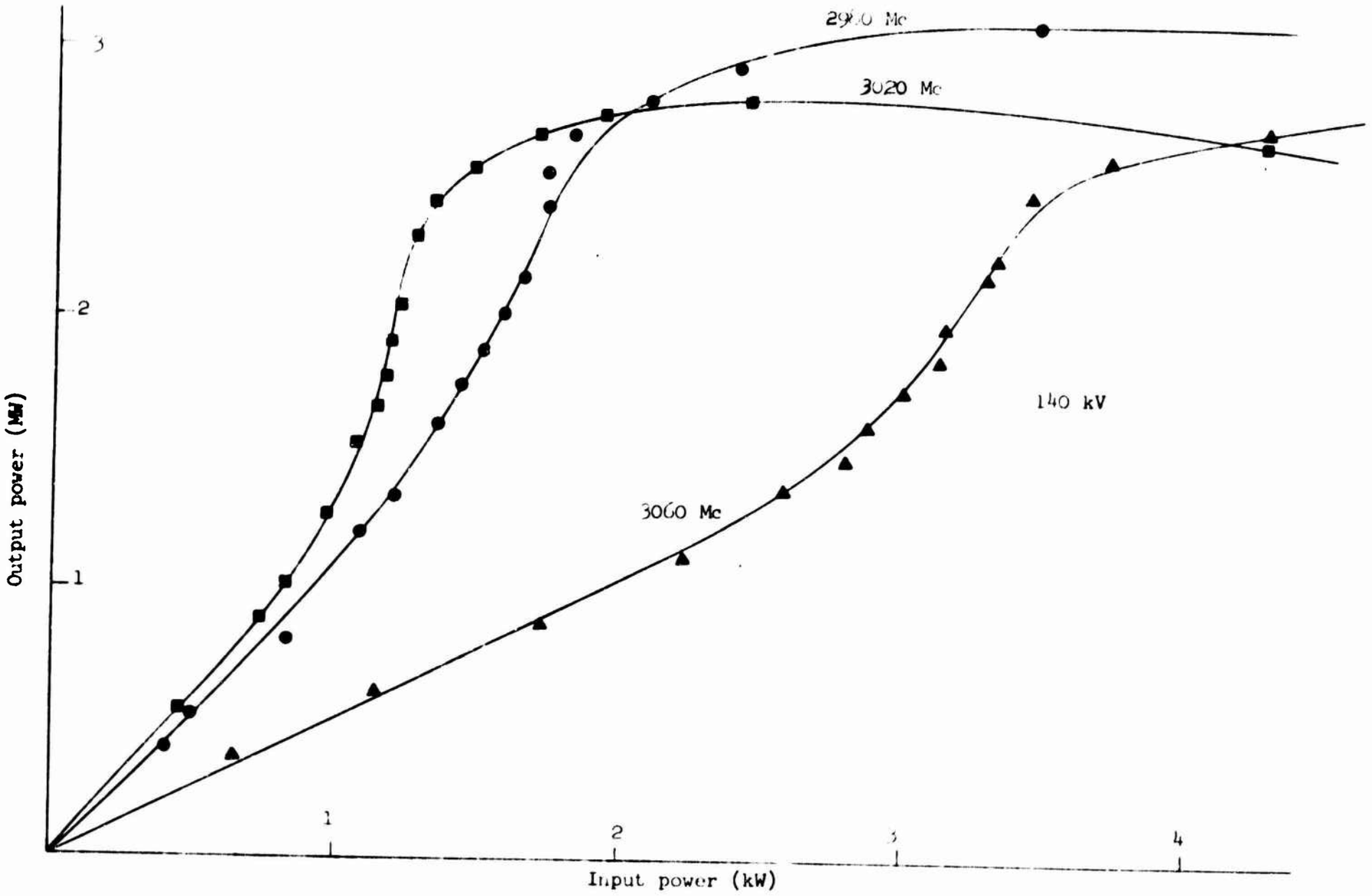

FIG. 4.7--Output power vs input power characteristics of linear tapered TWT with beam voltage at 140 kV.

about one percent of the small-signal gain at this frequency. Therefore, it is believed that the approximating method used in Chapter II for estimating this effect is quite reliable

In order to compare these results with those of uniform circuit tubes using an identical circuit, but not tapered in the output section, the results are normalized to their saturation values and plotted in decibels in Fig - 8 for a beam voltage of 120 kV It can be seen that for small-signal operation the normalized output power is a linear function of the normalized input power over a wide dynamic range The normalized characteristic curve for a small-signal operation will be a straight line with a slope of unity since the normalized input and output always have the same increment When the drive power is increasing, the characteristic reaches the nonlinear region If the gain in this region is lower than that in small-signal operation, the slope of the characteristic curve will be less than unity and the curve will go below the original 45 degree line Conversely, if the gain is higher in the nonlinear region, the characteristic curve will have a slope greater than unity and will lie above the 45 degree line. For a frequency of 2920 Mc/s the characteristic curve, (which is typical of those obtained at frequencies below the midband frequency) gradually bends below the 45 degree line when the input power increases beyond the small-signal values This curve shows a close resemblance to that obtained from an untapered tube built by the General Electric Microwave Laboratory with identical untapered cavities It will be noted that the output characteristic of the GE tube has a nonlinear region beginning at 5 db below saturation output power, while the tapered tube shows a noticeable departure from linearity only about 1 db below saturation At a frequency of 3000 Mc/s the tapered case shows an increase in gain beginning about 5 db below the saturation point of the output power. The maximum increase in gain in this case is about 0 8 db For a frequency of 3060 Mc/s the increase in gain is even higher, having a value of 2.3 db and beginning about 4 db below output power saturation

It is important to note that in all three cases the tapered tube requires a much smaller drive power change in order to bring the tube from the linear region to the point of saturation than did the GE tube

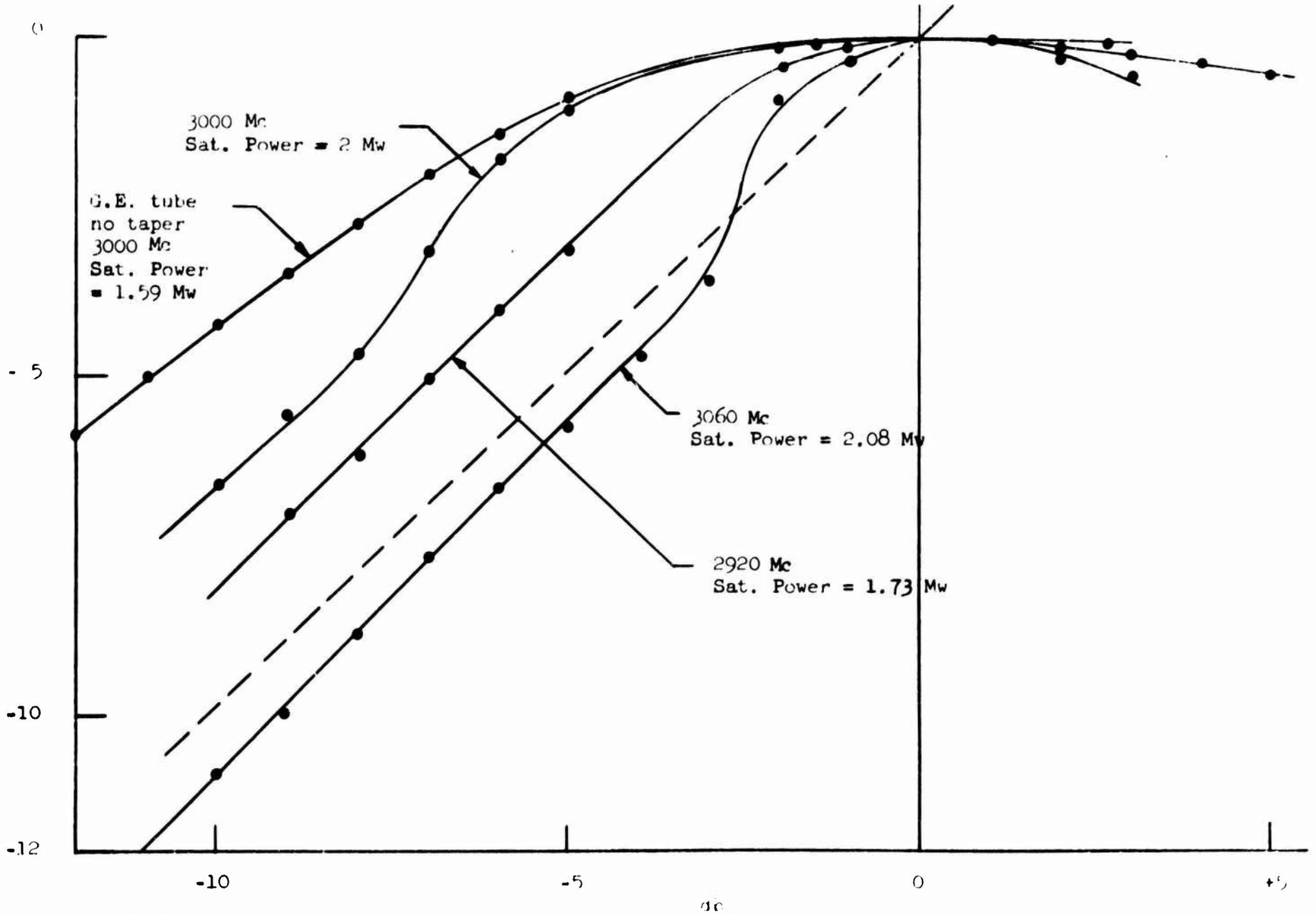

FIG. 4.8--Normalized power characteristics with beam voltage at 120 kV. Both the input and the output powers are normalized to their saturation levels.

which required a variation of about 15 db. This effect is especially noticeable at the higher frequencies where merely doubling the drive power brings the tube from the linear region to complete saturation.

Alternatively, the total gain of the tapered tube is plotted vs input rf power for three different frequencies in Fig. 4.9. The manner and the amount of gain increase, as well as the corresponding rf drive levels at these frequencies, is clearly shown in the figure.

A plot of saturation power output as a function of frequency at a beam voltage of 120 kV is shown in Fig. 4.10. The maximum power output obtained was 2 MW at 3000 Mc/s with a 3 db bandwidth of 12.2%. The efficiency based on the cathode current is 22.3 percent, but since the beam transmission is poor, the efficiency based on collector current is probably more realistic, and is about 28 percent. The actual overall efficiency should be somewhere between these two values, probably 26 percent. Results obtained at higher beam voltages, namely 130 and 140 kV, indicate a continuous increase in saturation power output. For these two voltages, the maximum output power increased up to 2.5 MW and 3.2 MW, respectively, with the center frequency shifting slightly to a lower value. The bandwidth, however remains nearly constant for all cases. The efficiency is believed to be slightly increased also, as the voltage is raised, but the collector current is difficult to measure due to the presence of the upper passband oscillations. The saturation power output for beam voltage at 140 kV is plotted as a function of frequency in Fig. 4.11. The center frequency can be seen to be 20 Mc/s lower than that at beam voltage of 120 kV. For higher beam voltages the power output is increased even more, but the measurement was limited by the capacity of the cathode seal to withstand the higher pulse voltages. Also, as the voltage was raised the higher passband oscillations become stronger and were more difficult to drive out with the rf drive; hence, no further data were taken.

D. CONCLUSIONS

In the present and previous chapters, it has been shown both theoretically and experimentally that by properly tapering the slow-wave structure of a traveling-wave amplifier the long persistent problem of pulse-edge oscillations can be

Figure 4.10 - Saturation power versus frequency for beam voltage at 120 kV.

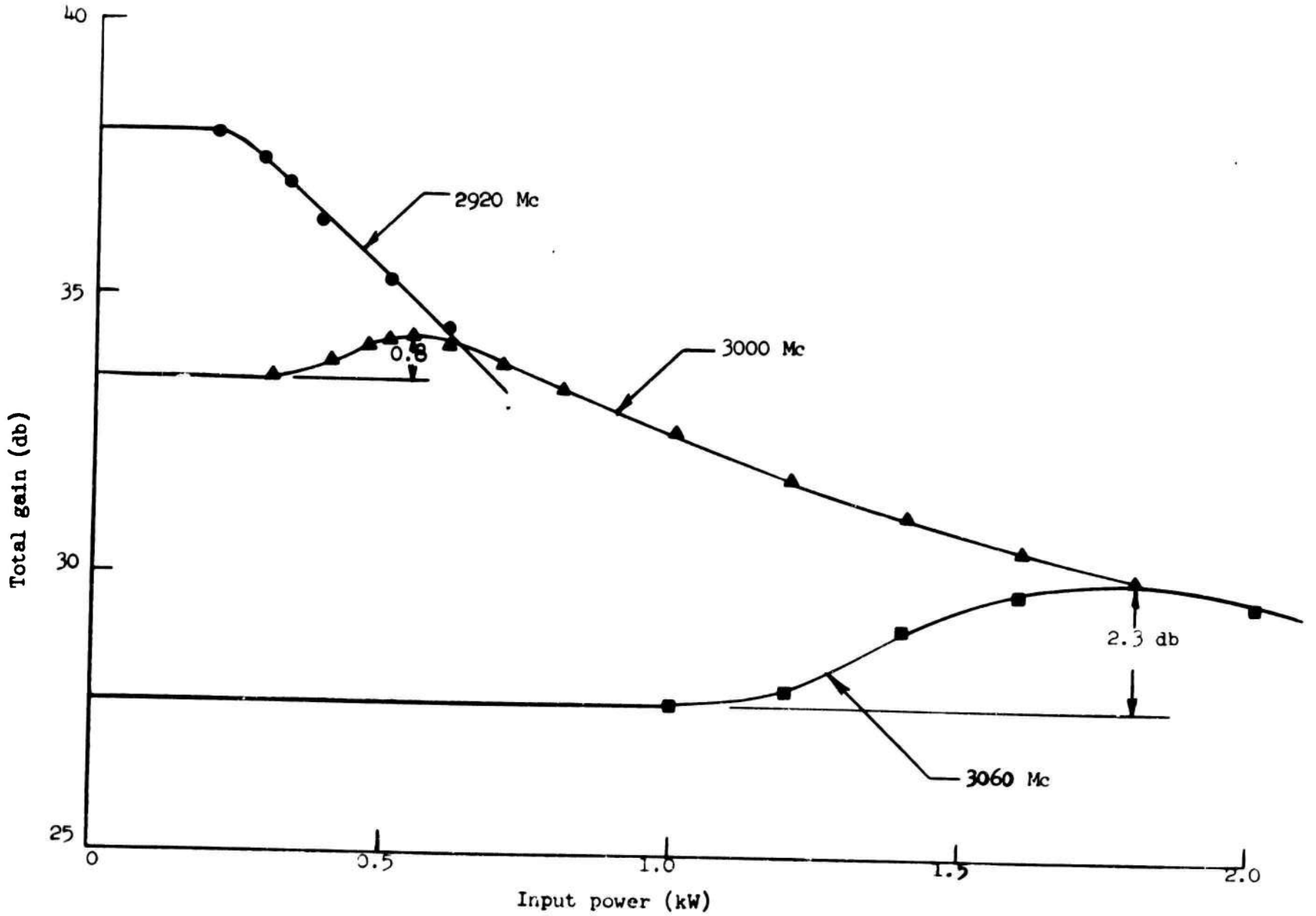

FIG. 4.9-- Total gain vs input power with frequency as parameter at 120 kV.

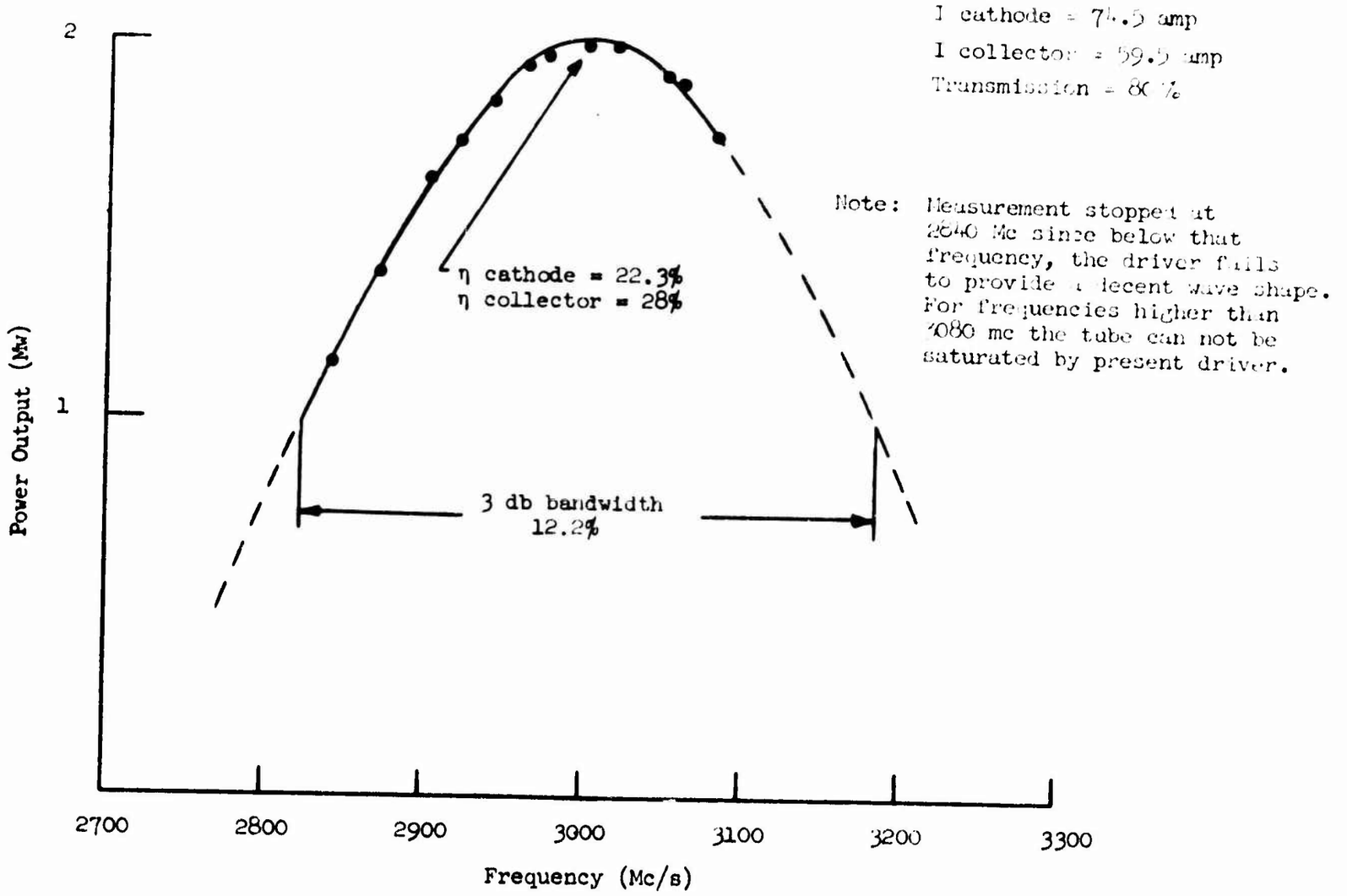

Figure 4.10 - Saturation power versus frequency for beam voltage at 120 kV.

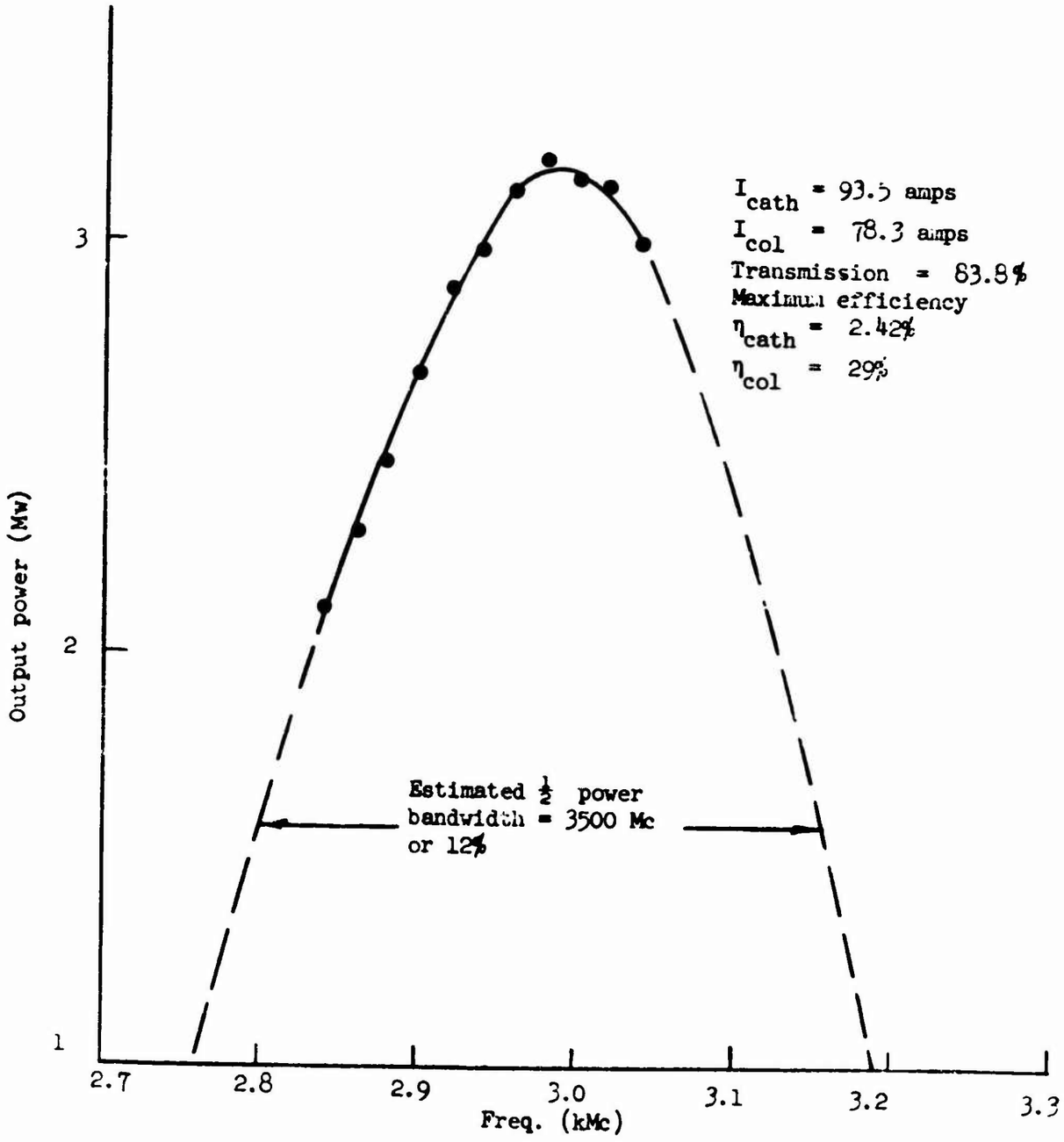

FIG. 4.11--Saturation power vs frequency for beam voltage at 140 kV.

eliminated without otherwise deleteriously affecting the amplifier's performance. By comparing the theoretical predictions and the experimental results, close agreement is found between them. From such close agreement, one can see that the methods used in Chapter II in predicting the performance of the tapered tube are well justified. These methods provide convenient ways for designing tapered traveling-wave tubes and also provide insight as to the operation of a tapered circuit.

Similarly, the forward-wave amplification at moderate input power level is shown to be considerably improved. For lower end frequencies in the passband, such improvement tends to extend the linear portion of the power-out vs power-in curve. And at the mid-band frequencies, the gain at moderate input power level is greater than the small-signal gain. These changes on the power-out vs power-in curves enable the tapered tube to be used in some special applications. As mentioned previously, both these changes are unattainable by the untapered tubes. Moreover, the empirical results obtained from the experimental tube are in close agreement with the prediction made in Chapter II. This means that the method used in Chapter II, though an approximate one, is quite capable of giving a good prediction and a decent interpretation of the operation of the tapered circuit in this input power range.

As can be seen from the foregoing results in this chapter, the efficiency of this experimental tube is about the same as that of the untapered tube. This is because, as mentioned before, the circuit tapering on the forward-wave amplification region is purposely made small so any effect on the efficiency of the tube was not evident. From a comparison of this tube with tapered tubes elsewhere,[24] it is believed that if the tapering in the forward-wave region can be made larger and more rapid, the tube efficiency should also be improved. For the clover-leaf slow-wave circuit, it is relatively simpler to make tapering larger and more rapid. For instance, instead of keeping the 0-mode frequency fixed, one may let it decrease; then at the lower end frequencies of the passband there will be quite a large circuit tapering. However, as stated in Chapter II, if a taper is properly designed for improving tube efficiency, it should have a proper

rate of tapering, a proper starting point of the taper, etc. But, all these factors are a function of frequency and circuit parameters. Therefore, a taper may be proper for some frequencies in the passband but may not necessarily be adequate for other frequencies. To date, no optimum taper design for improving efficiency has been found. Nevertheless, as mentioned in Chapter II, several authors[1] have delved far into this field, and many results have been accumulated. It is believed that from these empirical results a set of universal curves for designing a proper taper to improve efficiency is possible to obtain by simply using proper normalization. For instance, the length of the taper may be normalized to the electron wavelength, such that the same curve can be used for different frequencies and beam voltages, etc. Since this report is mainly concerned with the elimination of pulse-edge oscillations, no further investigation has been made in this direction.

The experimental tapered tube used for this study has been shown to have the effects of eliminating the pulse-edge oscillations and of improving the amplifications at moderate input power level simultaneously. It is interesting to know whether one can design a taper which can also improve the tube efficiency. To the author, it appears to be that one can either improve the amplification and stability or improve the efficiency and stability. The reason is that to improve efficiency, the tapering must be quite rapid. Under this condition, the gain in the tapered cavity will be decreased drastically, such that no noticeable amplification improvement can be obtained even if the average electron velocity is decreased in the taper region as the input power is increased.

In this paper, only the clover-leaf slow-wave structure was considered. However, the results are believed to be adaptable immediately to other types of circuits. But in some slow-wave circuits the work involved in achieving a practical taper is sometimes tremendous, as was learned by the author in working with other slow-wave structures.

---

[1] See Chapter II, Section D.

APPENDIX

EVALUATION OF SMALL SIGNAL PARAMETERS OF THE LINEARLY TAPERED TRAVELING-WAVE AMPLIFIER

From the measured ω-β diagram shown in Fig. 2.12 and the frequency perturbation results shown in Fig. 3.6, two sets of small-signal parameter computations are performed for the untapered cavities and the last cavity of the linear taper. The parameters computed are those introduced by J. R. Pierce, and the procedure used is summarized briefly in the following paragraphs.

By definition, Pierce's gain parameter, C, is given by

$$C^3 = \frac{E^2}{2\beta^2 P} \frac{I_0}{4V_0} = \frac{I_0 Z}{4V_0} , \qquad (A.1)$$

where, $Z = E^2/2\beta^2 P$ is the interaction impedance, and $I_0/4V_0$ is the beam admittance.

By using the perturbation method, the interaction impedance of a circuit can be determined empirically by measuring the frequency shift when the axial E-field is perturbed by a known subject.[29,30] In our measurement, a 0.100 in. diameter sapphire rod with dielectric constant of 10.3 is used to perturb the axial E-field, and the results are shown in Fig. 3.9.

The conversion equation used to compute the interaction impedance from the measurement results is

$$\frac{E^2}{W} = \frac{480\ C}{(\epsilon' - 1) r_d^2} \cdot F \cdot D \cdot \left(\frac{\Delta f}{f}\right) \cdot \left[I_0^2(\gamma r) - I_1^2(\gamma r)\right] , \qquad (A.2)$$

where $\Delta f/f$ is the normalized frequency perturbation by the sapphire rod, E is the amplitude of the fundamental forward-wave component, r_d is the radius of the sapphire rod, F is the correction factor for the rod, and D is the space harmonic factor with the form of

$$D = \frac{A_0^2}{\sum_0^\infty A_n^2} \cong \frac{1}{1 + \left(\frac{A_1}{A_0}\right)^2} , \qquad (A.3)$$

where

$$A_n = \frac{\sin\left(\frac{\beta_m \ell}{2}\right)}{\left(\frac{\beta_m \ell}{2}\right)} \cdot \frac{1}{I_0(\gamma a)} . \qquad (A.4)$$

The last $[I_0^2(\gamma r) - I_1^2(\gamma r)]$ term is the averaging factor over the whole beam cross area, where $I_0(\gamma r)$ and $I_1(\gamma r)$ are zero- and first-order modified Bessel functions.

Equation (A.2) is derivable from the perturbation equation

$$\frac{\Delta f}{f} \cong - \frac{(\epsilon - \epsilon_0) A \int_0^L E_c \cdot E_c^* \, dz}{4 W_c} , \qquad (A.5)$$

where ϵ = dielectric constant of the rod,

ϵ_0 = dielectric constant of free space,

E_c = total axial E-field,

W_c = energy stored in the cavity, and

A = cross section area of the rod.

In Fig. A.1 is shown the computed value of gain parameter, C, vs frequency for these two cases. One may notice that the difference between these two cases is essentially the largest difference obtainable in the taper, since for any intermediate cavity the difference will be smaller than that shown in the figure, although the differences are not too large themselves.

In obtaining the C parameters, several assumptions have been made, namely: (i) the perveance of the beam has been assumed to be 2 μperv.; (ii) the beam diameter is assumed to be 0.8 of the circuit aperture; (iii) the beam voltage in the last section is assumed to be the same as that in the first section of the taper.

The velocity parameter, b, is obtained by

$$b = \frac{1}{C}\left(\frac{u_0}{v_p} - 1\right) \quad , \tag{A.6}$$

where u_0 is the relativistic electron velocity, v_p is the circuit phase velocity, and C is the gain parameter. The results are plotted vs frequency in Fig. A.2. It can be seen that the values of b increase as one proceeds from the first to the last section of the taper as expected.

In Fig. A.3, the space-charge parameter, QC, is shown vs frequency which is obtained by the following equation under the same assumptions as in computing the above parameters.

$$2C\sqrt{QC} = \sqrt{4QC^3} = \frac{\omega_q/\omega}{1 + \omega_q/\omega} \quad , \tag{A.7}$$

where ω_q is the reduced plasma frequency calculated from the plasma frequency, ω_p, , and the reduction factor is obtained from Mihran and Branch's paper[32] by assuming $R = 2$.

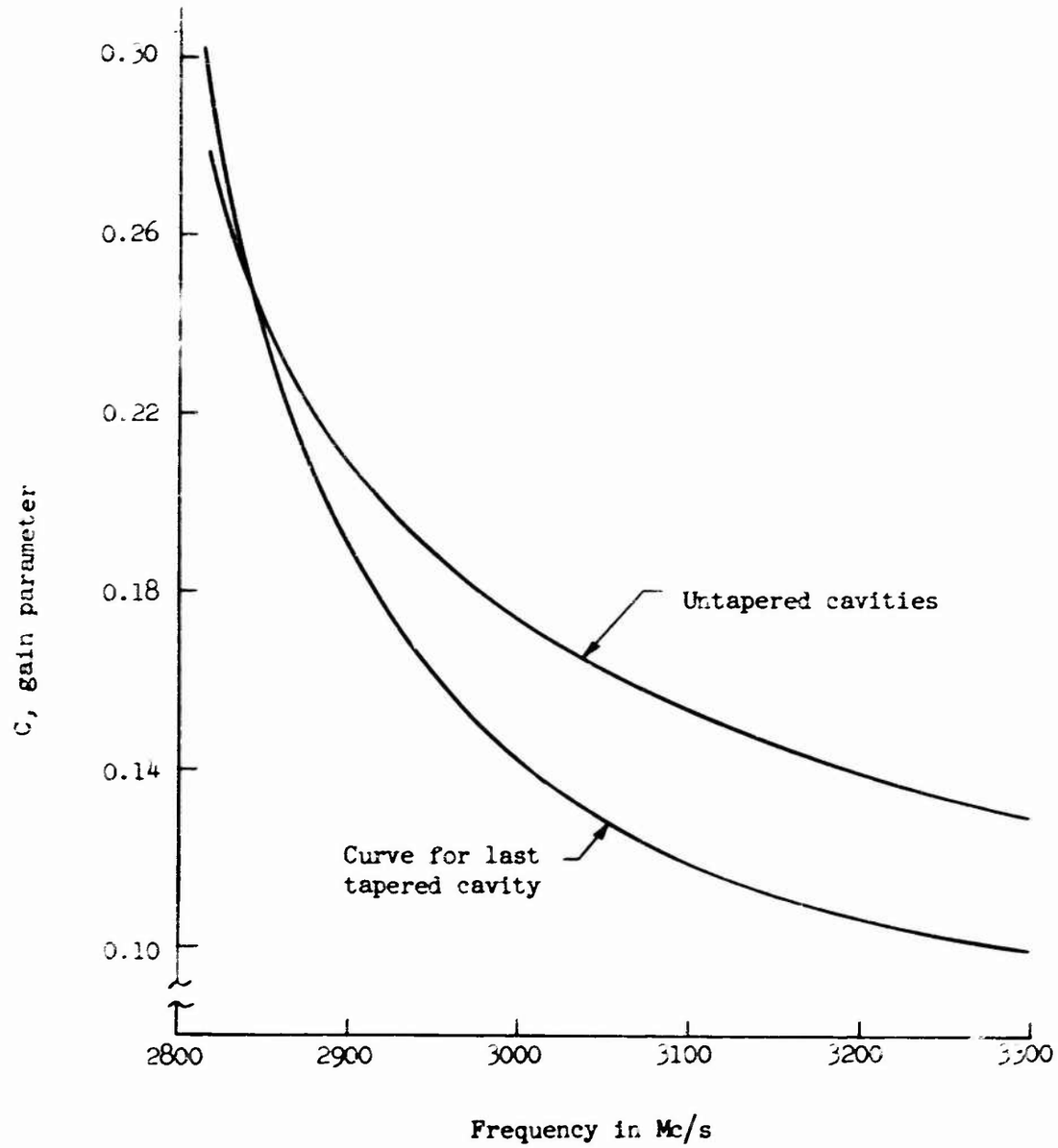

FIG. A.1--C vs frequency.

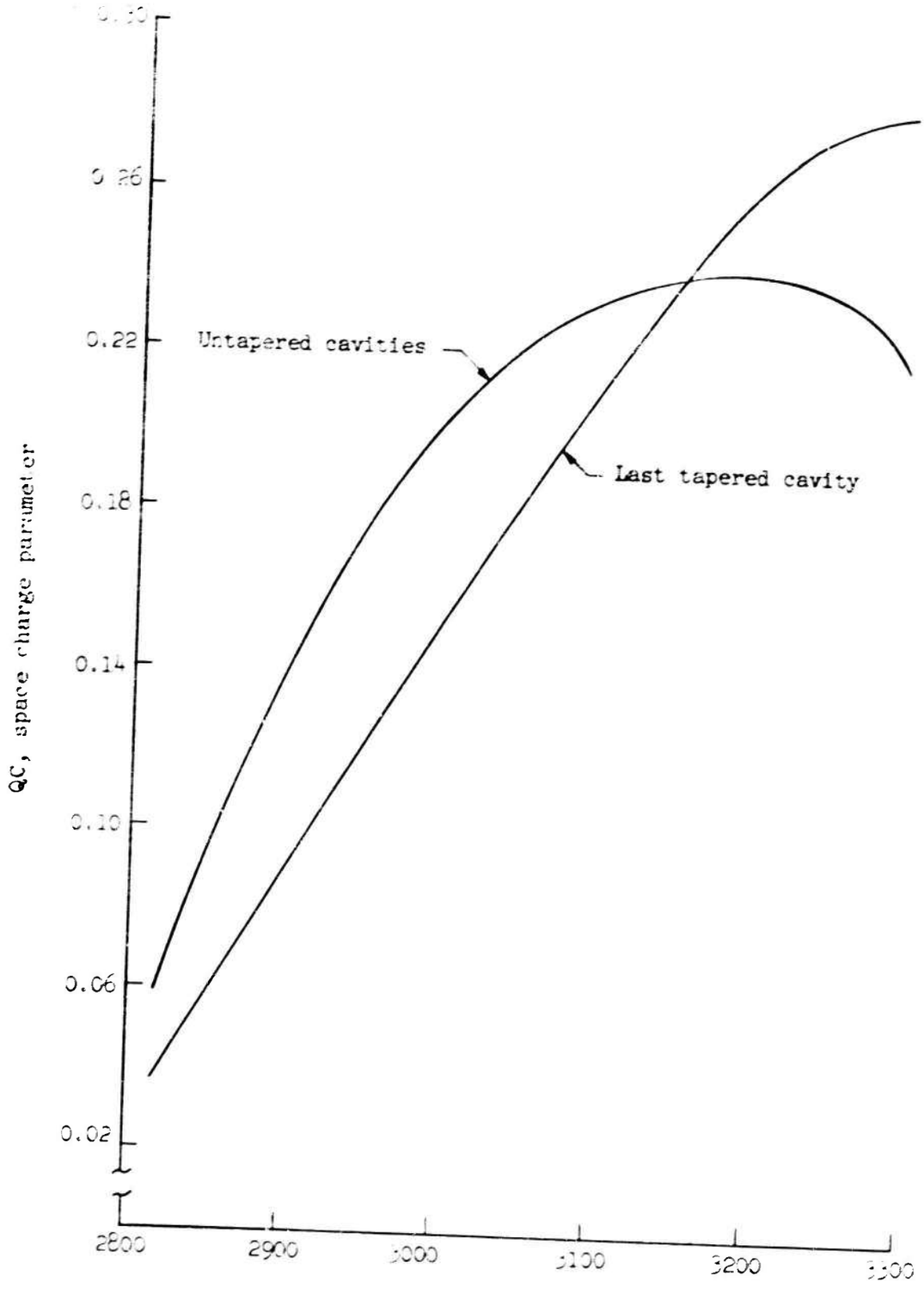

FIG. A 2--QC vs frequency.

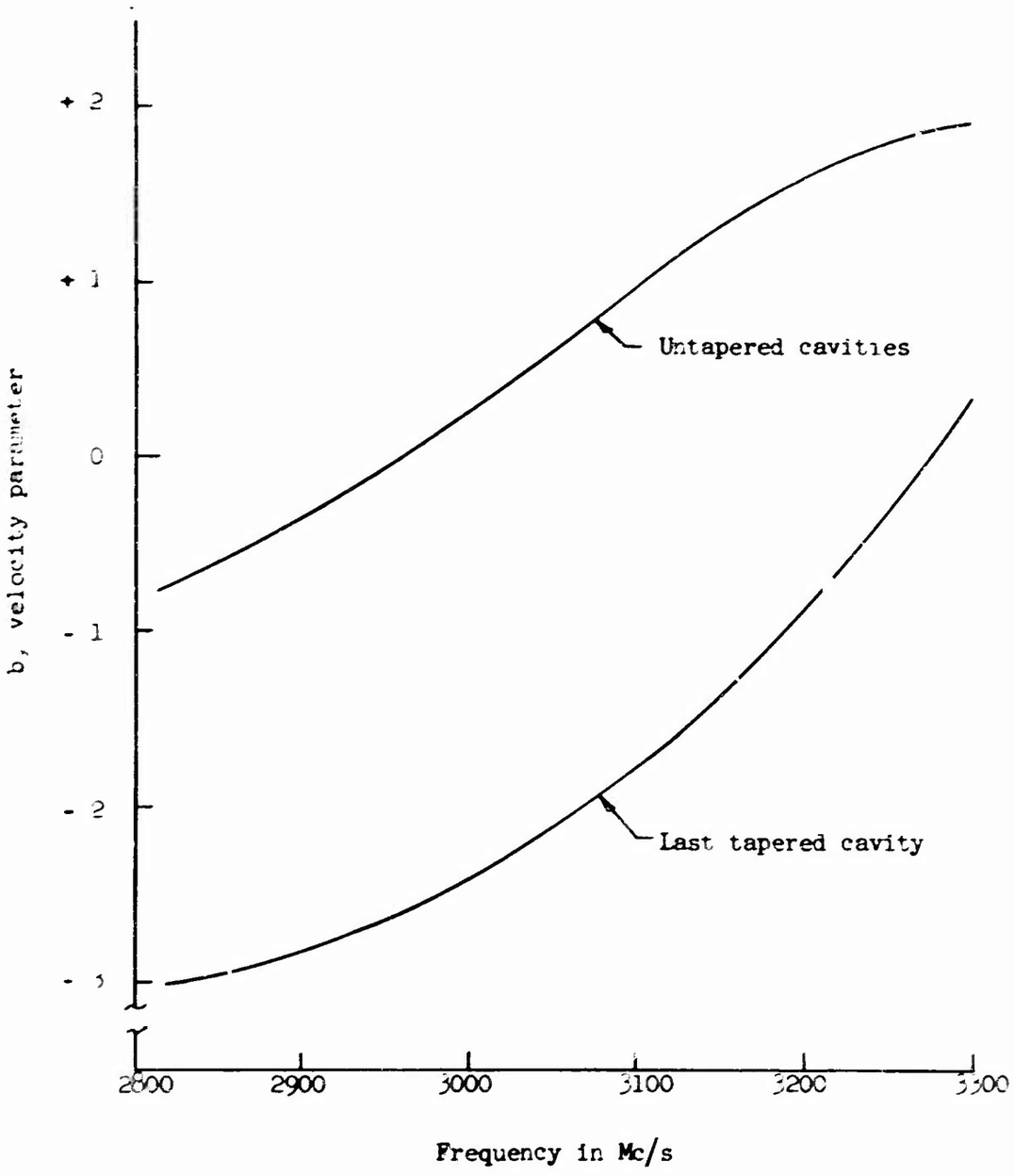

FIG. A.3--b vs frequency.

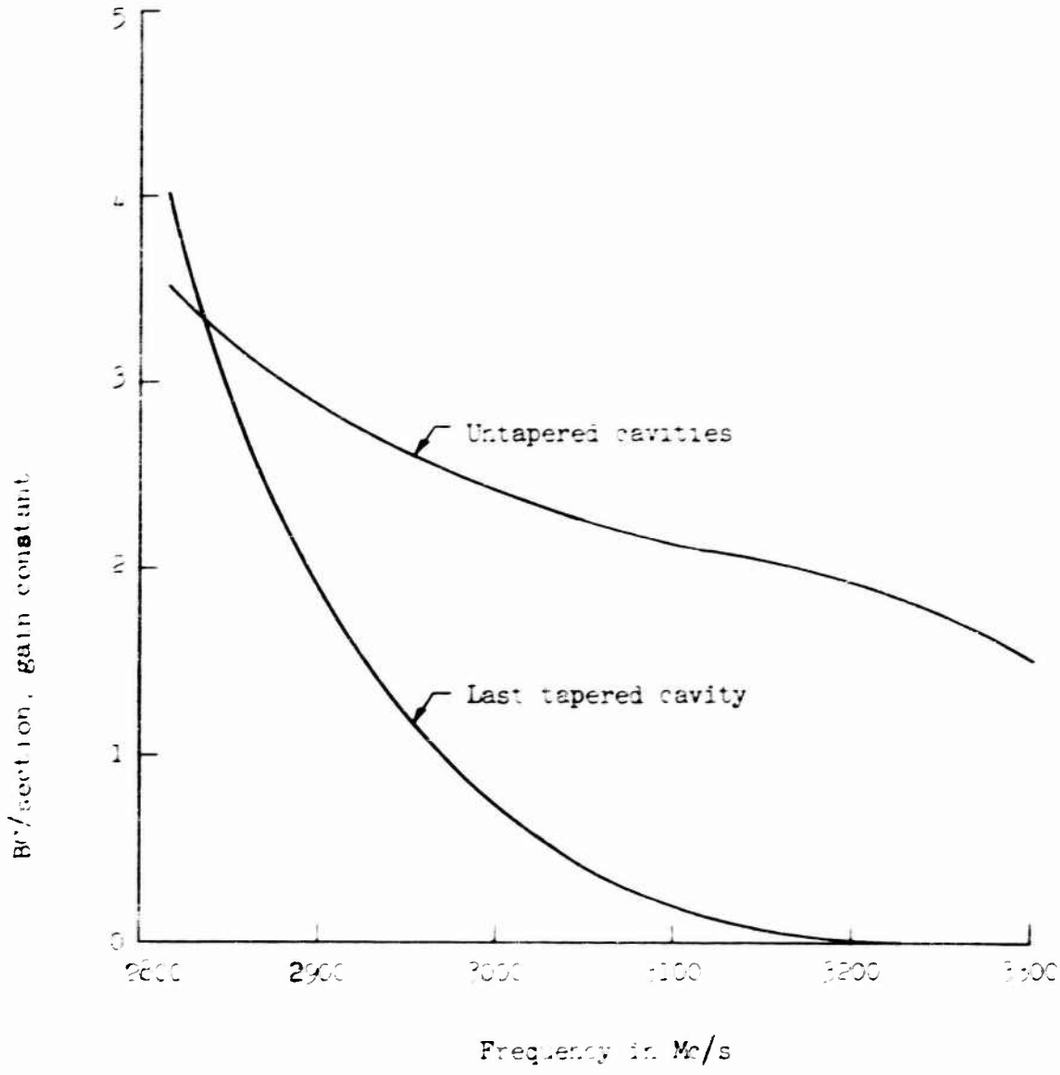

FIG. A.4---Bℓ/section vs frequency.

With the above parameters, one can find the x_1 parameter from Birdsall and Brewer's published results.[12] It is seen that $b = 54.6x$, the gain per section (Bc/section) can be obtained as shown in Fig. A 4

LIST OF REFERENCES

1. R. A. Craig, personal notes.
2. R. W. Gould, "Characteristics of Traveling-wave Tubes with Periodic Circuits," IRE Trans. PGED ED-5, 186-95 (July 1958).
3. D. G. Dow, "Behavior of Traveling-wave Tubes near Circuit Cutoff," IRE, Trans. PGED, ED-7 123-31 (July 1960).
4. M. Chodorow, "Recent Progress in High-Power Traveling-wave Tubes," Proceedings of International Congress on Microwave Tubes, Munich, Germany (1961), p. 88
5. C. C. Cutler, "The Nature of Power Saturation in Traveling-wave Tubes," Bell Syst. Tech. J. 35, 841-875 (July 1956).
6. R. L. Hess, private communication.
7. M. Chodorow, A. F. Pearce, D. K. Winslow, "The Centipede High-Power Traveling-wave Tube," Microwave Laboratory Report No. 695, Stanford University (May 1960).
8. J. R. Pierce, Traveling-wave Tubes, D. Van Nostrand Co., Inc., 1950.
9. H. Heffner "Analysis of the Backward-wave Traveling-wave Tube," Proc. IRE 42 930-37 (June 1954).
10. H. R. Johnson, "Backward-wave Oscillator," Proc. IRE 43, 684-97 (June 1955).
11. First and Second Annual Reports for Contract AF 30(602)-1844, Microwave Laboratory Report No. 773, Stanford University (January 1961), and Third Annual Report for Contract AF 30(602)-1844, Microwave Laboratory Report No. 854, Stanford University (February 1962).
12. C. K. Birdsall and G. H. Brewer, Tech. Memo No. 331, Hughes Aircraft Co. Also in IRE, Trans. EDI, (1954)
13. J. G. Meeker and J. E. Rowe, "Phase-focusing in Linear-beam Devices," IRE, Trans. PGED, ED-9, 257 (May 1962).
14. R. L. Hess, "Traveling-wave Tube Large Signal Theory, with Application to Amplifiers Having DC Voltage Tapered with Distance," Ph.D. Dissertation, University of California, Berkeley (July 1960).

15. A. Nordsieck, "Theory of the Large-signal Behavior of Traveling-wave Amplifiers," Proc. IRE 41, 630 (May 1953).

16. H. C. Poulter, "Large-signal Theory of the Traveling-wave Tube," Electronics Research Laboratory Technical Report No. 73, Stanford University (January 1954).

17. P. K. Tien, L. R. Walker and V. M. Wolontis, "A Large-signal Theory of Traveling-wave Amplifiers," Proc. IRE 43, 260 (1955).

18. P. K. Tien, "A Large-signal Theory of Traveling-wave Amplifiers," Bell System Tech. J. 35, 349 (1956).

19. J. E. Rowe, "Design Information on Large-signal Traveling-wave Amplifiers," Proc. IRE 44, 200 (1956).

20. J. E. Rowe, "A Large-signal Analysis of the Traveling-wave Amplifier: Theory and General Results," IRE, Trans. PGED, ED-3, 39 (1956).

21. J. E. Rowe, "One-dimensional Traveling-wave Tube Analyses and the Effect of Radial Electric Field Variations," IRE, Trans. PGED, ED-7, 16 (January 1960).

22. C. C. Cutler, "The Nature of Power Saturation in Traveling-wave Tubes," Bell Telephone Laboratories, Inc., Monograph, p. 24, (no date).

23. M. Chodorow and R. A. Craig, "Some New Circuits for High-power Traveling-wave Tubes," Proc. IRE 45, 1106-18 (August 1957).

24. J. Ruetz, D. Robinson and J. Pavkovich, "The Effect of Tapered Circuits on Efficiency, for High-power Traveling-wave Tubes," presented at Electron Devices Meeting. Washington, D. C., October 27-28, 1960.

25. D. J. Bates and A. W. Scott, "The Effect of Circuit Tapering on the Efficiency Bandwidth Characteristics of Dispersive Traveling-wave Tubes," IEEE, Trans. PGED, ED-10 (March 1963).

26. R. A. Craig, private communication.

27. H. A. Bethe, "Theory of Diffraction by Small Holes," Phys. Rev. 66, 163 (October 1 and 15, 1944).

28. S. V. Yadavalli, private communication

29 E. L. Ginzton, Microwave Measurements McGraw-Hill, Inc., New York, 1957.

30. R. P. Lagerstrom, "Interaction-Impedance Measurements by Perturbation of Traveling Waves," Stanford Electronics Laboratory Technical Report No. 7, Stanford University (February 1957).

31. R. A. Craig, Stanford Electronics Laboratory Technical Report No. 36, Stanford University (November 1954).

32. G. M. Branch and T. G. Mihran, "Plasma Reduction Factors in Electron Beams," IRE, Trans. PGED, ED-2, 3-11 (April 1955).